USGS
science for a changing world

Global Mineral Resource Assessment

Geology and Undiscovered Resource Assessment of the Potash-Bearing Central Asia Salt Basin, Turkmenistan, Uzbekistan, Tajikistan, and Afghanistan

Scientific Investigations Report 2010–5090–AA

U.S. Department of the Interior
U.S. Geological Survey

This page intentionally left blank

Global Mineral Resource Assessment

Michael L. Zientek, Jane M. Hammarstrom, and Kathleen M. Johnson, editors

Geology and Undiscovered Resource Assessment of the Potash-Bearing Central Asia Salt Basin, Turkmenistan, Uzbekistan, Tajikistan, and Afghanistan

By Jeff Wynn, Greta J. Orris, Pamela Dunlap, Mark D. Cocker, and James D. Bliss

Scientific Investigations Report 2010–5090–AA

U.S. Department of the Interior
U.S. Geological Survey

U.S. Department of the Interior
SALLY JEWELL, Secretary

U.S. Geological Survey
Suzette M. Kimball, Director

U.S. Geological Survey, Reston, Virginia: 2016

For more information on the USGS—the Federal source for science about the Earth, its natural and living resources, natural hazards, and the environment—visit http://www.usgs.gov or call 1–888–ASK–USGS.

For an overview of USGS information products, including maps, imagery, and publications, visit http://www.usgs.gov/pubprod/.

Suggested citation:
Wynn, Jeff, Orris, G.J., Dunlap, Pamela, Cocker, M.D., and Bliss, J.D., 2016, Geology and undiscovered resource assessment of the potash-bearing Central Asia Salt Basin, Turkmenistan, Uzbekistan, Tajikistan, and Afghanistan: U.S. Geological Survey Scientific Investigations Report SIR 2010–5090–AA, 106 p., and spatial data, *http://dx.doi.org/10.3133/sir20105090AA*.

ISSN 2328-0328 (online)

Acknowledgments

This publication represents the work of the authors and many reviewers, GIS specialists and figure preparers, as well as people familiar with stratabound and halokinetic potash-bearing salt deposits. Steve Jasinski (USGS), Lori Apodaca (USGS), Helen Folger (USGS), and Mark Gettings (USGS) provided formal technical reviews. Series edit was provided by Kate Johnson (USGS). The authors acknowledge Michael Zientek and Jane Hammarstrom of the USGS, who provided logistical guidance through the late stages of the USGS global potash assessment.

Bruce Lipin, Greg Spanski, and Steve Ludington participated in the three-part form of assessment of the Gissar tact. Chao Yang (Saskatchewan Geological Survey), Mirosław Słowakiewicz (Polish Geological Institute–National Research Institute), and Robert J. Ryan (Nova Scotia Department of Natural Resources) provided insights into potash deposits in their respective countries, and assisted in the three-part assessment of the Gissar tract.

Assistance with the GIS part of this report was provided by a large number of people, especially Karen Bolm (deceased), Deborah Briggs, Leila Gass, Robert Miller, and Connie Dicken. Drew Luders, Joe Miles, Heather Parks, and Kassandra Lindsey assisted in preparation of figures. All these individuals are USGS employees, students, or contractors.

This page intentionally left blank

Contents

Contents—Continued

Contents—Continued

Figures

Figures—Continued

Tables

Tables—Continued

Conversion Factors

Inch/Pound to International System of Units

Multiply	By	To obtain
	Length	
foot (ft)	0.3048	meter (m)
mile (mi)	1.609	kilometer (km)
yard (yd)	0.9144	meter (m)
	Area	
acre	0.4047	hectare (ha)
acre	0.004047	square kilometer (km^2)
square mile (mi^2)	259.0	hectare (ha)
square mile (mi^2)	2.590	square kilometer (km^2)
	Mass	
ounce, troy (troy oz)	31.015	gram (g)
ounce, troy (troy oz)	0.0000311	megagram (Mg)
ton, short (2,000 lb)	0.9072	megagram (Mg)

International System of Units to Inch/Pound

Multiply	By	To obtain
	Length	
meter (m)	3.281	foot (ft)
kilometer (km)	0.6214	mile (mi)
meter (m)	1.094	yard (yd)
	Area	
hectare (ha)	2.471	acre
square kilometer (km^2)	247.1	acre
hectare (ha)	0.003861	square mile (mi^2)
square kilometer (km^2)	0.3861	square mile (mi^2)
	Mass	
gram (g)	0.03215	ounce, troy (troy oz)
megagram (Mg)	1.102	ton, short (2,000 lb)
megagram (Mg)	0.9842	ton, long (2,240 lb)

Datum

Vertical coordinate information is referenced to the World Geodetic System 1984 (WGS 84), reported in decimal degrees.

Horizontal coordinate information is referenced to the World Geodetic System 1984 (WGS 84), reported in decimal degrees.

This page intentionally left blank

Geology and Undiscovered Resource Assessment of the Potash-Bearing Central Asia Salt Basin, Turkmenistan, Uzbekistan, Tajikistan, and Afghanistan

By Jeff Wynn,[1] Greta J. Orris,[2] Pamela Dunlap,[2] Mark D. Cocker,[2] and James D. Bliss[2]

Abstract

Undiscovered potash resources in the Central Asia Salt Basin (CASB) of Turkmenistan, Uzbekistan, Tajikistan, and Afghanistan were assessed as part of a global mineral resource assessment led by the U.S. Geological Survey (USGS). The term "potash" refers to potassium-bearing, water-soluble salts derived from evaporite basins, where seawater dried up and precipitated various salt compounds; the word for the element "potassium" is derived from potash. Potash is produced worldwide at amounts exceeding 30 million metric tons per year, mostly for use in fertilizers. The term "potash" is used by industry to refer to potassium chloride, as well as potassium in sulfate, nitrate, and oxide forms (Neuendorf and others, 2005). For the purposes of this assessment, the term "potash" refers to potassium ores and minerals and potash ore grades. Resource and production values are usually expressed by industry in terms of K_2O (potassium oxide) or muriate of potash (KCl, potassium chloride).

The CASB hosts significant discovered potash resources and originated in an inland sea during Late Jurassic time. Seawater flowed into the CASB, mostly from its extreme northwestern margin near the modern Caspian Sea, during several evaporation episodes that deposited at least five different packages of evaporites, with virtually all potash in the second and fourth packages. In this study, the CASB was subdivided into three tracts (permissive areas) for evaluation: the Amu Darya tract in the west, the Gissar tract in the center, and the Afghan-Tajik tract in the east. The Gissar and Amu Darya tracts were quantitatively assessed, whereas the Afghan-Tajik tract was only qualitatively assessed because of the commonly extreme depth (as deep as 7 km) of the Jurassic salt, extensive deformation, and a lack of known potash deposits.

Two approaches were used to estimate amounts of undiscovered potash in the CASB. Stratabound evaporite deposits in the Amu Darya tract were evaluated using an Adaptive Geometric Estimation (AGE) approach, which estimates in-place potash volumes and tonnages. The Gissar tract was evaluated by using the AGE approach for stratabound deposits and the three-part form of assessment of Singer and Menzie (2005) for discrete halokinetic deposits. In the three-part form of assessment, numbers of undiscovered deposits were estimated and combined with grade and tonnage models to probabilistically forecast the amount of undiscovered potash. The Amu Darya tract is estimated to contain 38 billion metric tons (Bt) of undiscovered potash as K_2O by using the AGE approach for stratabound deposits. The hybrid stratabound-halokinetic Gissar tract is estimated to contain between 1 and 16 Bt of undiscovered potash as K_2O.

Chapter 1 of this report provides an overview of the history of the CASB and summarizes evaporite potash deposition, halokinesis, and dissolution processes that have affected the current distribution of potash-bearing salt in the CASB. Chapter 2 describes the Gissar tract, an uplifted region that contains a mix of stratabound and halokinetic potash deposits and all of the discovered and exploited potash deposits of the CASB. Chapter 3 describes the Amu Darya tract, where evaporite deposits remain flat-lying and undeformed since their original deposition. Chapter 4 describes the highly deformed and compressed Afghan-Tajik tract and what is known of the deeply-buried Jurassic salt. Chapter 5 describes the spatial databases included with this report, which contain a collection of CASB potash information. Appendixes A and B summarize descriptive models for stratabound and halokinetic potash-bearing salt deposits, respectively. Appendix C summarizes the AGE method used to evaluate the Gissar and Amu Darya tracts. Appendixes D and E contain grade and thickness data for the Gissar and Amu Darya tracts. Appendix F provides the SYSTAT script used to estimate undiscovered K_2O in a CASB tract. Appendix G provides a potash glossary, and appendix H provides biographies of assessment participants.

---

[1]U.S. Geological Survey, Vancouver, Washington, United States.

[2]U.S. Geological Survey, Tucson, Arizona, United States.

This page intentionally left blank

Chapter 1. Overview of the Geology and Assessment of Undiscovered Potash Resources in the Central Asia Salt Basin, Turkmenistan, Uzbekistan, Tajikistan, and Afghanistan

By Jeff Wynn[1] and Greta J. Orris[2]

Introduction

The Central Asia Salt Basin (CASB) is a major Jurassic to Early Cretaceous (?)[3] evaporite basin that spans four countries (Uzbekistan, Turkmenistan, Tajikistan, and Afghanistan) and contains a significant amount of the world's potash resources. The basin covers more than 770,000 square kilometers (km^2) and the area underlain by salt is estimated to be approximately 192,800 km^2 (fig. 1-1). The hachured area on figure 1-1 represents the approximate extent of Jurassic evaporites that contain a significant amount of salt; the area would have been larger, but less useful for accurately assessing potash, if we had included anhydrite and limestone. Figure 1-1 also shows that the extent of the basin containing Jurassic salt does not correspond to more modern basin extents (basins defined by Tellus, USGS, and AAPG); in fact, there is no single modern system of recognized basins. The three potash tracts shown in figure 1-2 represent the part of the CASB that is likely partially to wholly underlain by potash.

The CASB evaporite deposits unconformably overlie a pre-Jurassic basement depression and are thought to have evolved through repeated inflow of seawater from the northwest (and possibly also the southwest), followed by repeated evaporation during the Jurassic and possibly into the Early Cretaceous. Known potash deposits in the Gissar tract (fig. 1-2) are distal to seawater inflow point(s) of the original CASB and this position is consistent with stratabound and halokinetic potash-bearing salt models (appendixes A and B). Additional, though less extensive, evaporites were also deposited in the CASB during Paleogene time. Salt deposition associated with known potash deposits is largely confined to the Upper Jurassic Gaurdak Formation. Sedimentary rocks enclosing the evaporites are generally sandstones and shales from terrigenous sources, or marine carbonates. During the Miocene, uplift of the Gissar Range divided the basin into the Amu Darya Basin to the west (fig. 1-1, blue shading) and the Afghan-Tajik Basin to the east (fig. 1-1, lilac shading). All known potash deposits and mines occur on the flanks of the Gissar uplift, most likely because they are shallow and thus more easily discovered and exploited than deep deposits.

Undiscovered potash resources in the CASB were assessed as part of a U.S. Geological Survey (USGS) global mineral resource assessment whereby we (1) delineated permissive areas (tracts) for undiscovered potash deposits at a scale of 1:1,000,000; (2) created a database of known potash deposits and occurrences; and (3) where possible, calculated probabilistic estimates of the amounts of undiscovered potash for each permissive tract (Harris, 1984).

Potassium is an essential nutrient for plants, animals, and humans and has no known substitutes (Jasinski, 2015). The most common potash minerals, from which potassium is derived, are listed with their physical properties in table 1-1. Potash demand is primarily driven by demand for fertilizer for use in production of food and biofuels (Jasinski, 2015); increasing global population, changing diets, and decreasing amounts of arable land have increased the need for fertilizer minerals, including potash (Magen, 2010). This increasing demand has led to upward pressure on prices since the beginning of 2008 and subsequent exploration for new potash sources, particularly in Europe and Asia (table 1-2). This exploration has produced more new data on the geology and occurrence of potash than has been available since potash exploration efforts of the 1960s and early 1970s. In addition, more properties are reported as "currently under development" than have been in the previous 30 years combined.

---

[1]U.S. Geological Survey, Vancouver, Washington, United States.

[2]U.S. Geological Survey, Tucson, Arizona, United States.

[3]Ages in this report are consistent with the International Chronostratigraphic Chart (Cohen and others, 2013).

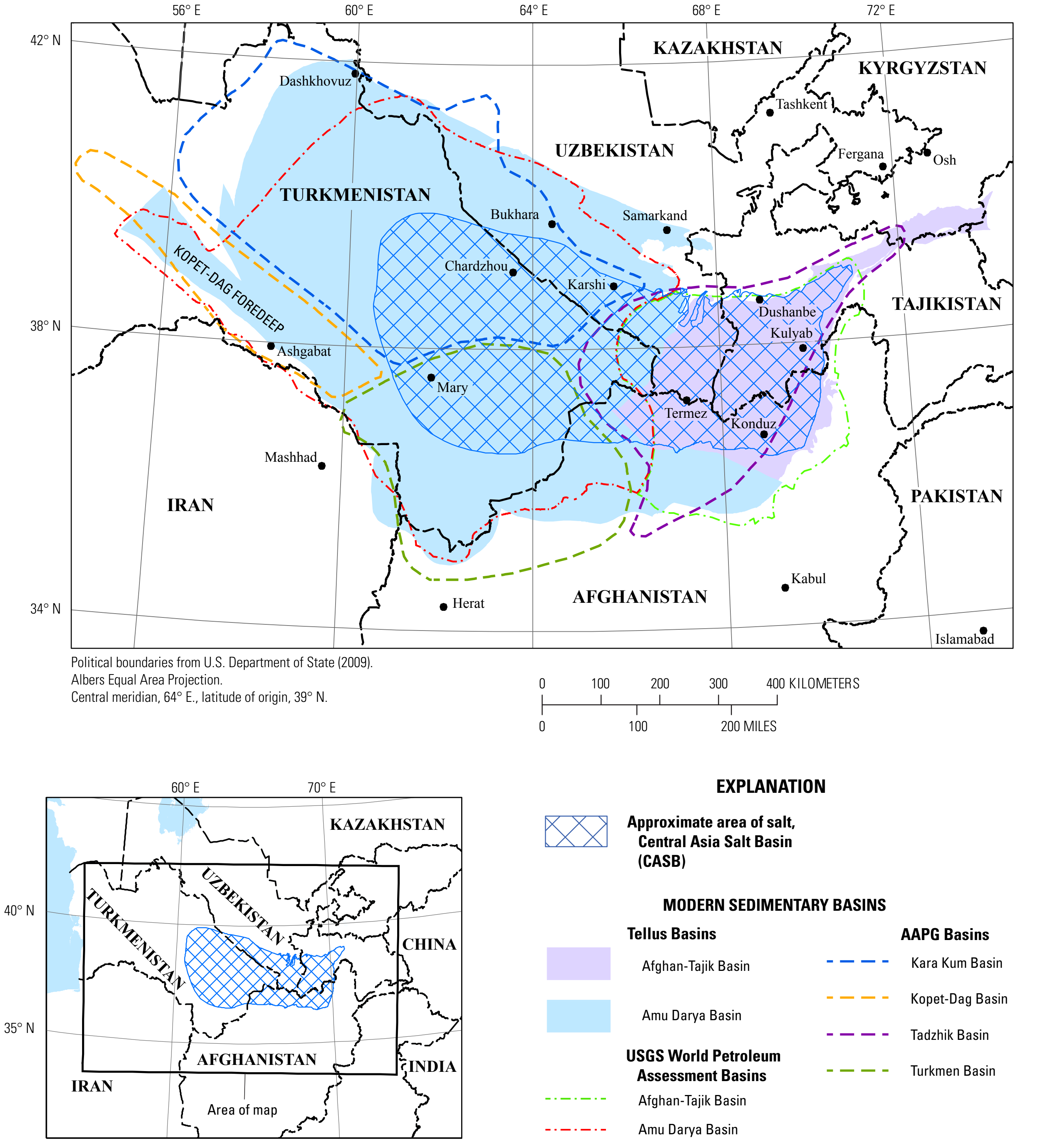

Figure 1-1. Map showing original Central Asia Salt Basin (CASB) compared with modern sedimentary basins. The two Tellus sedimentary basins, the Amu Darya and Afghan-Tajik to the west and east of the Gissar Range, respectively, are those defined by the World Petroleum Assessment (U.S. Geological Survey World Energy Assessment Team, 2000).

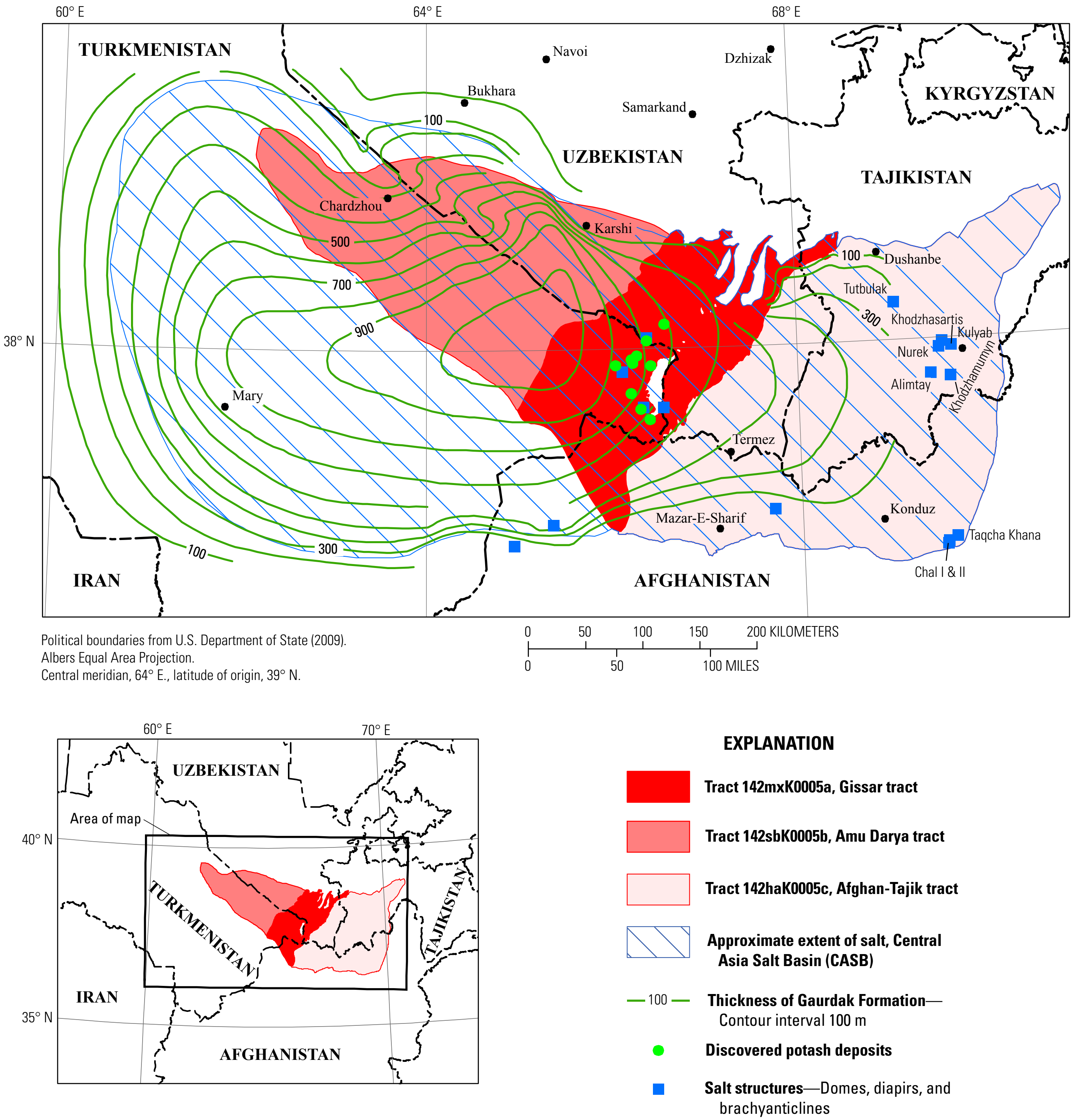

Figure 1-2. Map showing the three assessed tracts within the Central Asia Salt Basin (CASB) compared with salt-bearing Upper Jurassic Gaurdak Formation (adapted from Steinshouer and others, 2006). Note salt structures to east outside approximate boundaries of assessment tracts, and thickness of evaporite salt from Steinshouer and others (2006).

Table 1-1. Potash ore minerals and their physical properties from Orris and others (2014).

[Composition formulas from Back and Mandarino (2008); potassium content and specific gravity from Harben and Kuzvart (1996) and Anthony and others (1997, 2003); > greater than]

Mineral or material	Composition	Potassium oxide (K_2O), percent	Density (tons/cubic meter)
Primary potash minerals			
Carnallite	$KMgCl_3 \cdot 6H_2O$	16.9	1.60
Kainite	$MgSO_4 \cdot KCl \cdot 3H_2O$	19.3	2.10
Langbeinite	$K_2Mg_2(SO_4)_3$	22.7	2.83
Polyhalite	$K_2Ca_2Mg(SO_4)_4 \cdot 2H_2O$	15.6	2.77
Sylvite	KCl	63.2	2.00
Primary potash ore materials			
Carnallitite	Mix of halite and carnallite	Up to 15	Variable
Hartsalz	Mix of sylvite, halite, anhydrite, and kieserite	Typically <15	Variable
Sylvinite	Mix of sylvite and halite	Typically <25	Variable
Accessory potassium minerals			
Aphthitalite (glaserite)	$(K,Na)_3Na(SO_4)_2$	42.5	2.69
Arcanite	K_2SO_4	54.1	2.66
Douglasite	$K_2Fe^{2+}Cl_4 \cdot 2H_2O$	30.2	2.16
Leonite	$K_2Mg(SO_4)_2 \cdot 4H_2O$	25.7	2.20
Niter (saltpeter)	KNO_3	44.0	2.1
Picromerite (schönite)	$K_2Mg(SO_4)_2 \cdot 6H_2O$	23.4	2.03
Rinneite	$K_3NaFe^{2+}C_6$	34.5	2.35
Syngenite	$K_2Ca(SO_4)_2 \cdot H_2O$	28.7	2.58
Accessory non-potassium minerals			
Anhydrite	$CaSO_4$	0	2.98
Bischofite	$MgCl \cdot 6H_2O$	0	1.59
Blödite	$Na_2Mg(SO_4)_2 \cdot 4H_2O$	0	2.23
Dolomite	$CaMg(CO_3)_2$	0	2.86
Epsomite	$MgSO_4 \cdot 7H_2O$	0	1.68
Gypsum	$CaSO_4 \cdot 2H_2O$	0	2.30
Halite	NaCl	0	2.17
Hexahydrite	$MgSO_4 \cdot 6H_2O$	0	1.76
Kieserite	$MgSO_4 \cdot H_2O$	0	2.57
Löweite	$Na_{12}Mg_7(SO_4)_{13} \cdot 15H_2O$	0	2.36-2.42
Tachyhydrite	$CaMgCl_6 \cdot 12H_2O$	0	1.67
Vanthoffite	$Na_6Mg(SO_4)_4$	0	2.69

Table 1-2. Select areas of potash exploration and development in eastern Europe and Asia since 2000.

[—, no data]

Project	Country	Basin	Company	Reference
Western Qaidam Basin	China	Qaidam	—	Ourchemical (2011), Xi'an Center of Geological Survey (2008)
Hanumangarh-Mahajan-Punrasar	India	Nagaur-Ganganagar	Pebble Creek Mining Ltd. (2008)	Pebble Creek Mining Ltd. (2008)
Thongman	Lao PDR	Sakhon Nakhon-Vientiane	China-Laos Minerals Development and Investment Corp. (2010)	Chinese Academy of Sciences (2010)
Satimola	Kazakhstan	Pricaspian	Satimola, Ltd. (2011)	Agapito Associates Inc. (2011)
Uvs Nuur	Mongolia, Russia	Uvs Nuur (Tuva)	General Mining Corporation Ltd. (2011)	General Mining Corporation Ltd. (2009)
Gremyachinsk	Russia	Pricaspian	EuroChem (2009)	Environmental Resources Management (2009)
Tajikistan project	Tajikistan	Central Asia Salt Basin	Mineral Mining PLC (2011)	Newswire Today (2011)
Udon and Somboon	Thailand	Sakhon Nakhon	Asia Pacific Potash Corp. (2011)	Lomas (2002)
Karlyuk (Garlyk)	Turkmenistan	Central Asia Salt Basin	Belgeologia (2010)	Belarusian Telegraph Agency (2010)
Tyubegatan	Uzbekistan	Central Asia Salt Basin	Western Ural Machine Building Concern	ITE Gulf FZ LLC (2010)

The USGS global potash assessment distinguishes two end-member subtypes of potash-bearing evaporite salt—stratabound deposits and halokinetic deposits. Stratabound deposits (appendix A) are extensive and tectonically undisturbed. These deposits vary in size and can underlie areas ranging from tens to hundreds of thousands of square kilometers. The maximum deposit size in each basin is limited by the size of the basin at the time of deposition, but in some places, only very small deposits may be present in extremely large basins, so basin size is not a reliable predictor of potash deposit size.

Deep burial, active tectonics, and regional faulting can result in halokinesis—salt flowage that can form salt structures such as brachyanticlines, salt walls, folds, and diapirs, localized thickening and thinning of potash and salt, repetition of beds, and other disruptions, including loss of original potash deposition. Halokinetic deposits (appendix B) contain, on average, smaller tonnages than stratabound deposits, although halokinetic deposits exceeding a billion metric tons are possible.

For the USGS global potash assessment, quantitative estimates of undiscovered potash resources in stratabound deposits were made using an adaptive geometric estimation (AGE) method (summarized in appendix C). Quantitative estimates of undiscovered potash resources in halokinetic deposits were made using the three-part form of assessment of Singer and Menzie (Singer, 1993; Singer and Menzie, 2005). The CASB hosts both stratabound and halokinetic potash occurrences; halokinesis is more prevalent in the eastern CASB and the original stratabound nature of the deposit is largely, if not completely, preserved in the western part of the basin. This range of deposit types allowed us to investigate and compare the newly developed AGE method with the three-part form of assessment (Singer and Menzie, 2005).

For purposes of potash resource evaluation, we divided the CASB into three tracts (figure 1-1): (1) the Gissar tract (chapter 2) composed of uplifted and, in places, deformed sedimentary rocks that form the Gissar Range and its buried extension south-southwest to the Repetek Fault; (2) the Amu Darya tract (chapter 3) that consists of a largely flat-lying and minimally-deformed sedimentary sequence to the west of the Gissar Range; and (3) the Afghan-Tajik tract (chapter 4) composed of downdropped, deeply buried, deformed, and compressed sedimentary rocks to the east of the Gissar Range. Detailed descriptions of the assessment processes and assessment results for these three tracts are described in the following chapters of this publication.

Geologic Overview

The Jurassic CASB comprises part of the Amu Darya Basin in the west and the Afghan-Tajik Basin in the east, which are separated by the Miocene Gissar Range (fig. 1-1). The salt basin is physically delimited by the North Afghan and Mary-Serakh Highs to the southwest, the Kyzyl Kum Plateau and Alai Mountains to the north, and the Pamir Mountains and Hindu Kush to the east (fig. 1-3).

Basin History, Tectonics, and Structure

The Miocene Gissar Range is a large, broad anticlinorium trending roughly N20E that uplifted basinal sedimentary rocks at least 1,000 meters (m) above their pre-deformation positions (Ulmishek, 2004; Steinshouer and others, 2006) and forms the divide between the modern Amu Darya and Afghan-Tajik Basins. The westernmost Amu Darya Basin pinches out gradually to the northwest; this boundary is ill-defined in the scientific literature, despite extensive oil and gas exploration during the past half century. The Afghan-Tajik Basin was deformed by block tectonics during evaporite deposition and most of the basin has been folded and compressed by as much as 50 percent in an east-west direction in southern Uzbekistan and southwestern Tajikistan. The deepest parts of the basin are in Tajikistan and contain more than 10 kilometers (km) of sedimentary rock. Marginal structural steps, including the North Afghan High, surround the depression and are uplifted as much as 3–8 km relative to the deepest parts of the basin (Klett and others, 2006).

Much of the development of the CASB and its subsequent modern basins has been related to the movement of the Eurasia, Africa, and Indian continental plates and accretion of various terranes (Ulmishek, 2004). Major events include (1) compression caused by the closing of the Paleotethys Ocean in the late Carboniferous to early Permian (Cassard, 2006); (2) extensional rifting and continental breakup in the late Permian to Triassic; (3) collision and associated deformation of the Cimmerian Block with Eurasia; (4) extension from Early to Middle Jurassic; (5) Middle Jurassic to Early Cretaceous formation of island arcs, passive margins, and postrift sags that caused marine transgression and deposition of continental and marine sediments; (6) movement of microcontinents in the Neotethys Ocean through the early Paleogene; and finally, (7) renewed compression and closing of the Neotethys Ocean (Cassard, 2006; Klett and others, 2006).

Deformation affecting the CASB during the basinal stage of development (Jurassic through Paleogene) is characteristic of block tectonics (Klett and others, 2006). Structural highs, such as the North Afghan High, experienced slower subsidence and occasional upward movements that resulted in local disconformities and absence of parts of the sedimentary rock sequence (Ulmishek, 2004). This deformation is most evident in the Gissar and Afghan-Tajik tracts. In contrast, evaporites in the Amu Darya tract have remained relatively undeformed since original deposition.

Basin Stratigraphy

The basement of the CASB is an accreted terrane formed during the Variscan Orogeny (Carboniferous to Permian) composed of deformed and metamorphosed Paleozoic rocks (Ulmishek, 2004). These units are overlain by upper Permian to Triassic rift graben fill, which in turn is overlain by Lower to Middle Jurassic rocks that are largely continental and are commonly coal bearing. Deep-water marine carbonate deposition dominated during the Callovian (Middle Jurassic) until evaporites were deposited in Kimmeridgian-Tithonian (Late Jurassic) time. Deposition of clastic marine rocks, with some continental sedimentary rock intervals, dominated from the Early Cretaceous through Paleogene (Ulmishek, 2004), and evaporites are distributed throughout the stratigraphic section.

Although a few references consider part of the thick evaporite deposits to be Lower Cretaceous Almurad Formation (Baikov and Sedletskiy, 2001), the majority of literature available to us considers the extensive potash-bearing salt deposition to be contained exclusively in the Upper Jurassic (Kimmeridgian-Tithonian) Gaurdak Formation. All known reserves, with the possible exception of parts (or all) of the Okuzbulak and Khodzhaikan occurrences (described in chapter 2; see Rayevskiy and Fiveg, 1973), are considered Jurassic in age. Within the CASB, all potash-bearing salts are assigned to the Jurassic Gaurdak Formation for the purposes of this assessment; we do not have enough information to definitively distinguish potash that might be in the Lower Cretaceous Almurad Formation. In most places, the Gaurdak section consists of five distinct evaporite layers (from top to bottom): (1) upper anhydrite, (2) upper halite, (3) intermediate anhydrite, (4) lower halite, and (5) carbonate-anhydrite (Gavril'cheva, 1981; Gavril'cheva and Pashaev, 1993; Baikov and Sedletskiy, 2001).

The maximum thickness of the Gaurdak Formation is about 1,200 m (Vysotskiy and others, 1988; Baikov and Sedletskiy, 2001). The total volume of the Gaurdak is estimated to be 121,000 cubic kilometers (km^3), with halite and potassium salt composing as much as 33 percent of the total volume (Baikov and Sedletskiy, 2001). Basin-wide stratigraphy (fig 1-4) (Ulmishek, 2004) shows that Gaurdak Formation evaporites occur throughout the basin and are thickest in the vicinity of the Gissar Range in the central part of the CASB. Numerous gas and occasional oil deposits are reported throughout the Amu Darya Basin, both above and below the salt horizons of the Gaurdak Formation. Non-potash-bearing parts of the Gaurdak Formation extend at least 350 km west and 450 km northwest of the contoured "33 percent salt" limit of Steinshouer and others (2006) that is shown in fig. 1-2.

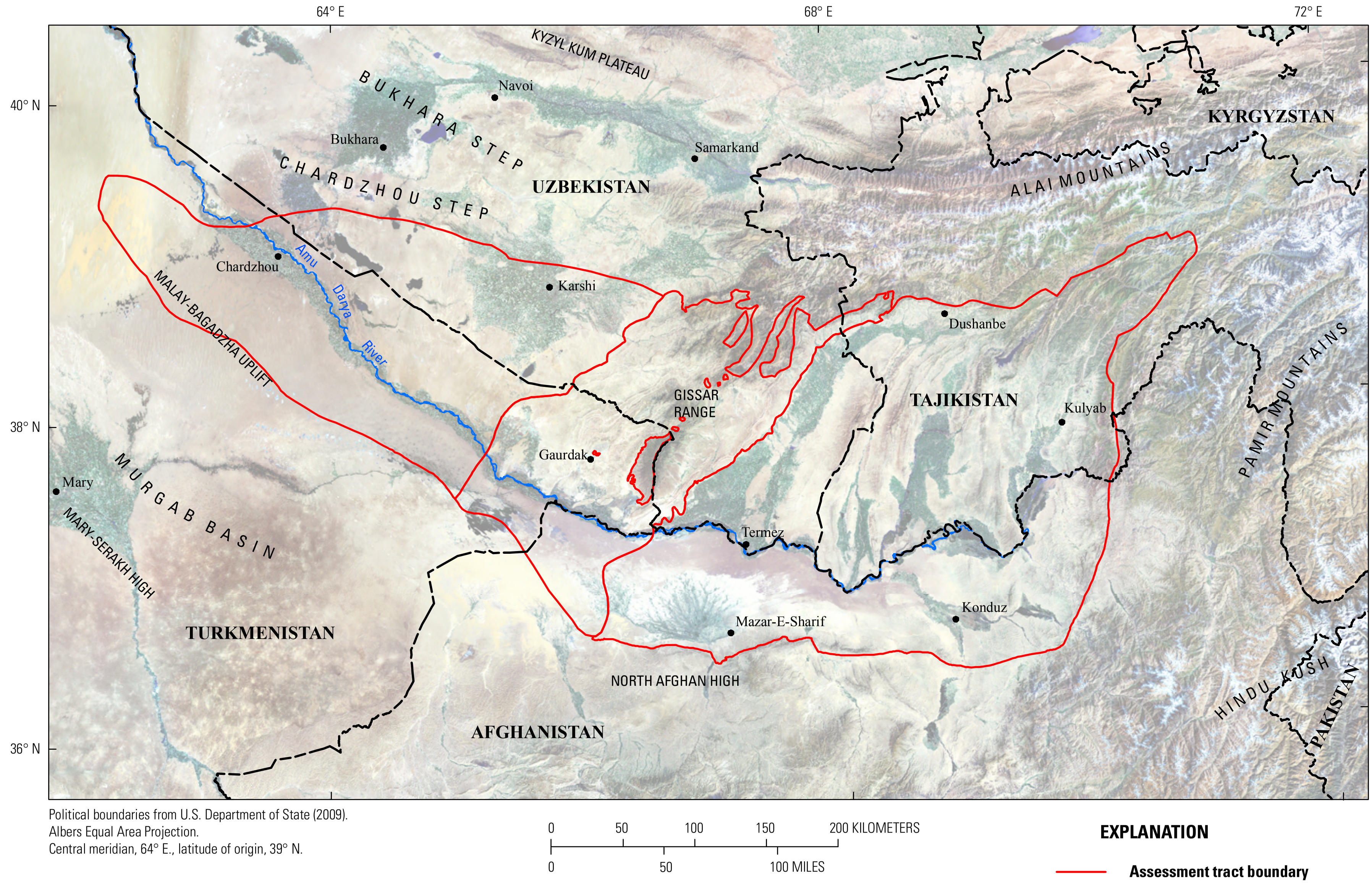

Figure 1-3. Map showing the three assessed tracts of the Central Asia Salt Basin (CASB) compared with modern geographic features on a Landsat image.

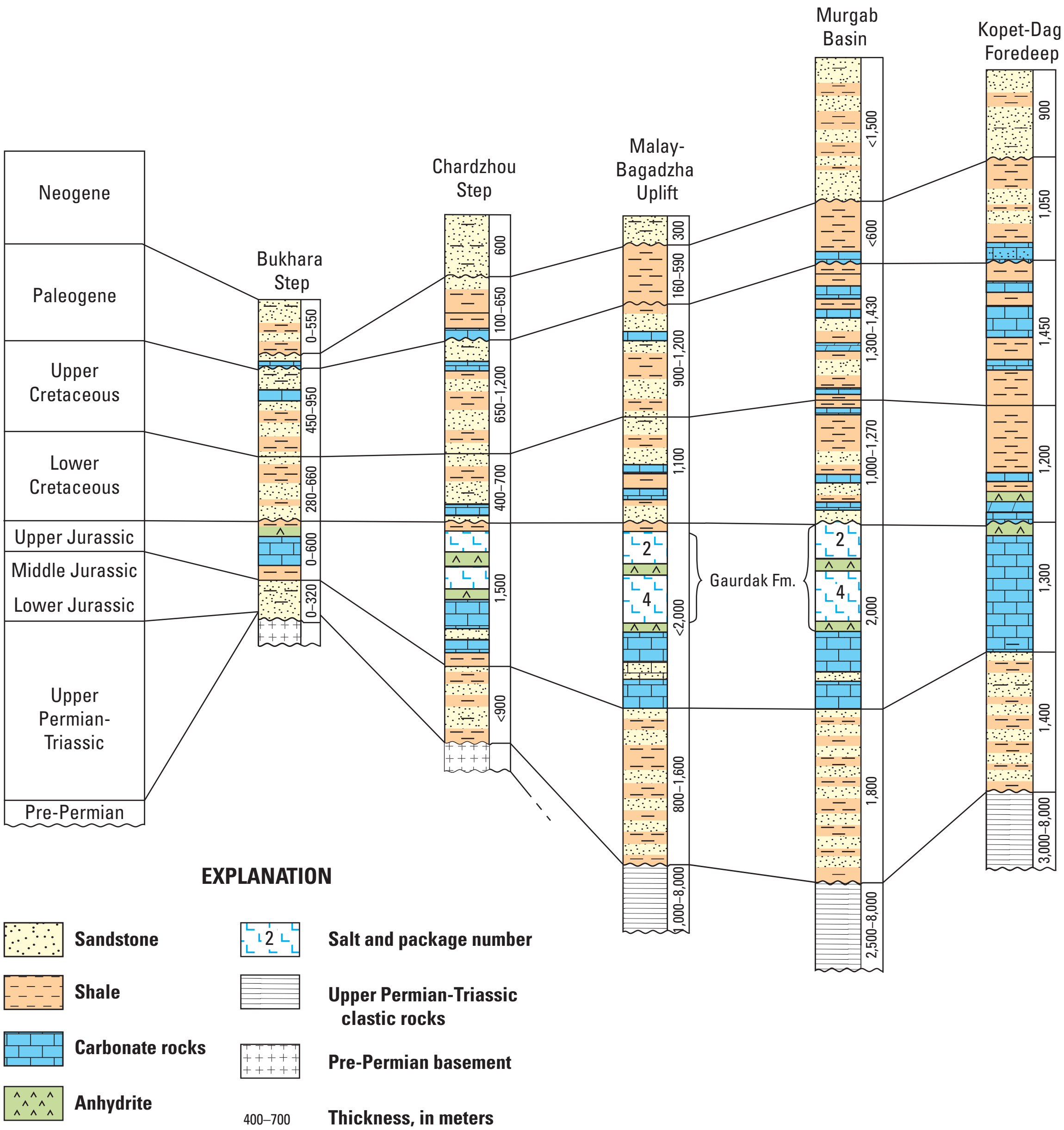

Figure 1-4. Stratigraphic columns showing generalized stratigraphy of the central and western Central Asia Salt Basin (CASB) (adapted from Ulmishek, 2004). Upper Jurassic Gaurdak Formation evaporite deposits are labeled, and potash-hosting, predominantly salt-bearing units within it are numbered. Potash locations adapted from Gavril'cheva and Pashaev (1993). Column locations are not available from original sources, but approximate locations labeled above columns are mapped in fig. 1-3.

Salt and Potash

The evaporite section in the CASB is best described in the Amu Darya Basin and Gissar Range areas; it is rarely exposed in the Afghan-Tajik Basin. Petroleum exploration has been largely confined to the periphery of the Afghan-Tajik Basin. According to Baikov and Sedletskiy (2001), the uppermost evaporite "package" (upper anhydrite, #1) may be Early Cretaceous in age, but this tentative Cretaceous age is copied from a single Baikov paper dating from 1974. It is unclear if any of the mineralized rock is Early Cretaceous, as the majority of available information indicates that potash mineralization occurred in the Late Jurassic, but two deposits may contain potash of earliest Cretaceous age. For the purposes of this assessment, all potash is assumed to be related and Late Jurassic in age, but the assessment of undiscovered resources should also be valid for any Late Jurassic-Early Cretaceous salts in the basin. Russian literature acknowledges that reporting on potash is inconsistent and incomplete (Popov and Osichkina, 1973), as it was incidental to oil and gas exploration in many parts of the CASB.

Most known halite deposits lie within the southeastern part of the Gaurdak Formation, which was outlined by Steinshouer and others (2006) as “33 percent salt” (fig. 1-2); the eastern boundaries of this salt area are not well defined and should extend east to include known salt domes that have been characterized as Jurassic in age (Vysotskiy and others, 1988; Bekker, 1996). The Gaurdak Formation west and northwest of the Amu Darya tract is not included in this assessment because only anhydrite, carbonates, and terrigenous sedimentary rocks (not potash-bearing) are shown in stratigraphic sections. Most potash is in the upper halite (package 2; Zharkov and others, 1982a, 1982b; Gavril’cheva and Pashaev, 1993) of the Gaurdak Formation (fig. 1-4), which has not been discovered outside the three delineated tracts of this study.

Potash in the CASB occurs as the minerals sylvite and carnallite (Petrov and Chistyakov, 1964; Rayevskiy and Fiveg, 1973; Sedletskiy and Derevyagin, 1980). Soluble sulfates of potassium, as well as sulfates of sodium and magnesium, are absent from the basin (Osichkina, 1978).

Assessment

The two westernmost tracts within the CASB, Amu Darya and Gissar, were evaluated using one or both of the global potash assessment methods (table 1-3). Tracts were delineated based on parameters of stratabound and halokinetic potash-bearing salt deposit models (appendixes A and B). Tracts permissive for halokinetic potash-bearing salt deposits were evaluated using the standard USGS three-part form of assessment (Singer, 1993; Singer and Menzie, 2005, 2010), and a grade and tonnage model was developed for this assessment (appendix D and table 1-4). Tracts permissive for stratabound potash-bearing salt deposits were evaluated using the AGE method developed for use with these deposits (appendix C). We prepared quantitative estimates for undiscovered potash resources in the Gissar and Amu Darya tracts, however, the assessment team had insufficient information to quantify undiscovered resources within the Afghan-Tajik tract. Moreover, geologic profiles of Bekker (1996) indicate that, unless uplifted by structural and halokinetic processes, most Jurassic sediments that might host potash are too deep for economic extraction.

Assessment Depth

An assessment depth limit of 3 km was used for potash tracts in the CASB; this is the standard depth limit used by the USGS to define potash worldwide.

Table 1-3. Estimates of potash in undiscovered deposits in the Central Asia Salt Basin, Turkmenistan, Uzbekistan, Tajikistan, and Afghanistan.

[km, kilometer; km^2, square kilometer; Bt, billion metric tons; NA, not applicable]

Tract name	Coded_ID	Type of assessment	Assessment depth (km)	Tract area (km^2)	Known potash resource (Bt K_2O)	Mean estimate of undiscovered potash resources (Bt K_2O)	Median estimate of undiscovered potash resources (Bt K_2O)	Consensus (Bt K_2O)
Gissar	142mxK0005a	AGE	3	26,669	1.63	27.9	25.3	NA
Gissar	142mxK0005a	Three Part	3	26,669	1.63	0.47	0.39	1 to 16
Amu Darya	142sbK0005b	AGE	3	40,224	0	41.1	37.8	38
Afghan-Tajik	142haK0005c	Qualitative	3	68,382	0	NA	NA	NA
Total								**39 to 54**

Table 1-4. Statistics for grade and tonnage model for halokinetic potash-bearing salt deposits.

[See appendix D; Mt, million metric tons]

	Distribution	Number of deposits	Mean	Quantiles		
				90	50 (median)	10
Tonnage (Mt)	lognormal	25	343.4	39.4	152.9	1,153
Grade (percent K_2O)	normal	25	16.5	9.2	15.8	24.7

Assessment Methods

The three-part form of assessment described by Singer (1993) and Singer and Menzie (2005, 2010) was used to estimate undiscovered potash resources in halokinetic deposits. In this method, an expert panel compared known deposits and permissive geology with a halokinetic potash-bearing salt deposit model, estimated the number of undiscovered deposits remaining in the tract, and then used a Monte Carlo simulation to combine a grade and tonnage model with the estimated number of deposits to arrive at a tonnage distribution for undiscovered potash resources. For potash, this is the remaining in-place K_2O value.

The AGE method (appendix C) was developed to estimate undiscovered potash resources in stratabound potash deposits. This method does not estimate undiscovered deposits, rather, it calculates a geometric estimate of in-place volumes and (or) tonnages of potash. The initial in-place values are then modified using simulations to estimate unknown or incompletely known parameters, such as grade and unmineralized areas (anomalies) caused by original non-deposition, replacement, dissolution, and erosion. Tonnages of known deposits are subtracted from this estimate.

Assessment and Results Summary

The Gissar tract, where mineralization is transitional, shows features of both halokinetic and stratabound potash-bearing salt deposits and was assessed for undiscovered potash resources using both assessment methods (table 1-3). Most of the available literature (for instance Vysotskiy and others, 1988) describes sedimentary rocks disrupted by tectonics and halokinesis; available information suggests these effects are highly variable throughout the uplifted Gissar tract. Numbers of undiscovered halokinetic deposits were estimated using a halokinetic potash-bearing salt descriptive model (appendix B), and were combined with the grade and tonnage model (table 1-4) to estimate tonnage distribution for undiscovered potash in halokinetic deposits for the Gissar tract. A number of factors (see chapter 2) suggest that the median of this estimate significantly underestimates undiscovered resources in the Gissar tract.

Undiscovered potash resources of the Gissar tract were also estimated using the AGE method. The tract boundary was interpolated from widely-dispersed no-potash-present drill-hole data, reports, and enclosed potash thicknesses of 1 m or greater as estimated from limited drill hole and point location data; this allowed in-place volume calculations to be made. A distribution of reported grades in the CASB, from potash intervals 1 m and greater in thickness, was randomly sampled and used to compute density and tonnage. This in-place tonnage was modified to account for unmineralized areas and postdepositional potash losses caused by erosion and other processes. The estimate for stratabound deposits was significantly larger than the estimate for halokinetic deposits, but it may be an overestimate (see chapter 2). The best estimate of undiscovered resources is probably between 1 and 16 Bt of potash as K_2O (table 1-3).

An estimate of undiscovered potash was also made for the Amu Darya tract. The stratabound potash-bearing salt model was determined to be the best fit for the tract and therefore the AGE method was used to produce the estimate (table 1-3). Within the Afghan-Tajik tract, where Jurassic evaporites are commonly deeply buried, there is potential for undiscovered potash in halokinetic deposits upraised by diapirs and block tectonics. Data for this tract were not adequate for a quantitative assessment; therefore, the assessment included delineation of the area within which potash could occur and a qualitative evaluation of potash potential.

Summary

In 2013 (the most recent year for which complete information is available), world potash production was 34.5 million metric tons (Mt) of K2O-equivalent. Canada was the leading producer of potash (10.1 Mt K2O-equivalent in 2013), followed by Russia, China, Belarus, Germany, Israel, Jordan, and Chile (Jasinski, 2015). Of the 12 known potash-producing countries in 2013, 8 produced 1 Mt or more; production in the United States was slightly less than 1 Mt, and production in Brazil, Spain, and the United Kingdom was less than 500,000 metric tons each (Jasinski, 2015).

Known potash resources in the CASB consist of 8.020 billion metric tons (Bt) of mineralized potash rock containing 1.63 Bt of K_2O, all in the Gissar tract. Our assessment indicates that between 39 and 54 Bt of K_2O exists in undiscovered deposits within the Gissar and Amu Darya tracts together (table 1-3). There is only one previous estimate of total resources for the CASB (or a portion thereof)—Zhang and others (2005) estimated a total resource of 20 Bt for the Gaurdak potash basin, but it is not clear how they defined area boundaries or exactly what they meant by “potash resources.” Based on incomplete table data, it is likely that Zhang and others (2005) estimated 20 Bt of ore in the explored potash area of the central Gissar Range. Our estimate of undiscovered potash for that area is larger and is for a defined area that includes the Gissar Range and the area between the uplifted range and the Repetek Fault to the south-southwest.

Chapter 2. Potash-Bearing Salt Assessment for the Gissar Tract (142mxK0005a)—Turkmenistan, Uzbekistan, Tajikistan, and Afghanistan

By Jeff Wynn,[1] Greta J. Orris,[2] Pamela Dunlap,[2] and Mark D. Cocker,[2] with contributions from Bruce R. Lipin,[3] Robert J. Ryan,[4] Mirosław Słowakiewicz,[5] Gregory T. Spanski,[6] and Chao Yang[7]

Introduction

A quantitative assessment of undiscovered potash resources was conducted for the Gissar tract of the Central Asia Salt Basin (CASB). This tract encompasses the Gissar Range, and extends northeast to southwest across the Uzbekistan-Turkmenistan border, with small areas in Tajikistan and Afghanistan (fig. 2-1). This tract contains the only known potash reserves and resources of the CASB, including the only operating potash mine at Tyubegatan. The Upper Jurassic (Tithonian) potash and host salt have been identified throughout the tract in a variety of salt structures and, in the areas of the Karabil and Karlyuk deposits, in undeformed pockets of stratabound potash-bearing salt. Documented potash reserves and resources in this tract are shared among 10 deposits and there are 18 additional known occurrences.

Potash deposits and occurrences within the Gissar tract are a mix of halokinetic and stratabound mineralization, that is, the area is probably transitional between the two end members. Because of this mix of mineralization styles, this study estimated undiscovered resources using two methods—one suited for halokinetic potash deposits and the other to stratabound potash deposits. Deposits in this tract are typically in the uplifted upper limbs of brachyanticlines and domes, where potash may be concentrated and thickened or disrupted by tectonic folding; this implies that halokinetic potash-bearing salt is the appropriate deposit type. However, the halokinetic deposit model and the three-part form of assessment of Singer and Menzie (2005, 2010) produce a mean estimate that appears to significantly underpredict undiscovered potash resources. This underprediction likely results from mineralized deposits that are transitional between stratabound and halokinetic potash-bearing salt. At least two deposits within the tract are relatively undisturbed and, in that sense, are stratabound, though they are not contiguous with any other deposits. The stratabound deposit model and the adaptive geometric estimation (AGE) method were used to estimate the in-place potash resource assuming the potash is continuous and not significantly impacted by halokinesis. Because the deposits in the tract are transitional between the deposit types, the undiscovered resource size probably lies between the halokinetic and stratabound estimates. Results of both estimates are presented in table 2-1.

Location

The Gissar tract encompasses the Gissar Range and its downdip extensions, and lies between the Amu Darya tract to the west (chapter 3) and the Afghan-Tajik tract to the east (chapter 4). It extends north to the flanks of the Kyzyl Kum Plateau, and to the south beyond the Amu Darya River into southeastern Turkmenistan and northern Afghanistan.

Basin History

Although the Gissar tract straddles the boundary between the modern Amu Darya and Afghan-Tajik Basins, the original Jurassic salt basin was continuous for more than 200 km east and west of this tract. Structural events that postdate the salt deposition, including Miocene uplift of the Gissar Range, differentiated the two basins. The Amu Darya tract, to the west of the Gissar Range, is relatively undeformed compared to the Afghan-Tajik tract to the east, which is highly deformed and deeply buried by east-west compression that has been ongoing since at least the Miocene. The Gissar tract is distinct from neighboring tracts because Miocene uplift has raised potash-bearing horizons to shallow levels where they are more easily discovered.

---

[1]U.S. Geological Survey, Vancouver, Washington, United States.

[2]U.S. Geological Survey, Tucson, Arizona, United States.

[3]U.S. Geological Survey, Reston, Virginia, United States.

[4]Nova Scotia Department of Natural Resources, Nova Scotia, Canada.

[5]Polish Geological Institute–National Research Institute, Warsaw, Poland.

[6]U.S. Geological Survey, Denver, Colorado, United States.

[7]Saskatchewan Energy and Resources, Regina, Saskatchewan, Canada.

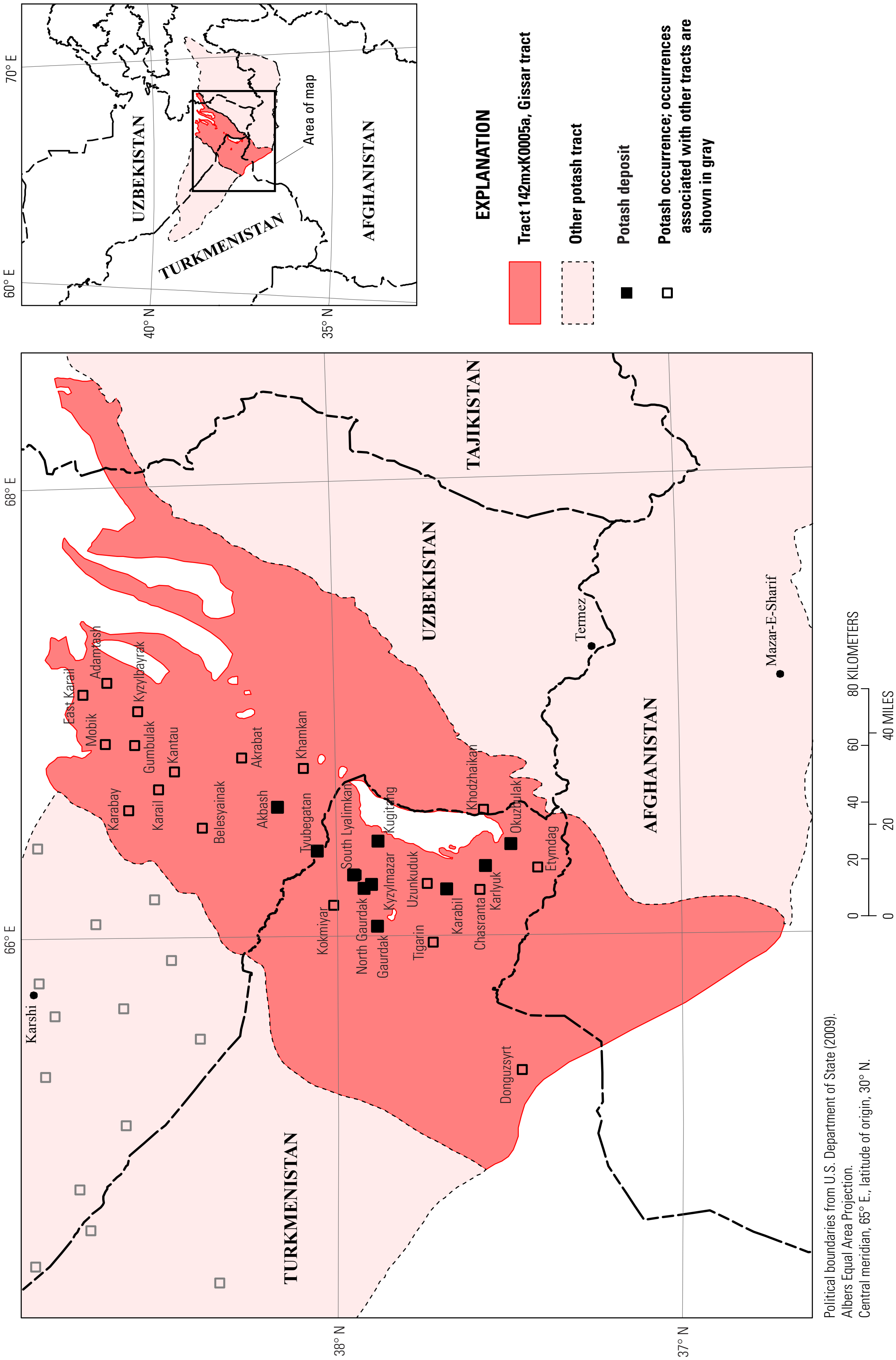

Political boundaries from U.S. Department of State (2009).
Albers Equal Area Projection.
Central meridian, 65° E., latitude of origin, 30° N.

Figure 2-1. Map showing location of the Gissar tract (142mxK0005a), Turkmenistan, Uzbekistan, Tajikistan, and Afghanistan, and known potash deposits and occurrences.

Table 2-1. Summary of potash resource assessment results for the Gissar tract, Turkmenistan, Uzbekistan, Tajikistan, and Afghanistan.

[km, kilometer; km^2, square kilometer; Bt, billion metric tons; —, no data]

Date of assessment	Assessment method	Deposit type	Assessment depth (km)	Tract area (km^2)	Known potash resource (Bt K_2O)	Mean estimate of undiscovered potash resources (Bt K_2O)	Median estimate of undiscovered potash resources (Bt K_2O)	Consensus (Bt K_2O)
May 2009	Three-part estimation	Halokinetic	3	26,669	1.63	0.47	0.39	1 to 16
June 2010	Adaptive geometric estimation (AGE)	Stratabound	3	26,669	1.63	27.9	25.3	—

Salt

The Late Jurassic basin of the CASB includes the five major stratigraphic units of the Gaurdak Formation (figs. 2-2*A*, 2-2*B*), of which the second and fourth units host potash (Gavril'cheva, 1981). In the Gissar tract, Jurassic salt is present in brachyanticlines and other salt structures resulting from Miocene uplift of the Gissar Range. Some salt and potash in the southeastern part of this tract has been attributed to the Lower Cretaceous Almurad Formation (Rayevskiy and Fiveg, 1973). Because of extremely limited and conflicting information on salt ages, the assessment team could not distinguish Cretaceous salt from Jurassic salt. Therefore, for the purposes of this assessment, Upper Jurassic and any possible Lower Cretaceous salt are assumed to result from the same evaporite event.

Assessment

The goal of the U.S. Geological Survey (USGS) potash assessment in the CASB was to estimate undiscovered potash as potassium oxide (K_2O) resources. This section describes the steps used to estimate undiscovered potash within the Gissar tract, including data collection and analysis, followed by identification of appropriate deposit model(s). The geology of the area is complex and poorly understood. Postmineralization tectonics and subsequent salt movement have shaped deposit features so that some fit the halokinetic potash-bearing salt deposit model and others are a better fit with the stratabound potash-bearing salt deposit model (appendixes A and B). Many deposits and occurrences within this tract are no longer flat-lying and continuous over large distances. A few deposits, such as Karabil, appear to be flat-lying and continuous within small areas that have been protected from postmineralization processes that disturbed other deposits and occurrences. The assessment team considered splitting this tract, but decided to keep the tract intact because (1) the entire tract shares a common depositional and postmineralization geologic history; (2) the southwestern part of the tract, largely covered and not well explored, is likely to contain the same mix of deposit characteristics at the same scales; and (3) subdividing would result in small (single mine and deposit-specific) areas relative to the assessment scale of 1:1,000,000.

Delineation of the Permissive Tract

A starting point for defining the Gissar tract was the Gissar Range, where all known deposits are found, along with potash-prospective zones 1 and II of Fedin (1981) and Vysotskiy and others (1988, their figure 73). The tract boundary was refined by excluding all geologic units older than Middle-Upper Jurassic (Gaurdak Formation) in the vicinity of the Gissar Range on the Central Asia Geologic Map (Seltmann and others, 2005). Next, the tract boundary was extended southwestward beyond the Upper Jurassic evaporites to follow the edge of the Beshkent Depression until it intersected the Repetek Fault Zone (fig. 2-3) and the Donguzsyrt occurrence (see fig. 2-1). The tract was further extended 3 km past the easternmost mapped Jurassic rock outcrops to include covered parts of Gissar Range, though some of the potash in the area may lie below the 3-km assessment depth limit. The tract was extended to the north until pre-Jurassic rocks were encountered, and then extended westward 3 km downdip below post-Jurassic rocks mapped at the surface, in order to enclose all potential potash-hosting geologic units in the tract. Finally, tract boundaries were modified where necessary to include all appropriate deposits and occurrences.

Definition of Resources

Known deposits (table 2-2) were considered to be those with documented reserves or resources in categories A, B, C1, or C2 of the Russian classification system (see Henley, 2004).

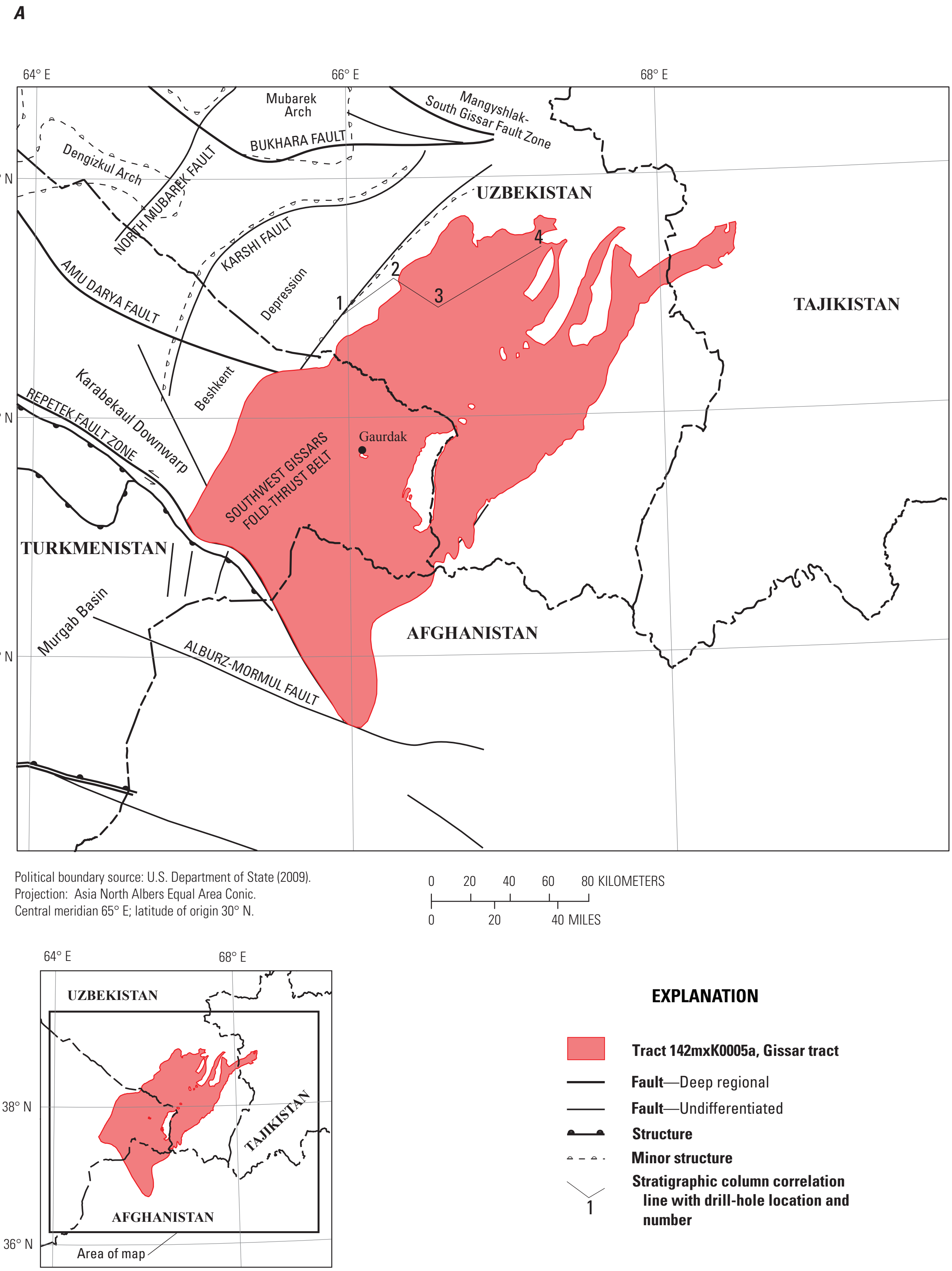

Figure 2-2. Map showing location of the Gissar tract (142mxK0005a), four drill holes,and corresponding stratigraphic columns. *A*, structural features influencing the Gissar tract (adapted from Zharkov and others, 1982a, and Blackbourn, 2008) and location of four drill holes. *B*, section of the Upper Jurassic Gaurdak Formation (Zharkov and others, 1982a). Drill holes 1 and 2 approximately mark eastern edge of Beshkent Depression. No potash was reported in these two drill holes by Zharkov and others (1982a), but it was reported to be present by Gavril'cheva (1981).

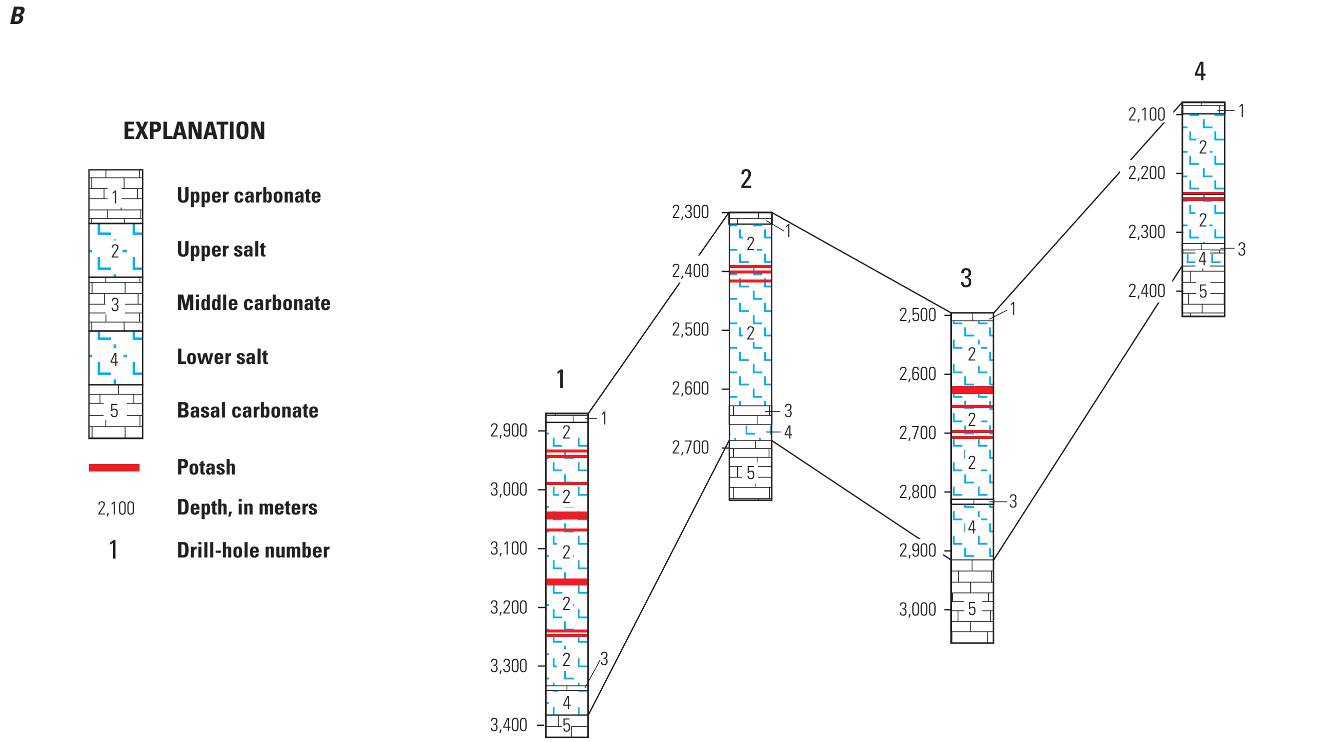

Figure 2-2.—Continued

Table 2-2. Known deposits of potash within the Gissar tract, Turkmenistan, Uzbekistan, Tajikistan, and Afghanistan.

[Mt, million metric tons; reserve and resource categories A, B, and C are described in the text]

Name	Latitude	Longitude	Reserves, resources (Mt ore rock, in place)	Grade (percent K_2O)	Contained K_2O (Mt)	References
Akbash	38.417	66.55	C2=266.5	12	31.98	Fedin (1981)
Gaurdak	37.588	66.346	A+B+C1=106.3	18.9	20.09	Fedin (1981)
Karabil	37.820	66.071	C2=3,500	21.65	757.75	Rayevskiy and Fiveg (1973); Fedin (1981)
Karlyuk	37.659	66.234	A+B+C1=2,015; C2=1,175	19.5	622.05	Levine and Wallace (2001); Fedin (1981)
Kugitang	37.844	66.393	C2=144	9.8–15.9	18.5	Rayevskiy and Fiveg (1973); Fedin (1981)
Kyzylmazar	38.54	66.883	A+B+C1=1.7; C2=2.2	9.9	0.39	Rayevskiy and Fiveg (1973); Fedin (1981)
North Gaurdak	37.920	66.209	C2=3.8	19.5	0.74	Rayevskiy and Fiveg (1973); Fedin (1981)
Okuzbulak	37.930	66.379	A+B+C1=96	18.3	17.57	Rayevskiy and Fiveg (1973); Fedin (1981)
South Lyalimkan	38.157	66.515	C2=24	19.9	4.78	Rayevskiy and Fiveg (1973); Fedin (1981)
Tyubegatan	37.435	66.340	A+B+C1=400.2; C2=285.6	22.4	153.62	Ashurmatov (2006); Uzbekistan Daily (2006); Fedin (1981)
Total			8,020.30		1,627.47	

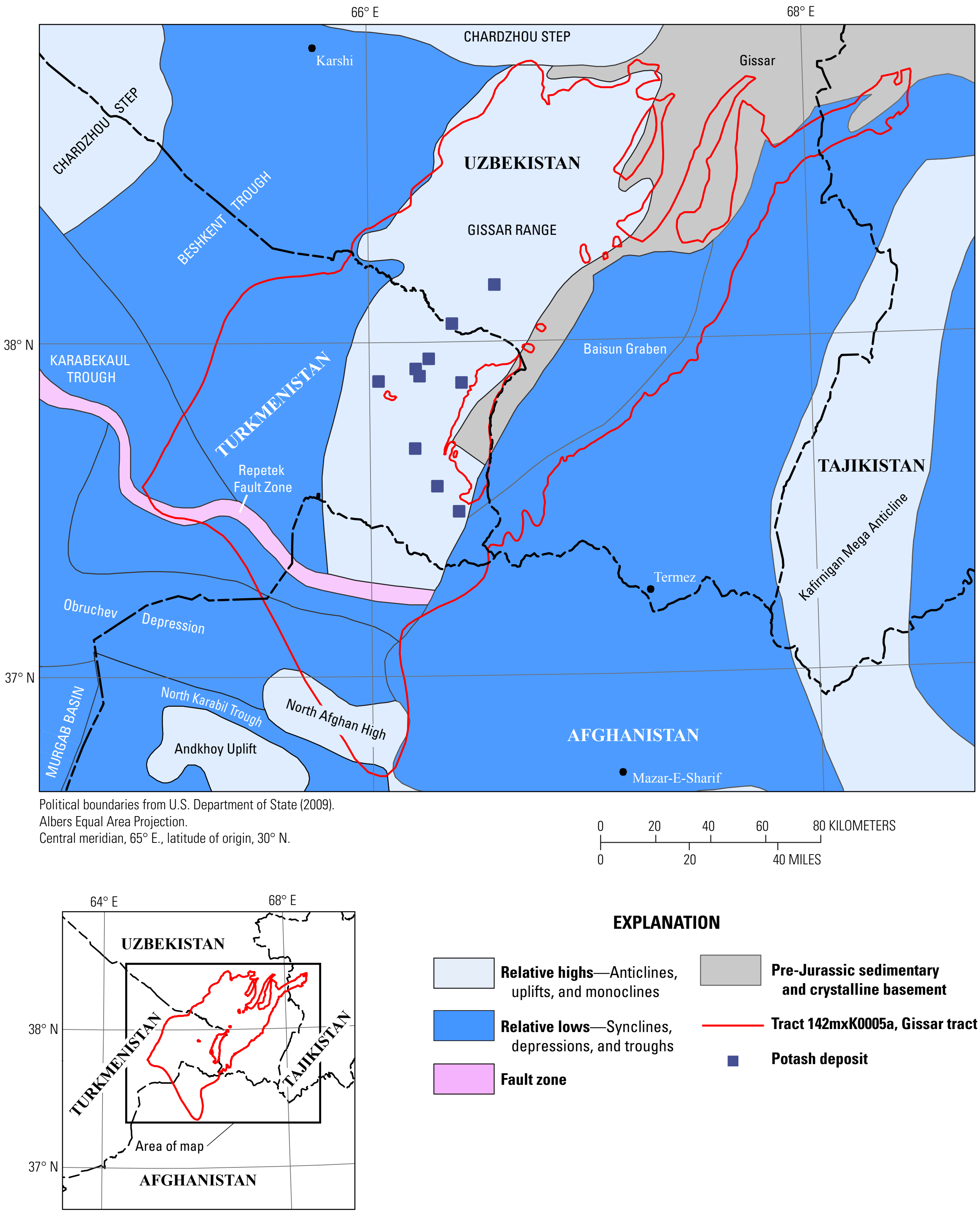

Figure 2-3. Map showing structural provinces in and near the Gissar tract (142mxK0005a), Turkmenistan, Uzbekistan, Tajikistan, and Afghanistan, based on Steinshouer and others (2006). Note that structural uplifts and downwarps (depressions, troughs) are not necessarily reflected in modern topography.

The Russian mineral resource categorization system divides mineral concentrations into seven categories in three major groups: fully explored reserves or resources (A, B, C1), evaluated reserves or resources (C2), and prognostic resources (P1, P2, P3). Category A is only distinguished from B by the amount of detail known about reserves (category B is based on less information), but both are roughly equivalent to the McKelvey classification of measured resources or proven and probable reserves. Reserves C1 and C2 are estimated with lower density gridding and trenching; C1 lies between B and C2, where C2 is estimated on the coarsest exploration grid. In the McKelvey classification, the Russian C1 and C2 may be equivalent to measured, indicated, and (or) inferred resources, or may be reserves. In the absence of specific definitions in the source literature, reserve and resource figures were assumed by the assessment team to represent in-place numbers for the purposes of the stratabound resource calculations.

Discovered Resources

All known potash deposits in the CASB (fig. 2-1, table 2-2) are within the Gissar tract. Ten potash deposits are recognized in this tract, and all deposits with reserves and resources lie within the Upper Jurassic (Oxfordian) Gaurdak Formation (fig. 2-4).

Summaries of known deposits are presented in the following report sections. Readers should note that many deposits and occurrences overlie locally recognized structures with the same names as the deposits. These structures are mentioned in deposit reports, but the extent of their areal coverages are not shown on maps. Mined potash-salt horizons are often not identified in the literature and are likely obscured by deformation. In the following report sections, any potash layers discussed are local to each particular deposit and do not correlate to the broader-scale numbering of Gavril'cheva (1981).

Akbash

The Akbash deposit (fig. 2-1, table 2-2) in Uzbekistan is approximately 20 km north of the Tyubegatan deposit in the central part of the Gissar tract. Two sylvinite (sylvite+halite) layers that are traceable from the Tyubegatan deposit were identified at this site during exploration drilling at depths ranging from 150 to 500 m (Sedletskiy, 1969; Rayevskiy and Fiveg, 1973). The upper potash layer is 3–3.5 m thick and contains 11.5–16.5 percent K_2O; the lower layer is 2–11.4 m thick and contains 11.3–12.1 percent K_2O (Rayevskiy and Fiveg, 1973; Fedin, 1981).

Gaurdak

The Gaurdak deposit (fig. 2-1, table 2-2) in Turkmenistan is approximately 8 km north of the town of Gaurdak, in the central part of the Gissar tract. Potash mineralization is found on the northwestern flank of the northeastern part of the Gaurdak brachyanticline, which dips variably at angles ranging from 6° to 30°. Paleozoic granite and metamorphic rocks comprise the core of this brachyanticline at a depth of 926 m. The otherwise continuous Upper Jurassic and Lower Cretaceous sedimentary rocks on the northwest limb of the Gaurdak brachyanticline are abruptly displaced by varying distances that may be related to deformation of underlying Paleozoic rocks during brachyanticline formation.

In the Gaurdak area, the Gaurdak evaporite salt deposits can be divided into a lower rock salt, which does not contain potash, and a potash-bearing sequence. A transitional horizon between the units contains lenses and uneven impregnations of potash minerals. Two sylvinite lenses lie in the transitional horizon; one is 0.5 m thick, the other 1.5 m thick, with K_2O contents of 18.4 percent and 17.6–18.0 percent, respectively.

The potash-bearing sequence of the Gaurdak Formation contains three persistent potash horizons with as many as seven potash beds separated by rock salt. Locally, these are called the “Lower II,” “Lower III,” and “Blue” horizons. The Lower II horizon consists of two sylvite (sylvite-carnallite in the south) layers, 2 and 3 m thick (total average thickness of 4 m), that range from 9.6 to 26.8 percent K_2O (Sedletskiy, 1969; Rayevskiy and Fiveg, 1973). The Lower III horizon lies higher in the stratigraphy, has a lower average K_2O content (13.4–17 percent K_2O), and contains less than 3 percent magnesium chloride (as carnallite). The Blue horizon is separated from the Lower III by 30–40 m of rock salt. This white and pink sylvite-bearing bed contains 13.7–24.5 percent K_2O and is 1.5–5 m thick (Sedletskiy, 1969). Garrett (1996) reported considerable leaching of salts and gradational mineralization from north to south in the Gaurdak deposit—from carnallitite (carnallite+halite), to carnallitite-sylvinite, to sylvinite, to halite.

Karabil

The Karabil deposit (fig. 2-1, table 2-2) in Turkmenistan is southeast of the town of Gaurdak in the central part of the Gissar tract. The deposit is on a brachyanticline, the northern and southern boundaries of which are cut by faults. The primary structural features of the deposit are the same as those at the Karlyuk deposit, though the potash-bearing stratum is somewhat thinner and deeper (Sedletskiy, 1969). Of ten potash layers, eight are relatively continuous sylvinite potash beds that contain a range of 16.1–27.2 percent K_2O and an average 1 percent magnesium chloride (Rayevskiy and Fiveg, 1973). Potash layer 4 is the most widespread with the most consistent thickness, but has a higher level of insoluble material than the other layers of interest. The central and western parts of this deposit are least disturbed by faulting and unfavorable hydrogeologic conditions (Rayevskiy and Fiveg, 1973).

Karlyuk

The Karlyuk deposit (fig. 2-1, table 2-2), discovered in the mid-1960s, is one of the largest in Turkmenistan. More than 100 drill holes were reported to have penetrated the potash at this deposit (Rayevskiy and Fiveg, 1973). In 1983, a large solution mining pilot plant was operated at this site (Garrett, 1996), but was soon discontinued.

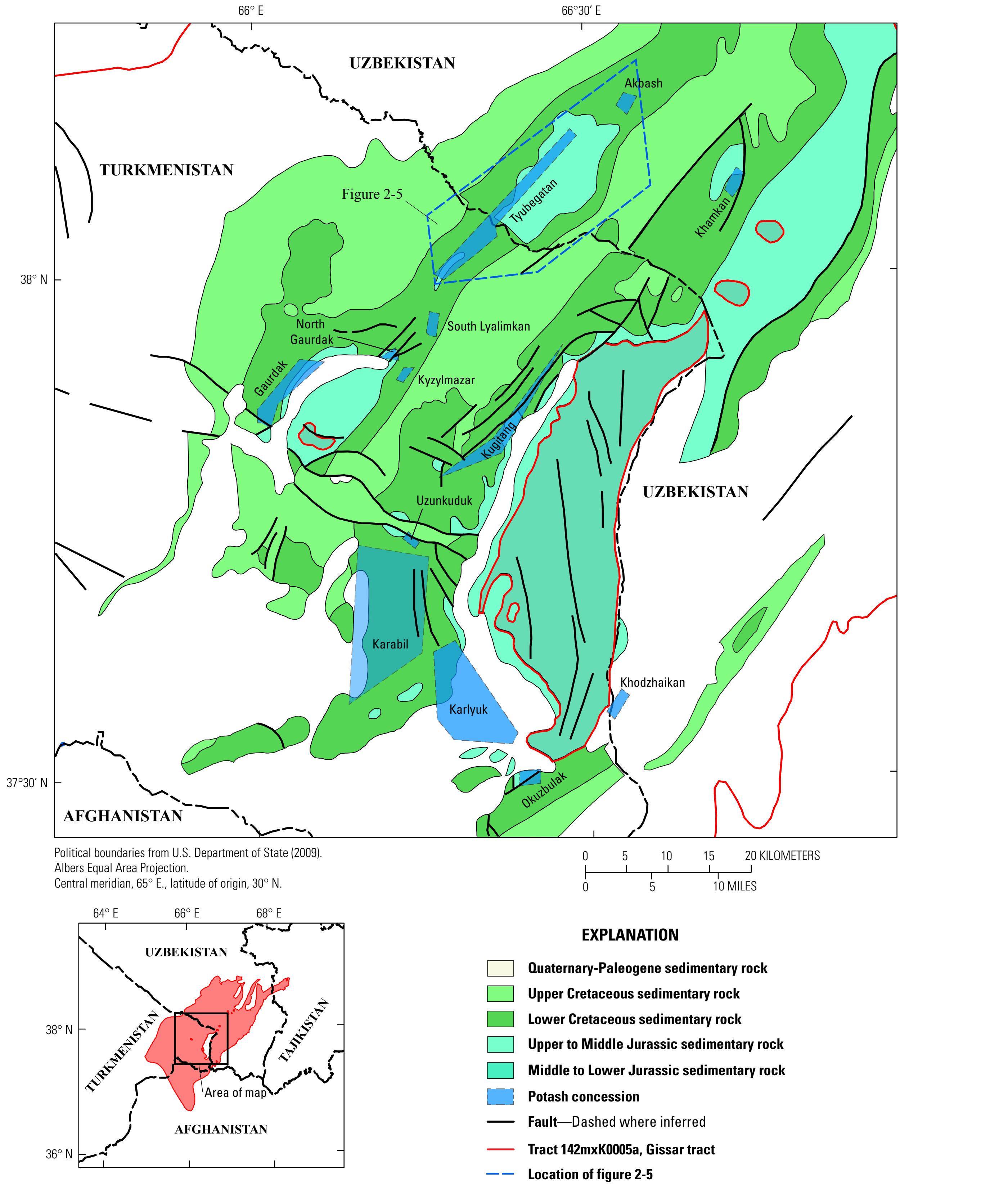

Figure 2-4. Map showing geology and concession areas in the central part of the Gissar tract (142mxK0005a), Turkmenistan and Uzbekistan. Middle to Lower Jurassic rocks are older than potash-bearing salt of the Gaurdak Formation and have been removed from the tract because they are not permissive for this deposit type. These areas are represented by the "anomalies" parameter in the adaptive geometric estimation process. This map is an interpolation of more detailed maps by Vysotskiy and others (1988, fig. 4) and Mirzakhanov (1989) with 1:1,500,000-scale geology of Seltmann and others (2005) mineral deposits map of central Asia. Blue, dashed line outlines map area shown in figure 2-5.

The deposit contains three main potash horizons with as many as 16 beds, lenses, and intercalations of potash salts with rock salt at depths of 200–1,200 m over an area of 75 km^2 (Sedletskiy, 1969). Three of the potash beds (locally labeled ninth, eighth, and seventh, counting up) are in the lower potash horizon of Gavril'cheva and Pashaev (1993) and contain most of the reserves. The mean grade of this horizon is more than 18 percent K_2O, but carnallite is locally abundant. Carnallite-free sylvite makes up the seventh potash bed and is considered secondary in origin (Sedletskiy, 1969).

The overlying sixth potash layer is composed of carnallite-bearing sylvite and averages more than 5 m thick. The fourth and fifth beds contain sylvite, and have grades of 14–15.5 percent K_2O, and a combined thickness of 1.5–43 m (Sedletskiy, 1969).

The upper potash-bearing horizon is largely composed of individual thin lenses and intercalations of potash salts and is only persistent in the central part of the deposit. The first, second, and third potash beds are dominantly low-grade sylvinite (Sedletskiy, 1969).

Carnallite beds lie at the top of both the lower and upper potash horizons; they are locally referred to as the "middle carnallite" and "upper carnallite". These beds contain 6–28 percent magnesium chloride. The middle carnallite is missing in some parts of the Karlyuk deposit (Sedletskiy, 1969; Rayevskiy and Fiveg, 1973).

Kugitang

The Kugitang deposit in Turkmenistan (fig. 2-1, table 2-2), is approximately 20 km south-southeast of the Tyubegatan deposit, in the central part of the Gissar tract. Six potash beds occur on the west limb of the Kugitang structure at depths of 500–550 m, but only three of these beds are persistent (Sedletskiy, 1969). The lowest bed is 0.7–2.2 m thick and consists of red sylvite with minor carnallite; the grade varies from 10.7 to 27.1 percent K_2O (Sedletskiy, 1969; Rayevskiy and Fiveg, 1973).

The middle potash horizon consists of two potash seams separated by a thin intercalation of gray to pink rock salt (Rayevskiy and Fiveg, 1973). Like the lower horizon, the middle horizon consists of red sylvite with scattered orange carnallite. The thickness and grade of this horizon are highly variable and potash thickness rarely exceeds 3 m. The average grade ranges from 9.8 to 15.9 percent K_2O (Rayevskiy and Fiveg, 1973). In places, the carnallite content is significant with some samples containing as much as 9.6 percent magnesium chloride. In these areas, the clay content may exceed 5 percent (Sedletskiy, 1969).

The upper potash horizon comprises one or two white to pink sylvinite layers intercalated with rock salt. Each potash layer is commonly 1 m thick or less, though in one drill hole, at least one layer exceeded a thickness of 3 m. The average potash grade is reported to range from 7.9 to 12.2 percent K_2O, but rarely exceeds 9 percent (Sedletskiy, 1969; Rayevskiy and Fiveg, 1973).

Kyzylmazar

The Kyzylmazar deposit (fig. 2-1, table 2-2) in Turkmenistan is 20 km north of the town of Gaurdak and less than 2 km south of the North Gaurdak deposit, in the central part of the Gissar tract. An unspecified number of sylvinite layers in the Gaurdak Formation lie at depths of 85–250 m (Rayevskiy and Fiveg, 1973) at the north end of the Gaurdak brachyanticline (Sedletskiy, 1969). The potash-bearing sequence is 5–50 m thick and contains an average of 9.9 percent K_2O (Rayevskiy and Fiveg, 1973; Fedin, 1981).

North Gaurdak

The North Gaurdak deposit (fig. 2-1, table 2-2) is in Turkmenistan, approximately 5 km north of the northernmost boundary of the Gaurdak deposit, in the central part of the Gissar tract. The area is a fault-bounded block of gently dipping rocks on the northwestern flank of a brachyanticline (Sedletskiy, 1969), the northern extension of the Gaurdak structure. One sylvinite layer (locally called "Lower II") has been identified at this deposit. The potash layer has an average thickness of 3.3 m and contains an average of 19.5 percent K_2O (Rayevskiy and Sedletskiy, 1969; Fiveg, 1973; Fedin, 1981).

Okuzbulak

The Okuzbulak deposit (fig. 2-1, table 2-2) in Turkmenistan is in the southern part of the Gissar tract about 20 km northwest of the point where Afghanistan, Turkmenistan, and Uzbekistan meet. The first discovery of potassium salts in the region was made here in the early 1930s (Rayevskiy and Fiveg, 1973). The deposit is on a brachyanticline which is overturned to the north, and is part of the southeastern limb of the larger Kugitang structure. The northern limb of the brachyanticline dips at 50–70°, the southern limb at 25°.

Initial reports on potash age, and most of the available reports published since the early 1970s, classify the potash reserves and resources in this region as Jurassic in age and belonging to the Gaurdak Formation (Fedin, 1981; British Sulphur Corporation, 1984; Schultz and others, 2000). Potash is also reported to occur in the Lower Cretaceous Almurad Formation in some parts of this site (Rayevskiy and Fiveg, 1973).

The British Sulphur Corporation (1979, 1984) reports that two sylvinite beds, 12 m apart, locally occur at the top of a gypsiferous section at Okuzbulak and are latest Jurassic (Gaurdak) in age. The lower bed is 3.5 m thick and contains 12.5–15.8 percent K_2O; the upper bed is 2.5 m thick and contains 8–11 percent K_2O. Rayevskiy and Fiveg (1973) also report two sylvinite beds. In this case, the lower horizon is reported to average 4 m thick and contain an average of 9.9 percent K_2O; the upper bed is reported to average 2.5 m thick with an average grade of 13.4 percent K_2O.

South Lyalimkan

The South Lyalimkan deposit (fig. 2-1, table 2-2) in Turkmenistan is southwest of the Tyubegatan deposit in the central part of the Gissar tract. The two deposits are separated by a salt plug that is exposed in a diapiric structure (Sedletskiy, 1969). Elevated potassium contents were noted at this site as early as the mid-1930s and later exploratory holes identified a bed of sylvinite 3.9–6.9 m thick (average 5.6 m in the drill core) containing 11.5–29.6 percent K_2O (Sedletskiy, 1969; Rayevskiy and Fiveg, 1973).

Tyubegatan

The Tyubegatan deposit (fig. 2-1, table 2-2) is in the central part of the Gissar tract and straddles the Turkmenistan-Uzbekistan border. The deposit is on the gently dipping (15–20°) northwestern limb of the Tyubegatan brachyanticline (fig. 2-5), which is approximately 30 km long and as much as 12–15 km wide. The southeastern limb of the brachyanticline is steeply dipping (as much as 50°). Ancillary structures such as the Lyalimkan dome (fig. 2-5) and the Akbash salt dome (fig. 2-5) are on or adjacent to the main structure (Rayevskiy and Fiveg, 1973). Most of the following discussion on the deposit has been extracted from Rayevskiy and Fiveg (1973).

Salt and potash at this site are considered part of the Kimmeridgian-Tithonian (Upper Jurassic) Gaurdak Formation. The potash-bearing material is underlain by pink rock salt with varicolored lenses of white and gray salt, veins of anhydrite, and rare inclusions of red argillaceous-carbonate material. The base of the potash-rich horizon(s) is composed of carnallite and impure halite that grades up-section from less than 0.6 percent K_2O to as much as 29.3 percent K_2O. Above the carnallite base, three sylvinite layers are separated by rock salt. The deposit's lower sylvinite layer is 2–20 m thick and contains less than 5.5 percent K_2O on average. The overlying "Tyubegatan" sylvinite layer is 0.8–10.6 m thick and comprises pink, red, and white sylvite and halite with thin veins of carnallite and anhydrite; this is the most continuous of the three layers reported by Sedletskiy (1969). The potash content of this layer ranges from 11.2 to 30.9 percent K_2O and was considered by Rayevskiy and Fiveg (1973) and Sedletskiy (1969) to be the main unit of economic interest. The upper sylvinite layer at Tyubegatan is rock salt with less than 2.5 percent K_2O as sylvite. The upper sylvinite is in turn overlain by the confusingly-named "intermediate salt unit." This intermediate salt contains less than 9.2 percent K_2O in the southwestern parts of the deposit, and decreases in potash grade and overall thickness to the northeast.

The rock salt and potash horizons are missing in parts of the structure (fig. 2-5), though the extent of this unmineralized area is not clear from the Rayevskiy and Fiveg (1973) discussion.

The middle sylvinite layer of Sedletskiy (1969) was evaluated by using data from 59 drill holes across 12 profiles. Reserves were calculated by using 45 of the drill holes in an area of approximately 80 km^2. Ore averaged 5.6 m thick at depths of about 100–800 m (table 2-2). In 2006, it was announced that the Uzbekistan part of this deposit would be developed for production (Ashurmatov, 2006; Shanghai Cooperation Organization for Economic Cooperation, 2006). In December, 2009, an unspecified amount of ore was mined from this deposit (Henley and Allington, 2010).

Mineral Occurrences

Potash prospects and occurrences in the tract were outlined by Russian geologists (Fedin, 1981; Vysotskiy and others, 1988) incidental to oil and gas exploration. The stratigraphy and structure of the potash-bearing zone were described by Russians from two-dimensional seismic data as well as from drill core and well logs. Brief descriptions in the Russian literature (Vakhabov, 1986; Popov, 1988) mention thinning and thickening of potash horizons from as little as 1 m on the edge of a typical mining concession to as much as 150 m in the core of the concession.

Eighteen potash occurrences are reported within the Gissar tract (fig. 2-1, table 2-3), all within the Upper Jurassic Gaurdak Formation (Petrov and Chistyakov, 1964; Popov, 1968; Rayevskiy and Fiveg, 1973; Sedletskiy and Fedin, 1981). Only 5 of the 18 known potash occurrences are discussed in the following section because of the extremely limited information available.

Adamtash

The Adamtash occurrence (fig. 2-1, table 2-3) is a potash-bearing structure in Uzbekistan, ~100 km northeast of the border with Turkmenistan. Potassium salt was detected using gamma-ray-log data at a depth of approximately 1,100 m (Popov, 1968). The potash occurs near the top of a rock salt horizon that exceeds 200 m in thickness (Popov, 1968).

Donguzsyrt

The Donguzsyrt occurrence (fig. 2-1, table 2-3; see also, location in fig. 3-1) in Turkmenistan is a potash-bearing salt structure expressed at the surface as a low-lying hill and is a brachyanticline in the extreme southwestern part of the Gissar tract. Although referred to as a salt dome in the literature, the salt structure and deformation of this occurrence result from folding and faulting related to the tectonism of the Gissar Range rather than depth of burial (Kutuzov and Popov, 1976). The surface expression of this salt structure occupies an area of about 2.5 km^2 and largely comprises anhydrite and (or) gypsiferous rock. The structure and lithology of this brachyanticline (fig. 2-6) is similar to those of the deposit at Tyubegatan (fig. 2-5). An explanation of the anhydrite that lies between the potash and the top of the rock salt at Donguzsyrt was not given in the available literature.

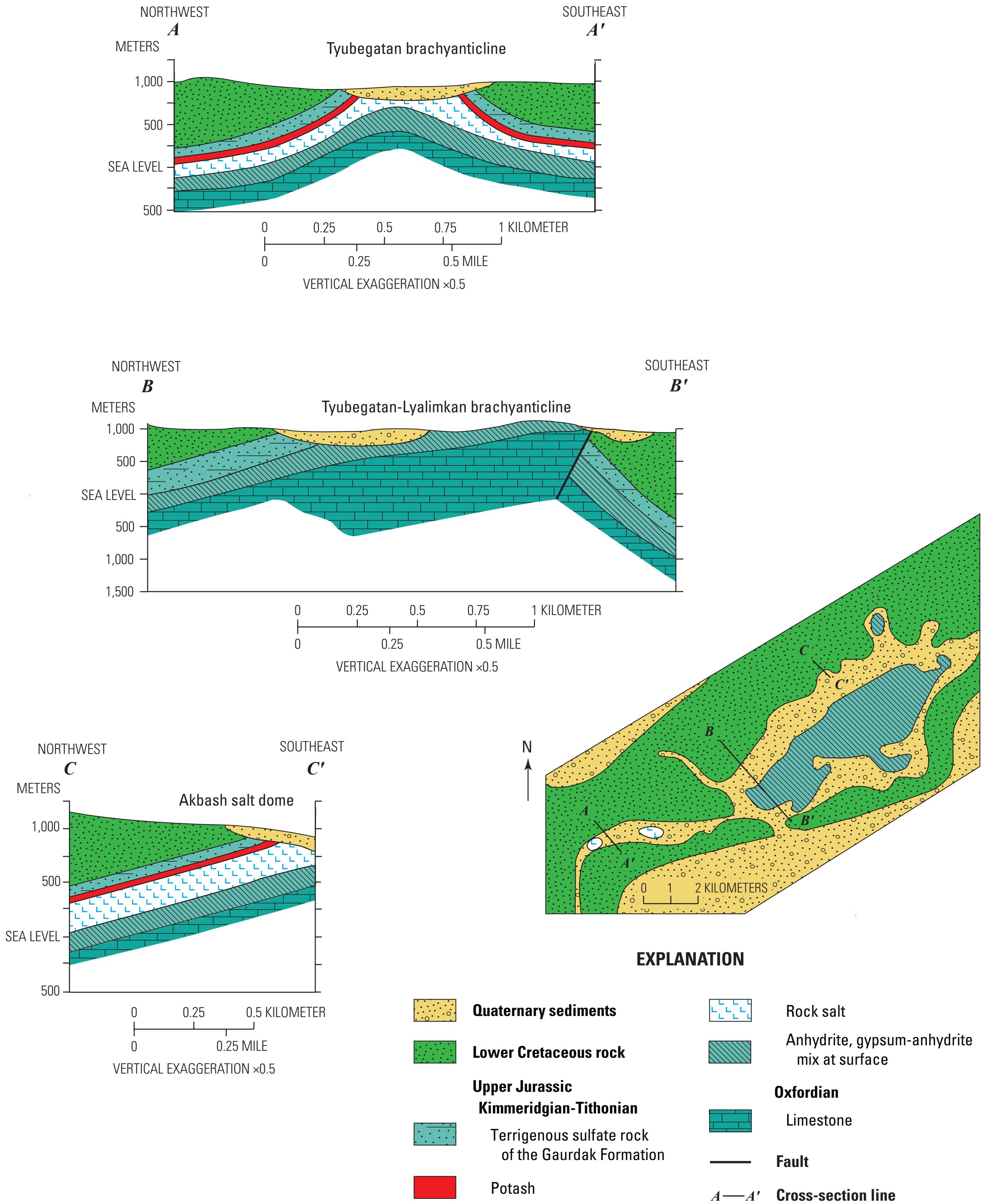

Figure 2-5. Map and cross sections showing parts of the Tyubegatan brachyanticline, the Lyalimkan area of the Tyubegatan brachyanticline, and the Akbash salt dome, Turkmenistan and Uzbekistan (modified from Rayevskiy and Fiveg, 1973). Location shown on fig. 2-4.

Table 2-3. Known occurrences of potash within the Gissar tract, Turkmenistan, Uzbekistan, Tajikistan, and Afghanistan.

[m, meter; Mt, million metric tons; —, no data]

Name	Latitude	Longitude	Comments	Reference
Adamtash	38.658	67.132	Potash detected using geophysics	Popov (1968); Sedletskiy and Fedin (1981); Vysotskiy and others (1988)
Akrabat	38.271	66.791	Potash detected using geophysics	Sedletskiy and Fedin (1981); Vysotskiy and others (1988)
Beleyainak	38.389	66.483	Potash is at depth of 2,200–2,500 m	Sedletskiy and Fedin (1981); Vysotskiy and others (1988)
Chashranta	37.586	66.197	Sylvite	Rodnov and others (2001)
Donguzsyrt	37.495	65.080	In Repetek Fault Zone, perhaps 100 Mt at depth of 300–350 m	Fedin (1981); Khudaykuliev (1986); Kutusov and Popov (1973)
East Karail	38.727	67.082	—	Sedletskiy and Fedin (1981); Vysotskiy and others (1988)
Etymdag	37.418	66.292	Could have significant potash resource	Fedin (1981)
Gumbulak	38.580	66.853	Potash detected using geophysics	Vysotskiy and others (1988)
Kantau	38.467	66.733	Potash detected using geophysics	Sedletskiy and Fedin (1981); Vysotskiy and others (1988)
Karabil	38.514	66.657	Potash detected using geophysics	Sedletskiy and Fedin (1981); Vysotskiy and others (1988)
Karabay	38.600	66.565	Potash bed is low grade	Sedletskiy and Fedin (1981); Vysotskiy and others (1988)
Khamkan	38.078	66.790	Sylvinite, carnallite lenses on Kugitangskoe brachyanticline	Rayevskiy and Fiveg (1973); Fedin (1981); Sedletskiy (1969)
Khodzhaikan	37.577	66.556	Sylvinite, carnallite lenses on Kugitangskoe brachyanticline	Garrett (1996); Osichkina (2006); Rayevskiy and Fiveg (1973)
Kokmiyar	38.010	66.136	—	Fedin (1981)
Kyzylbayrak	38.570	67.005	Potash detected using geophysics	Vysotskiy and others (1988)
Mobik	38.665	66.862	Potash detected using geophysics	Vysotskiy and others (1988)
Tigarin	37.723	65.970	Promising salt structure with potash at about 1,200 m depth	Fedin (1981)
Uzunkuduk	40.572	67.147	Associated with salt diapir of Malikokoy syncline	Rayevskiy and Fiveg (1973); Popov (1968)

Mineralized rock at Donguzsyrt consists of two potash layers that have poorly constrained thicknesses and grades resulting from poor preservation of the drill core (Kutuzov and Popov, 1976). Potash was identified at depths of 356 m to almost 600 m in the few documented drill holes. Fedin (1981) estimated that 100 million metric tons of so-called “potash salts” could be present in the brachyanticline. A more definitive estimation would require additional drilling and geologic information.

Khamkan

The Khamkan occurrence (fig. 2-1, table 2-3) in Uzbekistan is approximately 17 km north-northeast of the Turkmenistan-Uzbekistan border in the central part of the Gissar tract. Two potash layers have been identified on an anticline on the western limb of the Kugitang structure. Sylvite occurs in the upper part of a rock salt unit more than 200 m thick (Popov, 1968). One layer consists of sylvinite that is reported to be 3.5 thick and contains 15.9 percent K_2O. The second potash layer consists of approximately 1.5 m of carnallitite for which no K_2O grade is reported; however, the bed contains more than 10 percent magnesium chloride (Sedletskiy, 1969; Rayevskiy and Fiveg, 1973; Fedin, 1981).

Khodzhaikan

The Khodzhaikan occurrence (fig. 2-1, table 2-3) is in extreme southeastern Uzbekistan, approximately 1 km from the Turkmenistan border in the south-central part of the Gissar tract. Three potash layers occur at depths of less than 403 m on the southeastern limb of the Kugitang brachyanticline in a rock salt unit that is locally as much as 200 m thick. The thicknesses of the three potash-bearing layers were 3.5, 20, and 19.2 m in a single drill hole; grades were 7.5–18.6 percent K_2O (Rayevskiy and Fiveg, 1973). Rayevskiy and Fiveg assigned these potash-bearing layers to the Lower Cretaceous Almurad Formation on the basis of red-colored sedimentary rocks of assumed Neocomian age below the salt.

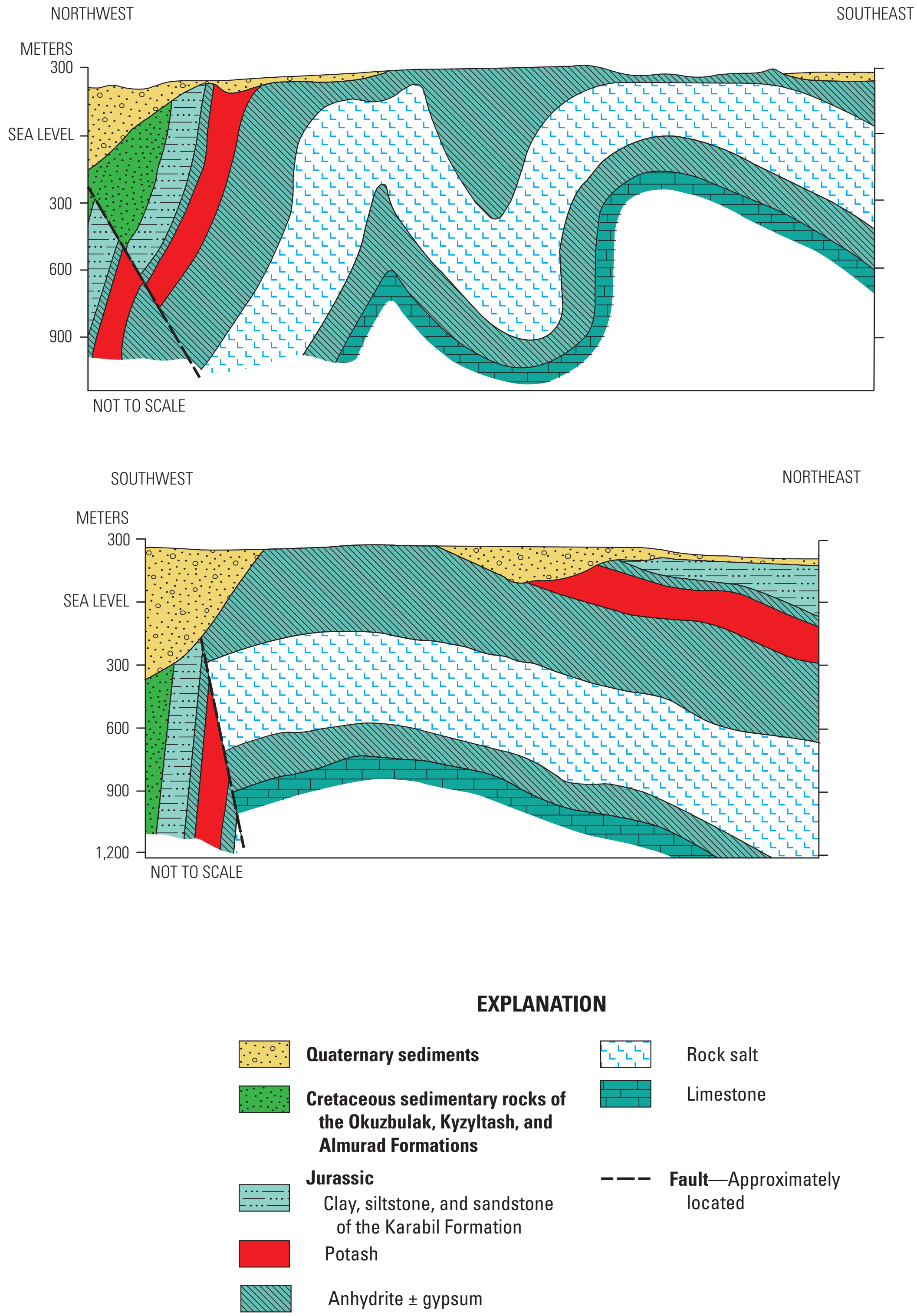

Figure 2-6. Cross sections of the Donguzsyrt potash-bearing salt structure, Turkmenistan (after Kutusov and Popov, 1976). Location coincides with the Donguzsyrt occurrence, shown in fig. 2-1. Horizontal scale is estimated.

Uzunkuduk

The Uzunkuduk occurrence (fig. 2-1, table 2-3) in Turkmenistan is approximately 20 km southeast of the town of Gaurdak in the central part of the Gissar tract. Potash mineralization is in a salt diapir in the Uzunkuduk Fault Zone. The diapir is 200–300 m wide and more than 2 km long (Popov, 1968). Potash was identified at depths of 215.8–250 m and consists of approximately 2 m of sylvinite and (or) carnallitite-sylvinite (Rayevskiy and Fiveg, 1973). No grades are reported for this site.

Exploration and Development History

Much of the known potash in the CASB was discovered incidentally during hydrocarbon exploration drilling, but potash exploration has occurred only in the central part of the Gissar tract. Written descriptions for individual deposits, occurrences, concessions, and structures in the Russian literature suggest that the central part of the tract is moderately to well explored.

The Tyubegatan deposit, Uzbekistan-Turkmenistan, containing a reported 400 Mt of potash reserves, was defined by drilling (Zhang and others, 2005; Ashurmatov, 2006) and the first ore was mined in December 2009 (Henley and Allington, 2010; Ansher Holding Limited, 2010). Limited production from a pilot solution mine at the Karlyuk deposit in eastern Turkmenistan occurred in 1983 (Garrett, 1996). Scattered reports suggest that the Karlyuk and Gaurdak deposits will be brought into production in the next few years. No production is reported or planned for the other known deposits.

Data Availability

Numerous reports describing the geology, geophysics, drill-hole logs, and mineral occurrences of the Gissar tract (table 2-4) are available. Many are more than 20 years old; most are published in Russian. The most useful publications in terms of data content include Baikov and Sedletskiy (2001), Fedin (1981), Rayevskiy and Fiveg (1973), Ulmishek (2004), and Vysotskiy and others (1988).

Quantitative Estimation

The Gissar tract is treated as a hybrid or transitional deposit of the end member stratabound and halokinetic potash-bearing salt deposits because the literature indicates that potash contiguity in this part of the Amu Darya Basin has been disrupted in places by salt structures and tectonics and, in some locations, is relatively undisturbed. As such, we decided it best to evaluate the tract as both stratabound and halokinetic in character.

The USGS global potash assessment recognizes two end-member subtypes of potash-bearing bedded salt—stratabound and halokinetic deposits (appendixes A and B). Stratabound deposits are extensive, flat-lying, and largely undisturbed since deposition. Halokinetic deposits have been disrupted by salt tectonics, fault movement, dissolution, or other processes that significantly changed thickness or continuity since original deposition; these deposits contain, on average, smaller tonnages than stratabound deposits.

Need for Two Estimation Approaches

Some known deposits, such as Karabil and Karlyuk, appear to be flat-lying (or at least stratabound) and have large reported reserves and resources; however, they are not as areally contiguous as most stratabound deposits. Observations that support a halokinetic deposit classification include erratic depths of mineralized rock, lack of continuity of mineralized rock over large areas of the tract, local significant thinning or thickening of potash-bearing unit(s), and highly developed halokinetic processes with increasing depth of evaporite burial in the southern part of the Gissar tract and eastward into the western boundary of the Afghan-Tajik tract. References in the Russian literature to “купола” (domes), “брахиантиклиналь” (brachyanticlines), and “линзы” (lenses) also suggest halokinesis.

Because alternate delineations of the tract did not resolve this complex, quasi-stratabound situation, except at a scale that defined targets instead of resources, and because we had no methodology for assessing a hybrid or transitional tract, we chose to estimate the undiscovered resources of the Gissar tract using two assessment methodologies. Undiscovered resources assumed to be halokinetic were assessed using the three-part form of assessment of Signer and Menzie (Singer, 1993; Singer and Menzie, 2005, 2010) and stratabound potash resources were quantitatively assessed using the Adaptive Geometric Estimation (AGE) methodology (appendix A).

Assessment of Undiscovered Potash Resources as Halokinetic Potash-Bearing Salt Deposits

Undiscovered potash resources in the Gissar tract were estimated by assuming they were halokinetic potash deposits (appendix C) and by using the three-part form of assessment described by Singer and Menzie (2005). The assessment team (appendix G) consisted of three international experts and five USGS experts, plus a USGS facilitator who was experienced in mineral resource assessments, and who also had a broad understanding of potash in evaporites. An estimate of the number of deposits (table 2-4) was made by members of the assessment team for the delineated tract using the global halokinetic grade and tonnage model (table 2-6) developed for the potash assessment.

Table 2-4. Principal sources of information for the Gissar tract, Turkmenistan, Uzbekistan, Tajikistan, and Afghanistan.

[CIS, Commonwealth of Independent States; GIS, geographic information system; M, million; USSR, Union of Soviet Socialist Republics]

Theme	Name or title	Scale	Citation
Geology	Potassium-bearing basins of the world	Unknown	Vysotskiy and others (1988)
	Some aspects of the genesis of halogenic sequences—Evidence from the Central Asian halogenic basin	Unknown	Baikov and Sedletskiy (2001)
	Tectonics of the Afghan-Tajik Depression	Unknown	Bekker (1996)
	Afghan-Tajik Depression	Unknown	Nikolaev (2002)
	Geologic map of Turkmenistan	1:500,000	Mirzakhanov (1989)
	Mineral deposits database and thematic maps of Central Asia	1:500,000	Seltmann and others (2005)
Mineral occurrences	An evaluation of prospects for potash-bearing capabilities in Upper Jurassic salt deposits, southern Central Asia	Unknown	Fedin (1981)
	World survey of potash resources	Unknown	British Sulphur Corporation (1979)
	Uzbekistan to extend its chemical industry	Unknown	Ashurmatov (2006)
	Upper Jurassic halogen deposits of southeast Central Asia	Unknown	Luchnikov (1982)
	Investigation of potassium resource, exploitation and utilization in Turkmenistan	Unknown	Zhang and others (2005)
	Deposits of potassium salts in the USSR	Unknown	Rayevskiy and Fiveg (1973)
	New data on the geology of Donguzsyrt, Southeast Turkmenia	Unknown	Kutuzov and Popov (1976)
	Industrial minerals of the CIS	Unknown	Troitskiy and others (1998)
Subsurface geology	Deposits of potassium salts in the USSR	Unknown	Rayevskiy and Fiveg (1973)
	Petroleum resource potential GIS of northern Afghanistan	Various	Steinshouer and others (2006)
	Petroleum geology and resources of the Amu-Darya Basin	Various	Ulmishek (2004)
	Facies zoning and conditions of sediment accumulation of Upper Jurassic salt-bearing formations in the territories of eastern Turkmenia	Unknown	Gavril'cheva (1981)
	Hydrogeologic conditions of gas reservoirs in Murgab Basin	Unknown	Semashev (1983)
	Amu Darya Basin and surrounding areas–generalized location map showing major structural elements, hydrocarbon provinces, hydrocarbon fields and well locations	1:1.35M	Blackbourn (2008)
Geophysics	Petroleum geology and resources of the Amu-Darya Basin	Various	Steinshouer and others (2006)
Exploration	Lithofacies and potassium potential of Upper Jurassic halogen deposits in Central Asia	Unknown	Sedletskiy and Fedin (1981)
	Jurassic Basins	Unknown	Vysotskiy and others (1988)
	World survey of potash resources	Unknown	British Sulphur Corporation (1979)
	Structure of the Upper Jurassic halogen complex and its role in predicting buried reefs in the Amu-Darya regional low	Unknown	Khudaikuliev (1989)

Three-Part Form of Assessment Process and Rationale

The team reviewed the deposit and grade and tonnage models and the process for delineating the tract, discussed the oil and gas exploration history of the Amu Darya Basin, and evaluated the following factors that suggest the presence of undiscovered halokinetic deposits in the Gissar tract:

- The marine evaporite section of the Gaurdak Formation is as much as 1,200 m thick and extends over a vast region. A limited number of stratigraphic sections in Russian reports suggest that combined salt and potash layers may be as thick as 800 m in places;
- Known deposits occur at Karabil, Gaurdak, Karlyuk, Tyubegatan, and other locations;
- Salt and potash are not present everywhere in the larger salt field or in specific structures (see, for example, fig. 2-5). Brief descriptions in other references (Belelovskiy and others, 1971; Vysotskiy and others, 1988; Baikov and Sedletskiy, 2001) all imply that deposits in the Gissar tract are not as continuous as would be expected of a purely stratabound deposit;
- Known deposits in the area of the Gissar tract are distal to the seawater inflow point of the original CASB to the northwest, which is consistent with the halokinetic potash-bearing salt model (appendix B);

The following factors argue against the presence of undiscovered halokinetic deposits:

- Tremendous east-west compression (as much as 50 percent) of the Afghan-Tajik Basin, adjacent to the eastern margins of the Gissar tract suggests at least the possibility of increased dissolution and alteration of potash on the east side of the tract;

- Geophysical evidence suggests that Upper Jurassic strata of the Afghan-Tajik (eastern) side was buried to depths of 7 km, which limits the eastward extension of potash lying above the 3-km assessment depth limit and within the Gissar tract;

- Known deposits appear to have been uplifted by the flanks of the Gissar Range, implying that they are deep and less accessible elsewhere;

- The relative flatness of the Karlyuk and Karabil deposits and their continuity is more consistent with stratabound potash-bearing salt deposits than halokinetic potash-bearing salt deposits.

The assessment team's estimate of numbers of undiscovered deposits incorporated the above factors and was made in part by analogy with estimated deposit densities in other tracts and similar environments (for example, Dnieper-Donets, Zechstein in Orris and others, 2014). The team also considered what little is known of the exploration history (that is, the relatively few potash deposits known for such a large evaporite basin), and the large number (nearly 50) of potash prospects (Fedin 1981; Vysotskiy and others, 1988) that were discovered incidental to hydrocarbon exploration to the west and northwest in the Amu Darya tract. It is reasonable to expect that deposits exploited on one limb of a brachyanticline could be mirrored in the other limb, as well as elsewhere along strike.

Results

Estimates of numbers of deposits by individual team members (table 2-5) vary, however, the consensus estimate is that there are 7.2 undiscovered halokinetic potash-bearing salt deposits in the Gissar tract (table 2-6). Contained potash (K_2O) in the tract was estimated by combining the consensus estimate with the grade and tonnage model developed for this study (table 1-2, appendix D), using the Economic Mineral Resource Simulator (EMINERS) program (Root and others, 1992; Bawiec and Spanski, 2012; Duval, 2012). The result is a mean of 470 Mt of K_2O (table 2-7). The complete results of the Monte Carlo simulation are presented as a cumulative frequency plot (fig. 2-7) showing estimated resource amounts associated with cumulative probabilities of occurrence, as well as the mean, for potash and for total mineralized rock.

Table 2-5. Deposit estimates by individual team members for the Gissar tract, Turkmenistan, Uzbekistan, Tajikistan, and Afghanistan.

[N_{xx}, estimated number of deposits associated with the xxth percentile]

Estimator	Estimated number of undiscovered deposits				
	N_{90}	N_{50}	N_{10}	N_{05}	N_{01}
1	1	5	10	10	10
2	1	4	6	6	6
3	1	5	20	20	20
4	1	2	5	5	5
5	3	7	15	15	15
6	1	5	5	5	5
7	6	12	25	25	25
8	2	6	16	16	16

Table 2-6. Undiscovered deposit estimates, deposit numbers, tract area, and deposit density for halokinetic potash-bearing deposits in the Gissar tract, Turkmenistan, Uzbekistan, Tajikistan, and Afghanistan.

[N_{xx}, estimated number of deposits associated with the xxth percentile; N_{und}, expected number of undiscovered deposits; s, standard deviation; C_v %, coefficient of variance; N_{known}, number of known deposits in the tract that are included in the grade and tonnage model; N_{total}, total of expected number of deposits plus known deposits; density, total number of deposits (N) per square kilometer (km^2). N_{und}, s, and C_v % are calculated using a regression equation (Singer and Menzie, 2005)]

Consensus undiscovered deposit estimate					Summary statistics					Tract area (km^2)	Deposit density (N/km^2)
N_{90}	N_{50}	N_{10}	N_{05}	N_{01}	N_{und}	s	C_v %	N_{known}	N_{total}		
1	7	14	14	14	7.2	4.5	63	10	17.2	26,669	0.001

Table 2-7. Results of Monte Carlo simulations of undiscovered potash resources in halokinetic potash-bearing salt potash deposits in the Gissar tract, Turkmenistan, Uzbekistan, Tajikistan, and Afghanistan.

[Mt, million metric tons]

Material	Probability of at least the indicated amount						Probability of mean or greater	Probability of zero
	0.95	0.9	0.5	0.1	0.05	Mean		
K_2O (Mt)	0	18	390	1,200	1,400	470	0.45	0.08
Rock (Mt)	0	110	2,500	6,100	7,100	2,900	0.45	0.08

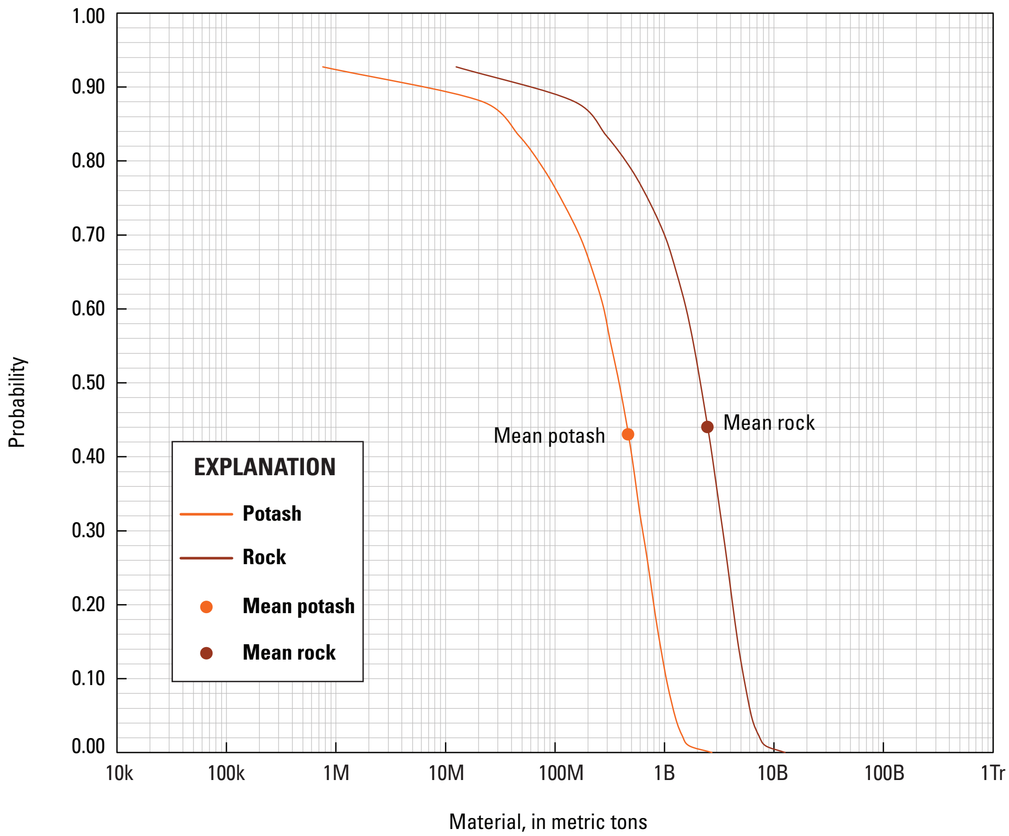

Figure 2-7. Cumulative frequency plot showing results of Monte Carlo simulation of undiscovered resources in halokinetic potash-bearing salt deposits in the Gissar tract (142mxK0005a), Turkmenistan, Uzbekistan, Tajikistan, and Afghanistan. k, thousands; M, millions; B, billions; Tr, trillions.

Assessment of Undiscovered Resources as Stratabound Potash-Bearing Salt Deposits

Assessment of stratabound deposits requires a method that considers the areal extent of the deposit, its thickness, and the range of ore grades throughout the deposit. The three-part form of assessment described in previous sections assumes that there is some number of discrete undiscovered deposits in the area being considered. Stratabound, relatively undeformed mineralized rocks that are contiguous within small to large parts of a depositional basin, may form a geologic deposit but are not always divisible into the physically discrete economic deposits needed to estimate the number of deposits needed for the three-part form of assessment. Therefore, for the global assessment of potash (K_2O), the AGE method was developed to estimate undiscovered resources in stratabound deposits.

The following observations support the presence of undiscovered potash in stratabound deposits:

- The marine evaporite section of the Gaurdak Formation is as much as 1,200 m thick and extends over a vast region according to the Russian literature. A limited number of stratigraphic sections in Russian reports suggest potash-hosting salt may be as thick as 800 m in places, suggesting a substantial potash resource;
- The large size of known deposits, such as Karabil and Karlyuk, suggests that disruption or loss of potash is more similar to stratabound potash-bearing salt deposits in some, but not all, parts of the tract;
- Blackbourn (2008) shows structure in the tract consisting of gently undulating folds;

The following observations do not support the presence of large stratabound potash deposits:

- At least two throughgoing faults in the same Blackbourn structural map suggest the possibility of local tectonic disruptions and dissolution;
- Older Russian literature refers to “lenses” of potash in the tract area, a word which has uncertain meaning, but generally refers to local thickening or a body of limited extent;
- The known presence of salt structures, some of which have pierced overlying sedimentary rocks or led to erosion and loss of salt and potash in the crests of the structures imply the presence of halokinetic-potash bearing salt deposits.

Overview of the Adaptive Geometric Estimation (AGE) Method

The AGE method (appendix A) follows a similar approach, albeit without the strict drill-hole density controls, to that used by most Canadian NI 43-101 standardized reports to estimate in-place volume of reserves and resources when applied to potash (Canadian Institute of Mining, Metallurgy and Petroleum, 2005, 2012), in that an in-place tonnage is calculated and then reduced by adjustments for anomalies and other factors. An AGE simulation can be modified to allow missing, incomplete, and unknown data to be estimated subjectively and (or) statistically through use of distributions based on partial data or analogous areas. Other approaches, such as a kriging method, were not used because of the large gaps between drill holes and other data points in the Gissar and Amu Darya tracts and the need to estimate the percent of unmineralized area, as well as missing variables such as thickness and grade.

In the AGE method, the volume of the tract being evaluated is first estimated using the tract area and thickness data. A grade is randomly selected from the grade distribution and the volume is converted to tonnage using a density based on the selected grade. The tonnage estimate is then adjusted to correct for areas of dissolution and lack of initial potash deposition, internal to the mineralized area (anomalies) and along the boundaries of the mineralized area (embayments). Lastly, known resources are subtracted from the calculated tonnage to determine the amount of undiscovered K_2O contained in the mineralized rock. All calculations are completed using a customized SYSTAT script (appendix F).

In the AGE method, unknown or incompletely known parameters may be (1) estimated from incomplete data available within the tract being studied, (2) estimated based on global averages for the deposit type, or (3) estimated subjectively. These estimates may be single numbers, but in this assessment they commonly are distributions that represent the variation of a particular parameter observed elsewhere, as well as the uncertainty in predicting its value(s). When assessing undiscovered resources, incomplete and missing data are the norm. Therefore, tract delineation and parameter estimation for missing data are critical for calculating a quantitative estimate of undiscovered resources. Parameter estimates for the Gissar tract (table 2-8) are discussed below.

Parameter Specification

(a) Volume

The volume of potash resources for the Gissar tract was calculated using a contoured set of potash thicknesses bounded by the tract, using an average, minimum, and maximum thickness. In the Amu Darya tract (chapter 3) we used data from drill holes to contour thickness because they covered a significant part of the tract (fig. 2-1). We averaged thicknesses in the Gissar tract to account for high data variability over short distances, a consequence of the Gissar Range uplift and deformation of potash-bearing salt. These thickness estimations are consistent with thickness estimations of the neighboring Amu Darya tract to the west. Average thickness for the Gissar tract was calculated as the weighted average of total potash thickness from all available data (appendix E).

Table 2-8. Parameters used to estimate undiscovered K_2O resources in stratabound potash-bearing salt deposits in the Gissar tract, Turkmenistan, Uzbekistan, Tajikistan, and Afghanistan.

[km^3, cubic kilometer; m, meter; min, minimum; max, maximum; %, percent]

Parameter	Source	Description
Thickness	Drill holes, other sources	Weighted average 4.5 m (min 3 m; max 10 m)
Volume	Triangular distribution	Triangular distribution (min 82 km^3; mode 123; max 273)
Grade (K_2O)	Drill holes, other sources	Normal distribution (mean 15.84%; standard deviation 4.42)
Anomalies	Global distribution	Triangular distribution (min 5%; mode 25%; max 40%)
Embayments	Global distribution	Triangular distribution (min 5%; mode 15%; max 30%)

Maximum and minimum thicknesses were taken directly from available drill-hole intercept data for this tract. These thickness values were used to calculate a minimum, average, and maximum distribution of possible potash volumes for the area of the tract using ArcMap.

(b) Grade

Available grade data for potash intervals of 1 m or greater in the Gissar and Amu Darya tracts were compiled and analyzed. The grade data (appendix D) form a normal distribution with a mean of 15.8 percent K_2O and a standard deviation of 4.42. Figure 2-8 provides a histogram showing grade distribution for potash in stratabound deposits in the Gissar tract. Conceptually, the mean or median are close to the actual average grade across the tract, and the tails of the grade distribution are much less likely to represent the tract as a whole. However, because data were not available for large parts of the Amu Darya tract, the higher and lower values of K_2O represented by the tails of the distribution cannot be completely eliminated as possibilities, however slight.

Two simplifications were necessary to use the grade data. There was limited point grade data across the tract extent, and no information on how typical any grade in the grade data we identified might be. Therefore, the grades in the grade distribution were treated as the range of possible average grades in the resource estimation simulation; in other words, a selected grade was applied to the entire tract during each pass of the Monte Carlo simulation. Because we do not know the potash mineral composition at most given points in the tract, it was assumed that average grades below 16.9 percent K_2O resulted solely from carnallite mineralization whereas grades of 16.9 percent or higher resulted from sylvite mineralization. This is based on experience with other potash-producing areas such as the Congo, Dnieper-Donets (Ukraine), and Zechstein (northern Europe); see Appendix C for a more detailed explanation. The density of carnallite is 1.6 (grams per cubic centimeter) g/cm^3, sylvite is 1.99 g/cm^3, and halite is 2.165 g/cm^3 (table I-1). With this information, an appropriate density can be determined for a select grade when estimating the undiscovered resource.

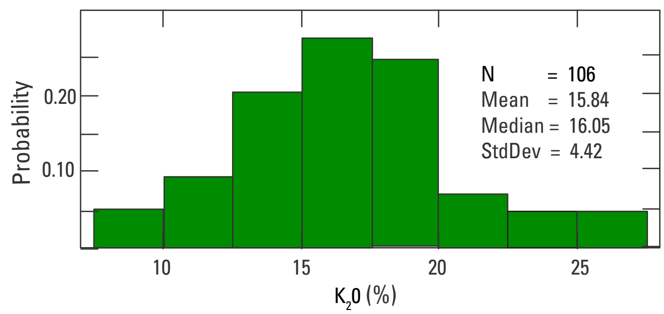

Figure 2-8. Histogram showing grade distribution for potash (K_2O) in stratabound deposits, Amu Darya and Gissar tracts, Turkmenistan, Uzbekistan, Tajikistan, and Afghanistan. N, number of grade distribution samples; StdDev, standard deviation. Data table is available in appendix D.

(c) Anomalies and Embayments

Unmineralized areas within stratabound potash deposit tract boundaries that are not connected to the edges of mineralization (and thus would be "embayments") are termed "anomalies" for the purposes of this assessment. Anomalies disturb the continuity of potash-bearing beds, and may range in size from less than one square meter to tens of square kilometers or more. Anomalies are usually composed of barren salt (halite) and commonly result from dissolution, diagenetic processes, or localized non-deposition of potash for unknown reasons. We used a range of 5–35 percent with a mode of 20 percent, based on better-known potash deposits elsewhere in the Monte Carlo simulation. The maximum is a conservative value and the minimum is based on the lowest reports of anomalies in the literature.

Potash and other salt deposits tend to have highly irregular tract boundaries that result from initial deposition and subsequent erosion. Where boundaries of stratabound potash have been mapped in detail, in places such as Carlsbad, New Mexico, they show pronounced embayments between unmineralized and mineralized areas. A more complete discussion of anomalies and embayments, including references, is in the method summary in appendix C.

Tectonism has uplifted and deformed the salt layers in this tract, increasing the possibility of erosion or dissolution. For example, a section of the central Gissar area is not permissive for potash because it has been eroded to below the level of the Upper Jurassic potash-bearing Gaurdak Formation (fig. 2-4). The anomalies parameter estimate has a higher mode and maximum for the Gissar tract than for the Amu Darya tract. This accommodates the greater evidence for tectonism in the Gissar tract than is found in the Amu Darya tract to the west. A more complete discussion of anomalies and embayments with references is in the Adaptive Geometric Estimation method summary in appendix C.

Simulation

The AGE approach for estimating undiscovered K_2O content of the Gissar tract (see Appendix C) assumes that potash deposits are dominantly stratabound and roughly flat-lying, consistent with the stratabound potash-bearing salt model (appendix A). The simulation begins with a calculation of the volume of potash-mineralized rock as the area multiplied by a variable thickness derived from very limited drill-intercept data.

After calculating the tract volume and other parameters, the next step is to run a Monte Carlo simulation, a random selection of a grade distribution done 5,000 times to obtain a distribution of the undiscovered potash. This grade is then used to determine whether carnallite or sylvite is the potash mineral (see previous discussion of grade), and thus determine the appropriate density value for converting tract volume to tonnage. The simulation actually calculates the volume and tonnage of sylvite (or carnallite) and of halite. The resulting tonnages are then adjusted for the expected proportions of anomalies and embayments, and finally the total tonnage is calculated and known resources are subtracted from this.

The simulations were run in SYSTAT 12, statistical analysis software. A generalized version of the SYSTAT script and a table defining the variables in the script is in appendix F.

Results

Our volume calculation assumes that stratabound potash mineralization varies from 82 to 273 km^3 (mode 234 km^3) depending on the average potash thickness assumed for the tract. This calculation results in a mean estimated resource of 27.9 Bt of K_2O (median 25.3) remaining undiscovered in the Gissar tract (fig. 2-9). The N=5,000 in the figure represents 5,000 Monte Carlo simulation runs using randomly selected grades and volumes to arrive at a most likely tonnage and to estimate uncertainty. At 90 percent confidence, there is at least 13.1 Bt of K_2O present; at 10 percent confidence, there is 47.0 Bt of K_2O present (table 2-1). These values compare well with the 20 Bt of K_2O estimated by Zhang and others (2005) for an apparently similar but ill-defined area.

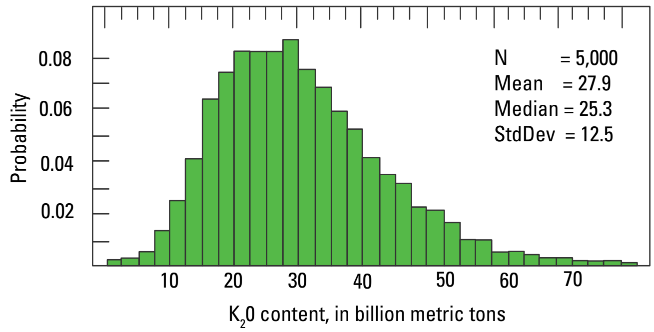

Figure 2-9. Histogram showing distribution of estimated in-place K_2O (potassium oxide) content in undiscovered stratabound potash deposits, Gissar tract (142mxK0005a), Turkmenistan, Uzbekistan, Tajikistan, and Afghanistan. N, number of in-place K_2O samples; StdDev, standard deviation.

Discussion

The Zhang and others (2005) estimate is consistent with ours if (a) they are discussing ore, not K_2O, and (b) we compare these numbers with the USGS AGE calculation. In Zhang and others (2005), the tract boundaries and estimation method are not clearly explained. If all potash in the Gissar tract occurs as halokinetic potash-bearing salt deposits, then the three-part form of assessment of Singer and Menzie (2005) predicts a mean undiscovered resource of 470 Mt of K_2O. Alternatively, if all potash in the Gissar tract occurs as stratabound potash-bearing salt deposits, then the AGE method predicts a mean undiscovered resource of 27.9 Bt of K_2O.

If we assume that Zhang and others (2005) estimated "nearly 20 billion tons" of potash ore in the central Gissar tract (fig. 2-4), then less than 20 percent of that ore (less than 4 Bt) is K_2O; this amount is more than one order of magnitude higher than the USGS halokinetic potash estimate and more than one order of magnitude lower than the USGS stratabound potash estimate. In other words, our end-member halokinetic and stratabound estimates for potash for the hybrid Gissar tract likely bracket the actual value. Note that our stratabound potash estimate is similar to the Zhang and others (2005) estimate of 20 Bt of K_2O. If the Zhang and others (2005) estimate is for the entire CASB, then the USGS estimate for halokinetic deposits is more consistent with theirs.

The USGS estimate of undiscovered potash resources in halokinetic deposits of the Gissar tract is likely an underestimate resulting from (1) conflicting information on the style and age of mineralization within known deposits and occurrences of the Gissar tract; (2) uncertainty about the mineralization and depth in the southwestern part of the tract; (3) an incorrect, or at least incomplete, understanding of the Donguzsyrt occurrence in the southwestern part of the tract (the Kutuzov and Popov [1976] paper was not available to us at the time of the assessment); (4) deliberate conservatism on the part of the assessment team in assessing additional potential for potash mineralization; and (5) sparse data in the global tonnage model to accurately represent the size range of the deposits in this tract (Karlyuk and Karabil are very large and were not part of the halokinetic grade and tonnage model).

Alternatively, the USGS estimate of undiscovered potash in stratabound deposits of the Gissar tract is six to eight times larger than Zhang and others (2005), although the Gissar tract almost certainly covers a much larger area than they considered. This USGS result may be an overestimate. The relatively shallow northern part of the Gissar tract was extensively explored by Soviet geologists, and most of the significant potash mineralization there has probably already been identified. This implies that the tract may contain much larger barren areas than would be expected from the less deformed stratabound potash-bearing salt deposits used as the analogues to determine the anomaly correction in the simulation.

An apparent lack of agreement between the two calculations does not invalidate either USGS estimate. The authors believe that the true amount of undiscovered and potentially economic potash resource in the Gissar tract lies between 470 Mt and 27.9 Bt of K_2O (table 2-1), placing it in the large tail of the distribution for worldwide halokinetic deposits and towards the smaller tail of distribution for worldwide stratabound deposits.

Additional data would lead to more optimistic estimates of numbers of halokinetic deposits in the three-part form of assessment or, in the AGE method, and would allow us to more closely define the parameters to reflect the actual geologic constraints of the area.

This page intentionally left blank

Chapter 3. Stratabound Potash-Bearing Salt Assessment for the Amu Darya Tract (142sbK0005b)—Turkmenistan and Uzbekistan

By Jeff Wynn,[1] Greta J. Orris,[2] Pamela Dunlap,[2] Mark D. Cocker,[2] and James D. Bliss[2]

Introduction

A quantitative assessment of undiscovered stratabound potash deposits was conducted for the Amu Darya tract of the Central Asia Salt Basin (CASB) that extends northwest from the Gissar Range along the Turkmenistan-Uzbekistan border (fig. 3-1). Upper Jurassic to Lower Cretaceous(?) potash and host salt of the Gaurdak Formation have been identified throughout the tract at or near the crests of abundant gentle anticlinal structures (fig 1-2). From the Russian literature, potash mineralization appears to be laterally continuous and stratabound, and to form a gently undulating surface. The assessment team interpolated limited available data (fig 3-2) to estimate a range of potash thicknesses for the Amu Darya tract that, in turn, allowed for estimation of volume and tonnage. Other parameters, such as grade and anomalies (unmineralized areas) were estimated from available data or analogous areas and were used to refine tonnage estimates of undiscovered potash resources. Our assessment team estimates a mean contained K_2O (potassium oxide) resource of 41.1 Bt for the Amu Darya tract (table 3-1).

[1]U.S. Geological Survey, Vancouver, Washington, United States.

[2]U.S. Geological Survey, Tucson, Arizona, United States.

Location

The Amu Darya tract is west of the Gissar Range and spans the border of Turkmenistan and Uzbekistan, including the city of Chardzhou. It is within the Jurassic CASB, and includes relatively undeformed parts of the northern Beshkent Trough, Karabekaul Trough, and Dengizkul Arch (figs. 3-3, 3-4, 3-5) that host potash occurrences. Maps shown in figures 3-3, 3-4, and 3-5 are derived from different sources and, in many places, do not agree; however, unique locations and features on each map (not found on the other) were used to define the Amu Darya tract and are thus included for completeness. We have made an effort to bring the figures into closer agreement in terms of feature names and locations (such as cities and fault names) but have not forced our own interpretations of what we believed to be the intent of the individual authors of the source maps.

Table 3-1. Summary resource assessment results for the Amu Darya tract, Turkmenistan and Uzbekistan.

[km, kilometer; km^2, square kilometer; Bt, billion metric tons]

Date of assessment	Assessment depth (km)	Tract area (km^2)	Known potash resources (Bt K_2O)	Mean estimate of undiscovered potash resources (Bt K_2O)	Median estimate of undiscovered potash resources (Bt K_2O)
2010	3	40,224	0	41.1	37.8

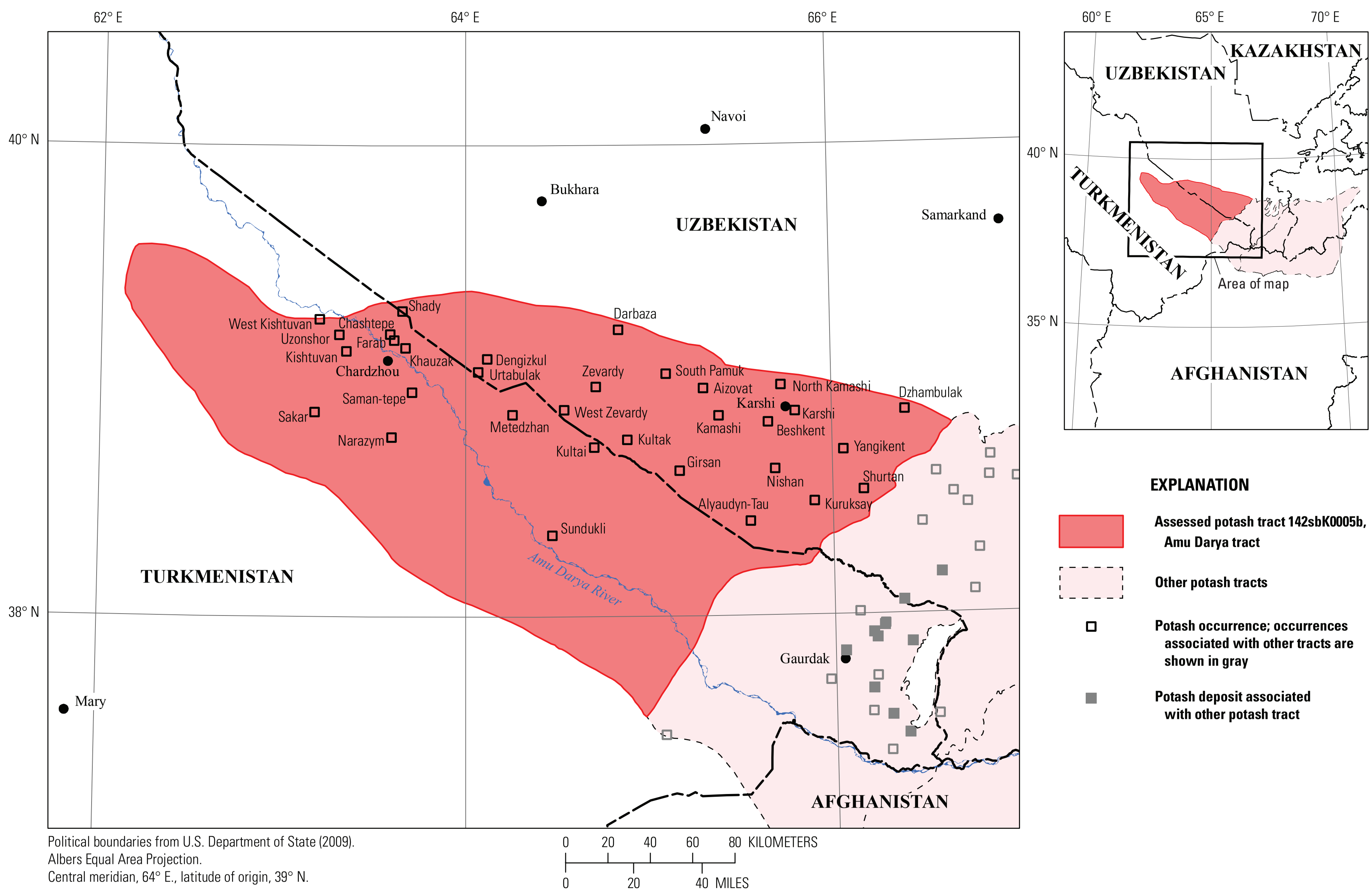

Figure 3-1. Map showing location of the Amu Darya tract (142sbK0005b), Turkmenistan and Uzbekistan, and potash occurrences.

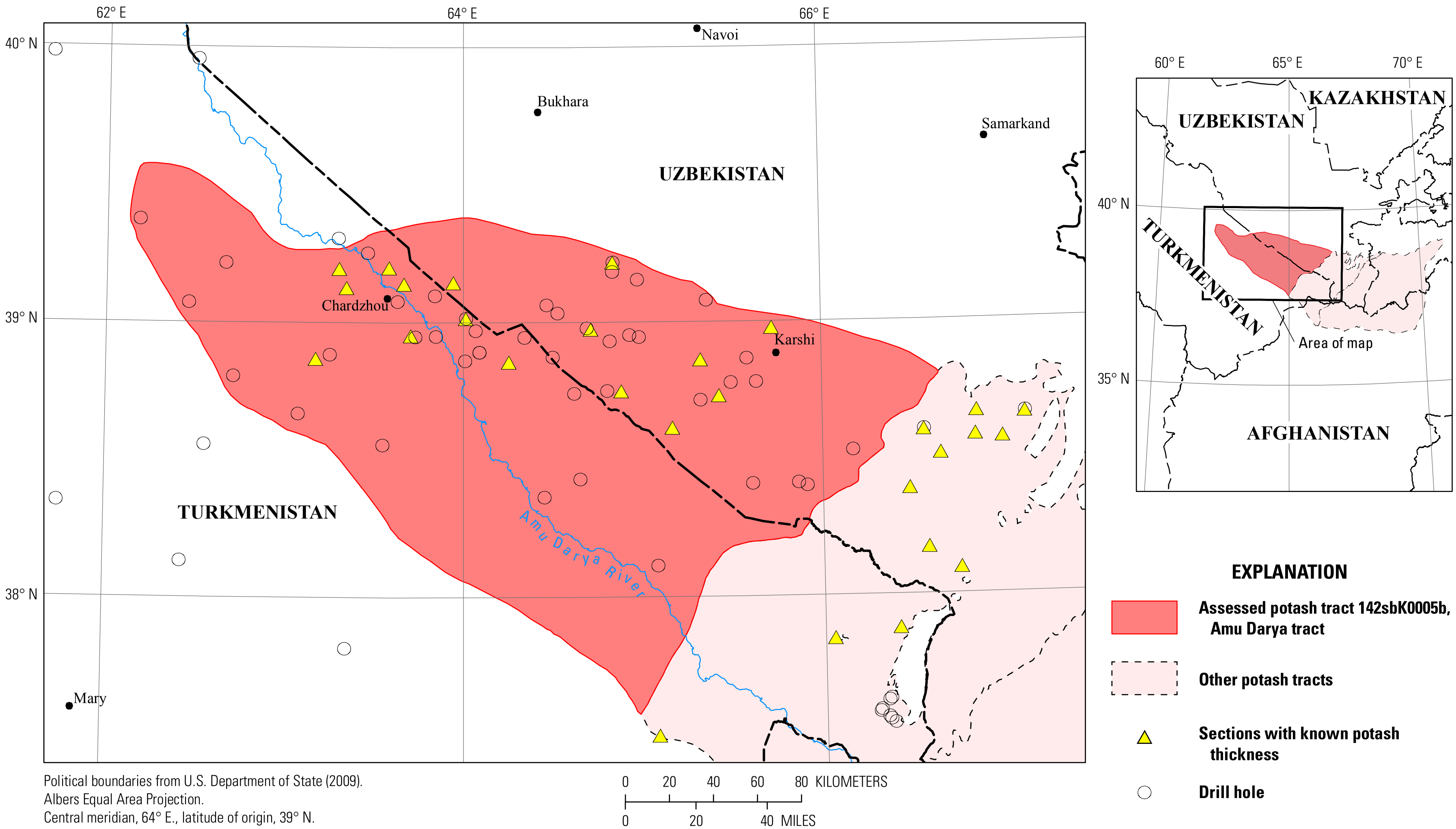

Figure 3-2. Map of the Amu Darya tract (142sbK0005b) showing drill holes and other point-source information indicating that at least one meter thickness of potash is present.

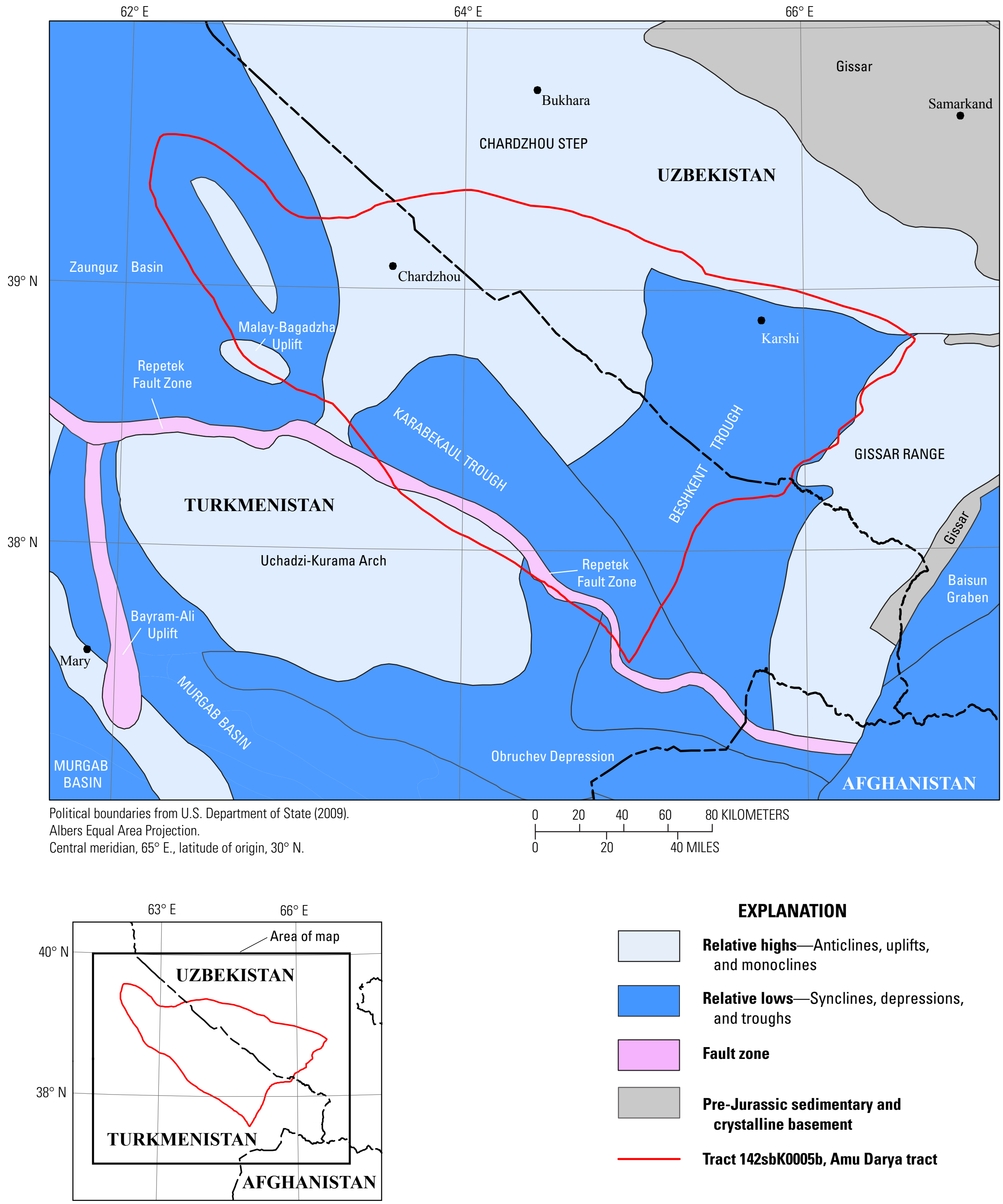

Figure 3-3. Map showing named structural provinces in and near the Amu Darya tract (142sbK0005b), Turkmenistan and Uzbekistan (adapted from Steinshouer and others, 2006).

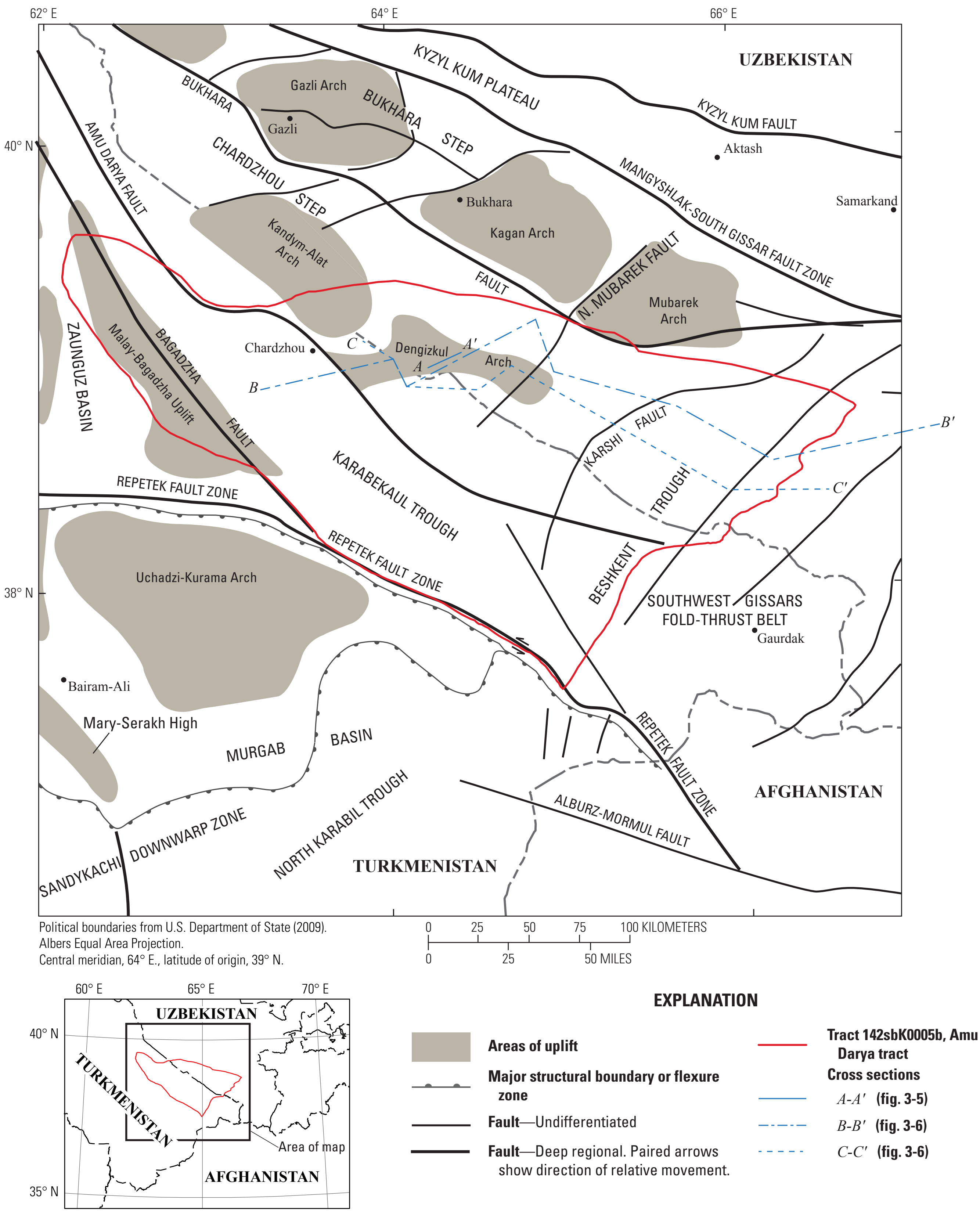

Figure 3-4. Map showing structural features and locations of cross sections in and near the Amu Darya tract (142sbK0005b), Turkmenistan and Uzbekistan (adapted from Blackbourn, 2008).

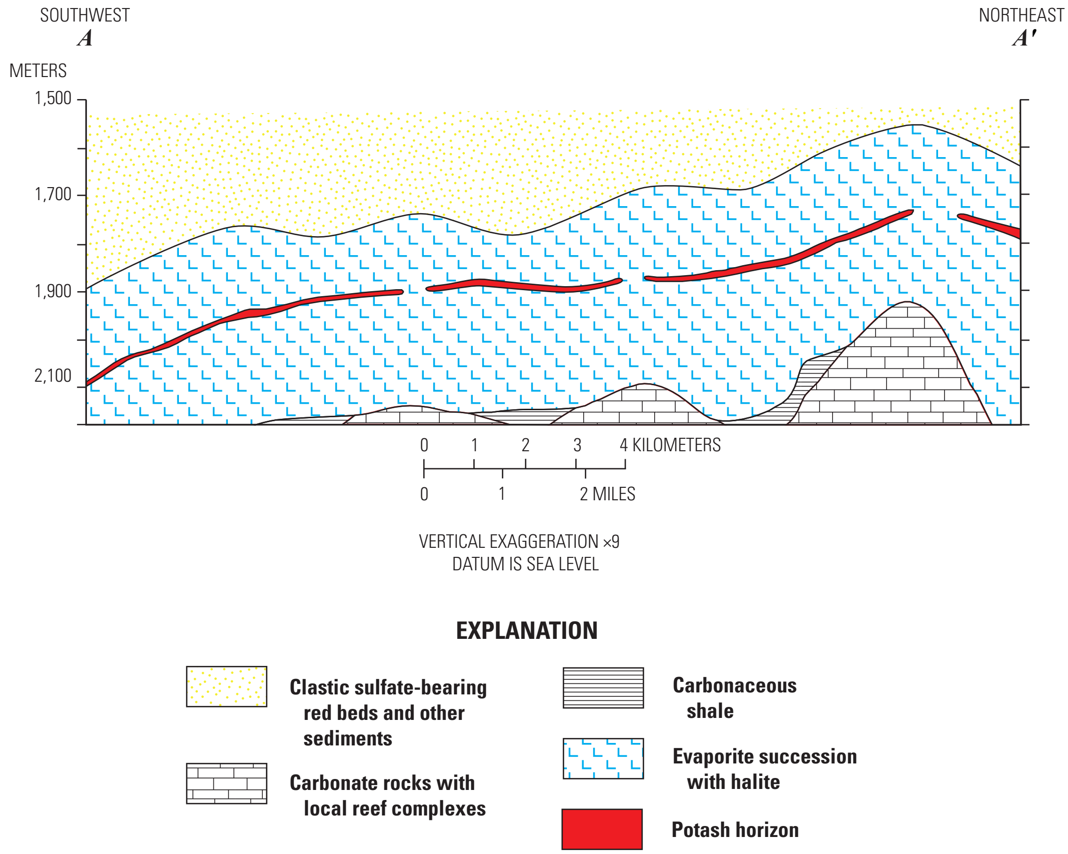

Figure 3-5. Cross section *A–A*' through the Dengizkul Arch, Turkmenistan and Uzbekistan (see fig. 3-4 for location). The potash horizon, referred to in Vakhabov (1986) and Popov and others (1984), is immersed in a much thicker evaporite succession with halite. Depth of Jurassic salt and potash increases to the south (adapted from Belenitskaya, 2000).

Basin History

The Amu Darya tract lies within the Amu Darya Basin, the relatively undisturbed part of the original CASB west of the area of Miocene uplift (the Gissar Range) that separated the CASB into two subbasins. Salt water inflow during Kimmeridgian-Tithonian (Late Jurassic) time appears to have come from the southwestern part of the modern Amu Darya Basin (Vysotskiy and others, 1988; Baikov and Sedletskiy, 2001). Subsequent basin infill, including that weathered from surrounding uplifted areas, such as the Kyzyl Kum Plateau to the north and the Uchadzhi-Kurama Arch to the south and southwest, has covered the Jurassic evaporite deposits with as much as 3 km of Cretaceous to Pleistocene sedimentary rocks. Whereas post-Miocene deformation continued in the eastern (Afghan-Tajik) subbasin, geophysical evidence (Ulmishek, 2004) suggests that little structural deformation or halokinesis has affected the salt in the Amu Darya tract, except near its contact with the neighboring Gissar tract and, possibly, adjacent to the Repetek Fault Zone.

Salt

The Amu Darya tract is within the boundaries of the CASB (fig. 1-2) and is underlain by salt and other evaporates of the Upper Jurassic Gaurdak Formation. In places, the salt is at least 100–300 m thick (Zharkov and others, 1982a, 1982b; Khudaikuliev, 1989). Stratabound potash-bearing salt is believed by Khudaikuliev (1986, 1989) and Zharkov and others (1982c) to be present within this unit. Whereas the morphology of potash-bearing salt is initially stratabound, dissolution, erosion, and halokinesis commonly result in less homogeneous and continuous mineralization, even when salt structures are not strongly developed. The entire area included within the tract is considered permissive for potash because we cannot precisely identify areas lacking potash within the tract boundaries. The depth of the Gaurdak evaporites increases in a southerly direction and, although much of the mineralization now lies at depths of 1 km or more, the potash remains mostly above the 3- km assessment depth limit (fig 3-6).

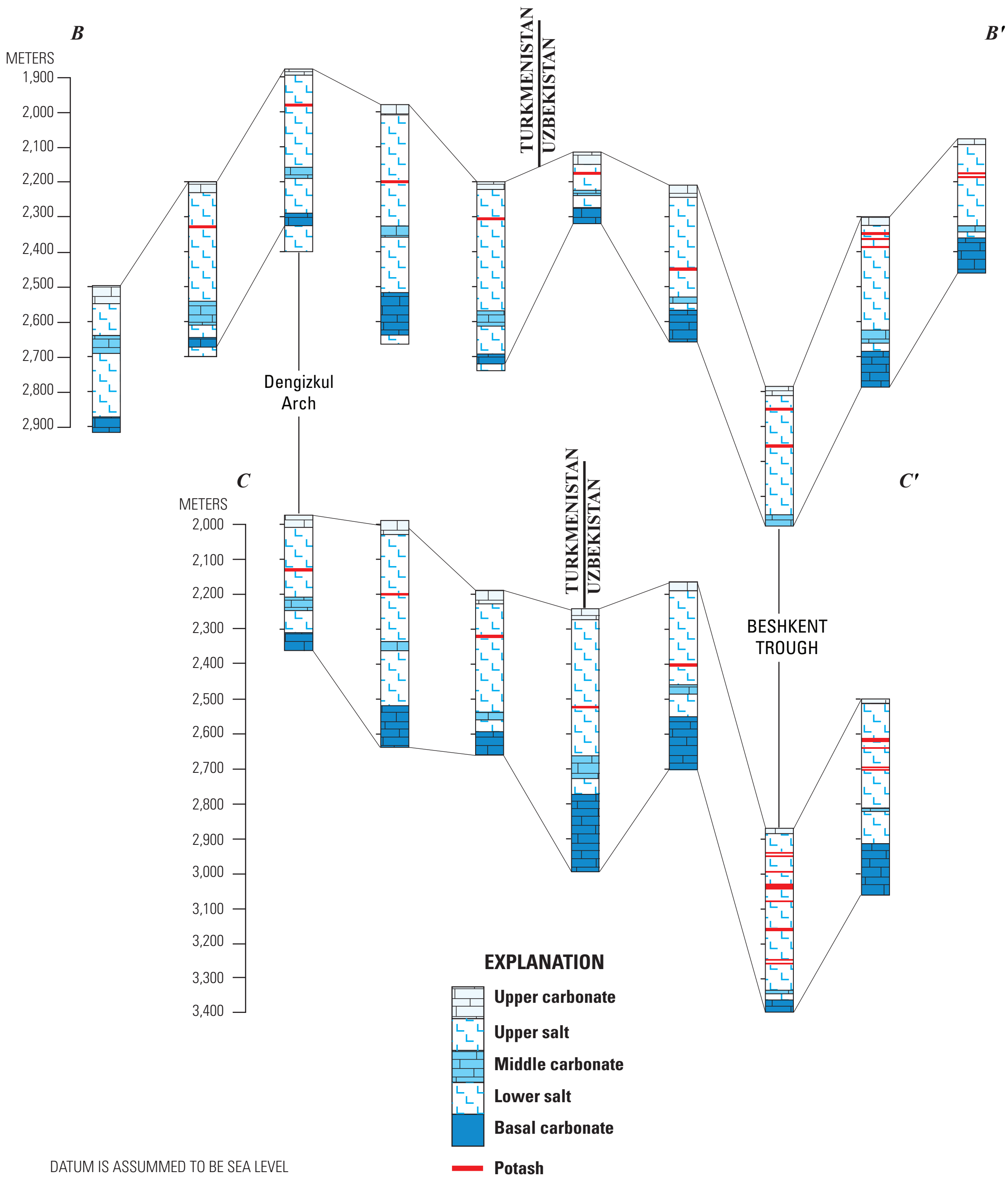

Figure 3-6. Stratigraphic sections *B–B*' and *C–C*' through the Amu Darya Basin, Turkmenistan and Uzbekistan (see fig. 3-4 for locations), derived from Zharkov and others (1982a) and Sedletskiy and Fedin (1981). Upper salt in this figure is the same as package 2, and lower salt is the same as package 4, of Gavril'cheva (1981), shown in figures 1-4 and 2-2.

The Repetek Fault Zone shown in figures 3-2 and 3-3 is coincident in places with a narrow arch (Repetek Arch). A lineament of small salt domes occurs within this fault zone along the southern boundary of the Amu Darya tract and part of the southern boundary of the Gissar tract. The only salt dome known to host potash is the Donguzsyrt occurrence in the adjacent Gissar tract. We included cumulative potash thicknesses (>1 m) reported from individual layers in our gridding and contouring of total potash thickness data (fig. 3-7; contours intersecting the tract boundary are explained in the following volume section).

Assessment

This section describes the steps used to estimate undiscovered K_2O resources in the Amu Darya tract, including data collection and analysis, and identification of the appropriate deposit model. Data available for the Amu Darya tract indicated that the stratabound potash-bearing salt model (appendix B) was most appropriate for this assessment. The Jurassic potash layers appear to be continuous and, where anticlines and (or) domes are present, these structures do not appear to be pronounced and mineralization is likely less disturbed than in the tracts to the east.

Although Zharkov and others (1982a, their fig. 4) report combined aggregate thicknesses of potash-hosting salt, we used their drill holes, in which no salt or potash is reported, to constrain the boundaries of the Amu Darya tract and thus constrain our calculation. The resulting potash thickness contours are within tract boundaries and approximate the “K-Prospective Zone III” of Vysotskiy and others (1988, their fig. 73) and Fedin (1981), increasing our confidence in our tract boundary.

Delineation of the Permissive Tract

The Amu Darya tract comprises the largely undisturbed part of the Beshkent Trough and regions farther northwest in the CASB (fig. 3-4) that contain potash occurrences. This tract is bounded to the east by the Gissar tract. Blackbourn (2008) and Belenitskaya (2000) show that the potash included in this tract is stratabound with gently undulating folds; the magnitude of structural modification apparently was not high enough to significantly disrupt the continuity of the potash-bearing salt layers (fig. 3-5). The Amu Darya tract lies south of the Kyzyl Kum Plateau, and includes all areas where potash one meter or greater in thickness has been reported or inferred. The K-Prospective Zone III of Fedin (1981) and Vysotskiy and others (1988) was the starting point to begin delineating the tract. The tract boundary was further refined by extending the boundaries to include known occurrences in the northeast and by using the high-resolution structural map of Blackbourn (2008), in addition to the structures shown by Steinshouer and others (2006). We used these structural maps to include the southern boundary of the Karabekaul Trough adjacent to the Repetek Fault, and to exclude areas where known total potash thickness is less than 1 m (Khudaikuliev, 1986; see fig. 3-2). The boundaries were slightly expanded south and west to include all known occurrences of potash (Zharkov and others, 1982a, 1982b), and potash occurrences shown in figure 3-1, even though earlier Russian reports said that there was no potash, for instance, west of the city of Chardzhou. The tract is consistent with reports that potash is only found north of the Repetek Fault Zone (Vysotskiy and others, 1988). Overall, the tract is believed to represent the extent of stratabound potash beds 1 m or greater in thickness.

The Murgab Basin (fig. 3-3, 3-4) is relevant to the resource discussion of the Amu Darya tract because it is part of the CASB; however, it is not included in the potash assessment. The Murgab Basin lies south and west of the Amu Darya tract, and is separated from it by the Repetek Fault Zone. The K-Prospective Zone IV of Vysotskiy and others (1988) includes the northern edge of the Murgab Basin, but was coarsely sketched in the original figure. Much of the Repetek Fault Zone is occupied by, or coincident with, a narrow arch that separates Fedin’s (1981) and Vysotskiy and others’ (1988) K-Prospective Zone III (approximately coincident with the Amu Darya tract) from another zone to the south that Russian geologists referred to as “K-Prospective Zone IV.” This latter zone was their lowest-potential potash resource zone, and includes the Murgab Basin.

The Repetek Arch is 450 km long and 12–15 km wide and is approximately coincident with the Repetek Fault Zone. Jurassic evaporite salt occurs in the Repetek Arch as a lineament of small salt domes that locally breach the surface and have 2,000–3,000 m in vertical relief (Semashev, 1983). This salt continues southwest and downdip into the Murgab Basin (Belelovskiy and others, 1971). Depth to basement, apparently ascertained by seismic-reflection data, ranges from 6 to 14 km. South of the Repetek Arch (coincident with the Repetek Fault Zone) is the Uchadzhi-Kurama Arch, which dips southward and forms the northern flank of the Murgab Basin. In the Mary-Serakh High, near the town of Mary, the base of the Jurassic lies at depths of 5–6 km, and is underlain by another 4–5 km of upper Paleozoic and Triassic sedimentary rock (Clarke, 1986; 1988). According to Vysotskiy and others (1988), no potash is reported in the Murgab Basin south and west of the Repetek Fault Zone. If potash is present, it lies well below the potash assessment depth limit of 3 km.

Definition of Resources

For the Amu Darya tract, known deposits were defined as those with documented reserves or resources with a category of A, B, C1, or C2 (the Russian classification system, see Henley, 2004, and also chapter 2 of this report). Using these criteria, no known deposits have been reported within the tract.

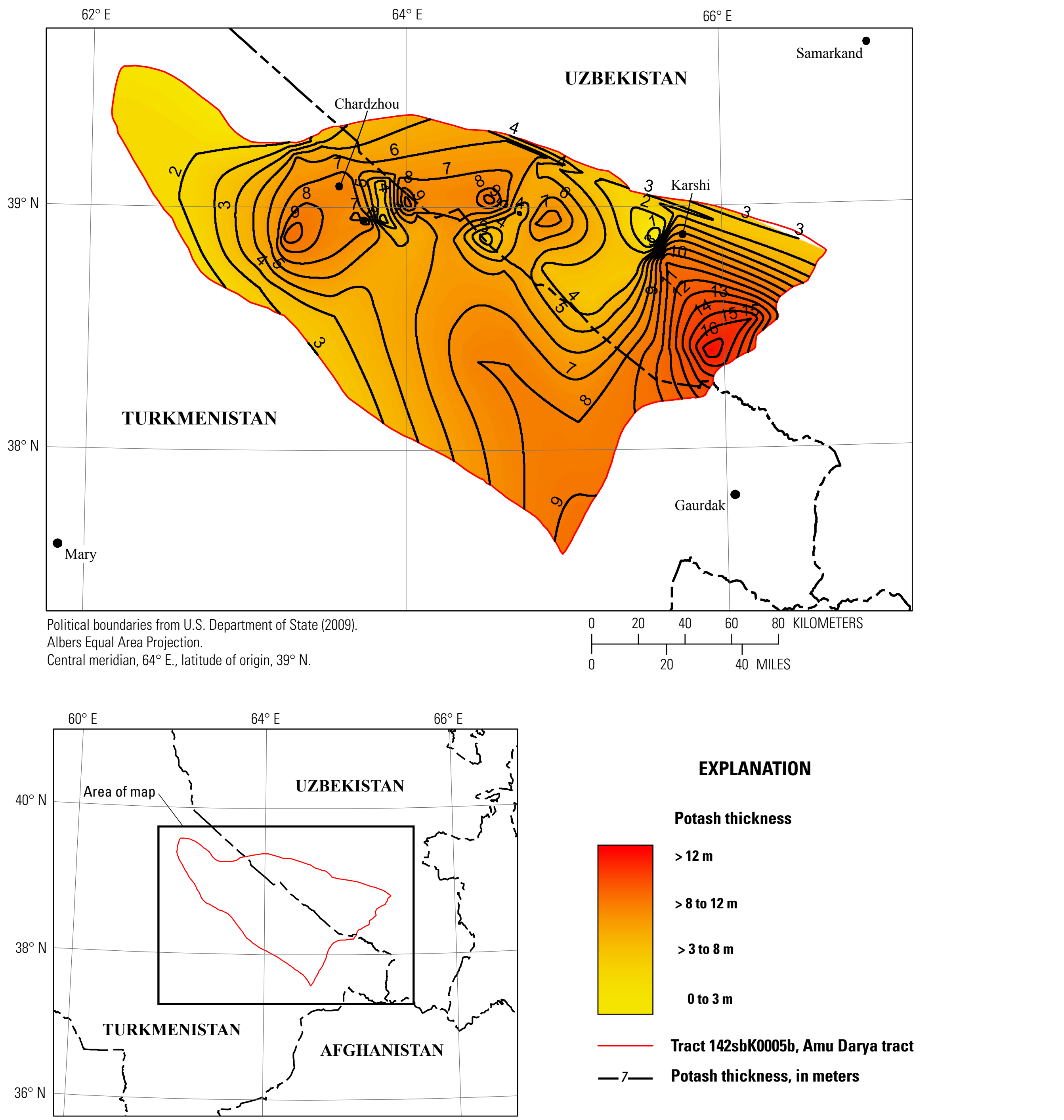

Figure 3-7. Map showing potash thickness contours in the Amu Darya tract (142sbK0005b), Turkmenistan and Uzbekistan. Contours were created by using drill-intercept data (appendix E) in ArcMap.

Mineral Occurrences

Many potash occurrences have been reported in this tract (table 3-2, fig. 3-1). Most reported potash appears to have been identified by using gamma-ray logs acquired during oil and gas exploration. Most, if not all, potash occurrences in the area are described as non-piercing salt structures (Fedin, 1981; Vysotskiy and others, 1988), which are undulations or flexures in the evaporite salt over local basement highs (fig. 3-5). Many of these structures were identified indirectly from "geophysical surveys" (probably seismic-reflection surveys) or gamma-ray logs, the latter being a standard technique used for characterizing stratigraphy in oil and gas exploration, but also useful for identifying potash. Potash descriptions by Sedletskiy and Fedin (1981), Belenitskaya (2000), and Khudaikuliev (1986) suggest that virtually all potash in the tract is shallower than 3 km (figs. 3-5, 3-6).

Exploration History

Although active potash resource exploration and development are occurring in the Gissar tract to the east, the assessment team was not able to identify any potash exploration in the Amu Darya tract during the past decade and, possibly, the past 30 years. Publications since the 1990s that reference potash mineralization in this tract appear to be based on earlier work or on data collected during oil and gas exploration (gamma-ray logs). Exploration for and development of potash within the Amu Darya tract is less likely than within the Gissar tract because deposits at shallower depths in the Gissar tract make them more attractive.

Table 3-2. Evaporite salt structures reported to contain detectable potash in the Amu Darya tract, Turkmenistan and Uzbekistan.

Name	Country	Latitude	Longitude	Reference
Chashtepe	Turkmenistan	39.199	63.584	Vysotskiy and others (1988)
Farab	Turkmenistan	39.174	63.608	Vysotskiy and others (1988)
Khauzak	Turkmenistan	39.142	63.669	Vysotskiy and others (1988)
Kishtuvan	Turkmenistan	39.128	63.345	Sedletskiy and Fedin (1981); Vysotskiy and others (1988)
Kultai	Turkmenistan	38.718	64.702	Sedletskiy and Fedin (1981); Vysotskiy and others (1988)
Metedzhan	Turkmenistan	38.857	64.256	Vysotskiy and others (1988)
Narazym	Turkmenistan	63.723	63.595	Sedletskiy and Fedin (1981); Vysotskiy and others (1988)
Sakar	Turkmenistan	38.869	63.173	Vysotskiy and others (1988)
Saman-tepe	Turkmenistan	38.953	63.705	Vysotskiy and others (1988)
Sundukli	Turkmenistan	38.345	64.471	Vysotskiy and others (1988)
Uzonshor	Turkmenistan	39.197	63.306	Sedletskiy and Fedin (1981); Vysotskiy and others (1988)
West Kishtuvan	Turkmenistan	39.283	63.197	Sedletskiy and Fedin (1981); Vysotskiy and others (1988)
Aizovat	Uzbekistan	38.967	65.300	Sedletskiy and Fedin (1981); Vysotskiy and others (1988)
Beshkent	Uzbekistan	38.821	65.653	Vysotskiy and others (1988)
Darbaza	Uzbekistan	39.218	64.838	Vysotskiy and others (1988)
Dengizkul	Uzbekistan	39.095	64.118	Vysotskiy and others (1988)
Dzhambulak	Uzbekistan	38.867	66.401	Sedletskiy and Fedin (1981); Vysotskiy and others (1988)
Girsan	Uzbekistan	38.617	65.167	Sedletskiy and Fedin (1981); Vysotskiy and others (1988)
Gumbulak	Uzbekistan	38.580	66.853	Vysotskiy and others (1988)
Kamashi	Uzbekistan	38.850	65.383	Sedletskiy and Fedin (1981); Vysotskiy and others (1988)
Karshi	Uzbekistan	38.867	65.800	Roskill (1989); Schultz and others (2000); Lefond (1969)
Kultak	Uzbekistan	38.750	64.883	Vysotskiy and others (1988)
Kuruksay	Uzbekistan	38.483	65.900	Vysotskiy and others (1988)
Mobik	Uzbekistan	38.570	67.005	Vysotskiy and others (1988)
Nishan	Uzbekistan	38.665	66.862	Sedletskiy and Fedin (1981); Vysotskiy and others (1988)
Shady	Uzbekistan	38.622	65.687	Vysotskiy and others (1988)
Shurtan	Uzbekistan	38.978	65.725	Vysotskiy and others (1988)
South Pamuk	Uzbekistan	39.298	63.652	Sedletskiy and Fedin (1981); Vysotskiy and others (1988)
West Zevardy	Uzbekistan	38.877	64.538	Vysotskiy and others (1988)
Yangikent	Uzbekistan	38.700	66.061	Vysotskiy and others (1988)
Zevardy	Uzbekistan	38.975	64.713	Vysotskiy and others (1988)

Data Availability

Most available data for the Amu Darya tract (table 3-3) were acquired in the 1970s and 1980s as a result of oil and gas exploration, and the assessment team believes that reports on the specific thickness of potash are largely derived from gamma-ray logs, though some potash was identified directly from drill core logs (for example, the Sakar occurrence, in Zharkov and others, 1982a, 1982b). Two 1:500,000-scale geologic maps (Seltmann and others, 2005) were available to the authors to use as a base, but only very coarse-resolution magnetic and gravity data were accessible. No original well logs were available. Figures from Russian reports lacked the detail and definitive geographic information needed to correlate map data and text was often abstracted from earlier, inaccessible or unpublished reports. Figure 3-2 shows the density of available information from which we built our resource estimate. Drill holes with measured and reported potash thicknesses of 1 m or greater are shown as yellow triangles. Open circles indicate drill holes where only the presence or absence of potash was noted, or other point sources of potash information including measured thicknesses. Drill holes and other point sources reporting at least one meter of potash (Khudaikuliev, 1986, 1989) are included within the tract boundary. The northwesternmost of these drill holes and occurrence data allowed us to extend the Amu Darya tract to the west beyond Chardzhou.

Table 3-3. Principal sources of information for the Amu Darya tract, Turkmenistan and Uzbekistan.

[CIS, Commonwealth of Independent States; GIS, geographic information system; NA, not applicable; USSR, Union of Soviet Socialist Republics]

Theme	Name or title	Scale	Citation
Geology	Potassium-bearing basins of the world	Unknown	Vysotskiy and others (1988)
	Central Asia Halogenic Basin	Unknown	Baikov and Sedletskiy (2001)
	Tectonics of the Afghan-Tajik Depression	Unknown	Bekker (1996)
	Afghan-Tajik Depression	Unknown	Nikolaev (2002)
	Geologic map of Turkmenistan	1:500,000	Mirzakhanov (1989)
	Mineral Deposits Database and Thematic Maps of Central Asia	1:500,000	Seltmann and others (2005)
Mineral occurrences	An evaluation of the prospects for potash-bearing capabilities in the Upper Jurassic salt deposits in southern Central Asia	NA	Fedin (1981)
	World survey of potash resources	NA	British Sulphur Corporation (1979)
	Uzbekistan to extend its chemical industry	NA	Ashurmatov (2006)
	Salt dome region of southwestern Tadzhikistan	NA	Luchnikov (1981)
	Potassium resource exploitation and utilization in Turkmenistan	NA	Zhang and others (2005)
	Industrial minerals of the CIS	NA	Troitskiy and others (1998)
	Deposits of potassium salts in the USSR	NA	Rayevskiy and Fiveg (1973)
Subsurface geology	Deposits of potassium salts in the USSR	Unknown	Rayevskiy and Fiveg (1973)
	Petroleum resource potential GIS of northern Afghanistan	Various	Steinshouer and others (2006)
	Petroleum geology and resources of the Amu-Darya Basin, Turkmenistan, Uzbekistan, Afghanistan, and Iran	Various	Ulmishek (2004)
	Hydrological conditions of gas accumulation in the Murgab depression	Unknown	Semashev (1983)
	Facies zoning and conditions of sediment accumulation of Upper Jurassic salt-bearing formations in the territories of eastern Turkmenia	Unknown	Gavril'cheva (1981)
	Amu Dar'ya Basin and surrounding areas	1:1,600,000	Blackbourn (2008)
Geophysics	Petroleum resource potential GIS of northern Afghanistan	Various	Steinshouer and others (2006)
Exploration	Prospects for potash-bearing capabilities in the Upper Jurassic salt deposits in southern Central Asia	Unknown	Fedin (1981)
	Jurassic Basins	Unknown	Vysotskiy and others (1988)
	World survey of potash resources	NA	British Sulphur Corporation (1979)
	Main structural features of the Upper Jurassic halogenous formation and its role in forecasting buried reefs in the Amu Darya syneclise	Unknown	Khudaikuliev (1986)

Quantitative Estimation

Undiscovered potash resources (K_2O) in tracts with thickness data for stratabound potash were estimated using an adaptive geometric estimation (AGE) method that follows the basic approach used by most Canadian NI 43-101 reports (Canadian Institute of Mining, Metallurgy and Petroleum, 2005, 2012) to estimate in-place volume of reserves and resources. The AGE method (appendix A) can be modified to allow missing, incomplete, and unknown data to be estimated subjectively and (or) through the use of distributions based on partial data or analogous areas.

Our AGE assessment of undiscovered potash in the Amu Darya tract was based on these encouraging observations:

- The marine evaporite section of the Gaurdak Formation is as much as 1,200 m thick and extends over a vast region. The potash-hosting salt may be as much as 800 m thick in places;
- Potash deposits, including Gaurdak, Karabil, Karlyuk, and Tyubegatan, are known in the adjacent Gissar tract directly east of the Amu Darya tract;
- Russian literature describes, within the area of the tract, potash occurrences with large areal extents and potash thicknesses in drill holes that suggest a substantial resource;
- Reported total thicknesses of potash-bearing layers in drill holes in the Amu Darya tract range from 1 to 17 m (fig. 3-6);
- Blackbourn (2008) shows structure in the tract consists of gently undulating folds.

Factors that do not support significant mineralization in the Amu Darya tract include the following:

- At least two throughgoing faults, the Amu Darya and the Bagadsha Faults (Blackbourn, 2008) suggest local tectonic disruptions and dissolution;
- Older Russian literature refers to “lenses” or local thickening of potash in the tract area, which implies some level of dissolution and disruption of the potash mineralization;
- Much of the potash intercept information was obtained incidental to oil and gas exploration, implying that there has been substantial drilling in the tract, which may have introduced pathways for local dissolution of potash;
- The tract is closer to the inflow source than the Gissar tract and thus the extent, grade, and thickness of the potash deposition may be more limited;
- Large gaps between some drill holes contribute to uncertainties about the character of potash mineralization.

Although the effect of the pessimistic factors cannot be quantified, the assessment team considered these factors during all phases of the assessment process. For the first, third, and fourth pessimistic factors listed above, this consideration included allowing for wider ranges of dissolution and non-deposition in the quantitative resource estimation process. A simplifying assumption, based on observations from other stratabound potash-bearing salt deposits with low levels of deformation in a similar climate, was that local lensing or changes in thickness are within the norm for stratabound potash-bearing salt deposits and are unlikely to affect the overall potash content of the tract.

Overview of the Adaptive Geometric Estimation (AGE) Method

In the AGE method, the area of the tract being evaluated is first multiplied by tract thickness to estimate volume. A grade is randomly selected from a grade distribution and the volume is then converted to tonnage using a density based on the selected grade. The in-place tonnage estimate is then adjusted downward to correct for areas of dissolution and nonmineralization, internal to the mineralized area (anomalies) and along the mineralization boundaries (embayments). Lastly, known resources are subtracted to determine the total amount of in-place, undiscovered K_2O contained in the mineralized rock. All calculations and simulations were completed using a customized SYSTAT script (appendix F).

In the AGE method, unknown or incompletely known parameters may be (1) estimated from incomplete data available within the tract being studied, (2) based on global averages for the deposit type, or (3) estimated subjectively. These estimates may be single numbers, but when estimating undiscovered resources, they are more commonly (as in this assessment) distributions that represent observed or expected variation of a particular parameter, as well as the uncertainty of predicting its value(s).When assessing undiscovered resources, incomplete and missing data are the norm; therefore, tract delineation and parameter estimation for missing data are critical for obtaining robust final quantitative estimates of undiscovered resources. For most areas assessed, much of the uncertainty in the final estimate results from uncertainty in parameter estimations, and this uncertainty reflects the quantity and quality of the initial inputs. Parameter estimates for the Amu Darya tract (table 3-4) are discussed below.

Parameter Specification

Volume

The volume of potash resources in the Amu Darya tract was calculated using a contoured set of potash thicknesses bounded by the tract (fig. 3-7), which represents our best estimate of the extent of potash 1 m or greater in thickness. A raster surface, built from contours in ArcMap, was used to approximate an undiscovered potash volume of 201 km^3.

Table 3-4. Parameters used to estimate the undiscovered K_2O resources of the Amu Darya tract, Turkmenistan and Uzbekistan.

[GIS, geographic information system; min, minimum; max, maximum; %, percent]

Parameter	Source	Description
Thickness	Drill holes, other sources	Data
Volume	GIS calculation	Point thickness data, including drill hole (see chapter 5)
Grade (K_2O)	Drill holes, other sources	Normal distribution (mean 15.84%; standard deviation 4.42)
Anomalies	Global distribution	Triangular distribution (min 5%; mode 20%; max 35%)
Embayments	Global distribution	Triangular distribution (min 5%; mode 15%; max 30%)

Before we did this, however, we generated a theoretical kilometer-diameter topographic hemisphere with a 1-m grid, and used raster and TIN surface methods to calculate a volume that we could compare with the analytic volume of a hemisphere. The TIN volume calculation gave the closest value to the analytical volume (within less than 2 percent), and this was used for the Amu Darya volume calculation.

Although the tract boundary was drawn using several different sources of information, thickness contours were constructed only using known, often sparse thicknesses of potash, which leads to the apparent contouring disparities in figure 3-7, such as the 4-m and 5-m contours intersecting the tract boundary on the south. Abrupt changes in thicknesses may result from faulting on some of these boundaries. Abrupt thickness changes in the northern part of the tract likely results from down-dropping along faults.

Grade

Available grade data for potash intervals 1 m or greater in thickness in the Gissar and Amu Darya tracts were compiled and analyzed. The grade data (appendix D) form a normal distribution with a mean of 15.8 percent K_2O and a standard deviation of 4.4 (fig. 2-8). This distribution provides a range of grades to sample in order to estimate the amount of K_2O in the basin.

Two simplifications were necessary in order to use the grade data. First, because point grade data across the Amu Darya tract were very uneven and there was no information on the frequency of any grade in the grade data, grades in the grade distribution were assumed to represent a range of possible average grades in the resource estimation simulation. Using Monte Carlo simulation, different grades within this range were applied to the entire tract. Secondly, because we did not know the potash mineral composition at any given point in the tract, it was assumed that average grades below 16.9 percent K_2O resulted from carnallite mineralization and grades of 16.9 percent or higher resulted from sylvite mineralization. The density of carnallite is 1.6 g/cm^3; sylvite is 1.99 g/cm^3, and halite is 2.165 g/cm^3 (table 1-1). With this information, an appropriate density was determined for a selected grade to estimate undiscovered resource tonnage.

Anomalies and Embayments

Unmineralized areas within stratabound potash deposit tract boundaries that are not along the edges of the mineralization are termed “anomalies” for the purposes of this USGS potash assessment. The term “embayment” refers to localized areas on tract margins where potash was never deposited because of local paleotopography, physical erosion, and other reasons including dissolution. See the chapter 2 (Gissar tract) where this issue was visited earlier. A more complete discussion of anomalies and embayments with references is in the method summary (appendix C).

Simulation

The AGE approach (appendix C) was used to estimate undiscovered stratabound K_2O in the Amu Darya tract. The process starts with a volume of potash-mineralized rock as a function of area and thickness. Values, or estimated distributions of values, have previously been determined or modeled for grade, anomalies, and embayments, and this information is entered into the simulation variables.

After determining tract volume and other parameters, the next step is to run a Monte Carlo simulation that starts with a random selection of a grade from the grade distribution. This grade is used to determine if carnallite or sylvite is the dominant ore mineral, which determines the density value to be used to convert the volume of potash-mineralized rock to tonnage. The simulation program actually calculates the volume and tonnage of sylvite (or carnallite) and of halite. Resulting tonnages are then adjusted for the expected proportions of anomalies and embayments (selected from distributions using Monte Carlo simulation), and finally, total ore and contained K_2O tonnages are calculated. Known resources are then subtracted to determine an estimate of in-place potash as K_2O. This process is repeated for 5,000 iterations to form a distribution of possible K_2O values.

Monte Carlo simulations were run in SYSTAT, a statistical analysis software package. A generalized version of the SYSTAT script and a table defining the variables in the script is in appendix F.

Results

Our calculation of potash-salt volume for the Amu Darya tract is 201 km^3. Converting volume to tonnage and using a Monte Carlo simulation to estimate the probable range of contained K_2O (fig. 3-8) yields a mean estimated resource of 41.1 Bt of K_2O (median of 37.8) undiscovered potash in the Amu Darya tract (table 3-1). At 90-percent confidence, there is 22.7 Bt of K_2O present; at 10-percent confidence, there is 64.9 Bt of K_2O present.

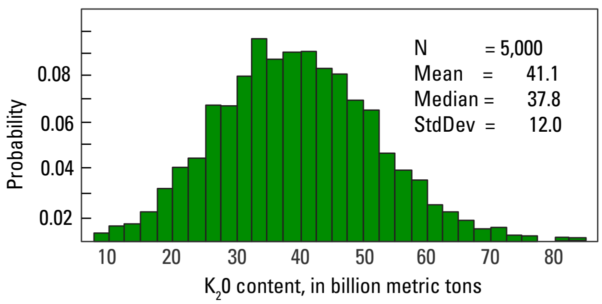

Figure 3-8. Histogram showing distribution of estimated in-place K_2O (potassium oxide) content of undiscovered potash deposits for the Amu Darya tract, Uzbekistan and Turkmenistan. N, number of in-place K_2O samples; StdDev, standard deviation.

Discussion

The Amu Darya tract contains a significant amount of potash. Our mean estimate of 41.1 Bt of K_2O is similar to our estimate of as much as 27.9 Bt of K_2O for the Gissar tract, given that the Amu Darya tract is almost 50 percent larger than the Gissar tract. However, this mean for the Amu Darya tract may overestimate or underestimate the resource actually contained in this tract. We expect that the true estimate lies within the distribution of estimated contained K_2O that was generated from the simulation. All grades in the grade distribution were obtained from the neighboring Gissar tract, where known deposits of the CASB occur. It is also possible that the grade distribution for the Amu Darya tract is significantly different than that for the Gissar tract. Given the lack of specific data, using the grade distribution from the contiguous and largely analogous Gissar tract was deemed appropriate. A similar uncertainty exists for most of the other estimated parameters, and readers should keep this in mind when using the results of this assessment. That said, the assessment team is confident that the predicted distribution of undiscovered potash resources encompasses the uncertainty of the estimate and that the mean of this distribution represents the best possible estimate.

Chapter 4. Potash-Bearing Salt Assessment for the Afghan-Tajik Tract (142haK0005c)— Uzbekistan, Tajikistan, and Afghanistan

By Jeff Wynn,[1] Greta J. Orris,[2] Pamela Dunlap,[2] and Mark D. Cocker[2]

Introduction

A qualitative assessment of undiscovered potash deposits was conducted for deeply buried salt in the eastern part of the Central Asia Salt Basin (CASB), which underlies much of the modern Afghan-Tajik Basin of Tajikistan and Afghanistan. The Afghan-Tajik tract shares its western boundary with the richly-mineralized Gissar tract (see chapter 2), and the assessment team believes that potash-hosting Jurassic evaporite units are likely present, but commonly at depths in excess of the 3-km assessment depth limit, especially in the western half of the tract near known reserves and resources of potash in the Gissar Range of Turkmenistan and Uzbekistan. In the Afghan-Tajik tract, the potential for potash is greatest where halokinesis and (or) faulting have resulted in potash occurring at depths of less than 3 km. Six, small, named potash occurrences have been reported (Sedletskiy, 1969; Rundkvist, 2001). Lack of exploration in the area and potential complexities and uncertainties inherent in potash deposits within halokinetic salt structures suggest that potential resources in this tract are unlikely to be developed.

Location

The Afghan-Tajik tract is east of the Gissar Range with parts of the tract in Uzbekistan, Tajikistan, and Afghanistan (fig 4-1). It comprises the eastern part of the original CASB, which is now separated by the Gissar Range into two modern basins: (1) the Amu Darya Basin in southern and eastern Turkmenistan and southwestern Uzbekistan, and (2) the Afghan-Tajik Basin in northern Afghanistan, western Tajikistan, and part of Uzbekistan (fig. 1-1).

Basin History

The Afghan-Tajik tract covers more than 68,000 km^2 and includes most of the modern Afghan-Tajik Basin. The Jurassic sedimentary rocks and evaporites of the basin are typically overlain by several kilometers of sedimentary rocks. Subsequent to the Gissar uplift of Miocene time, the Afghan-Tajik Basin has been continually compressed by the complex collision of the Indian subcontinent with Asia. Sedimentary rocks of the basin have been folded and compressed by as much as 50 percent in the east-west direction forming the Obigarm and Kafirnigan Mega Anticlines (open to the east) (Bekker, 1996; fig. 4-2). Geologic mapping and two-dimensional seismic profiles show that Upper Jurassic to Lower Cretaceous(?) evaporite units in the Afghan-Tajik tract have undergone extreme halokinesis during this tectonic compression (fig. 4-3*A*). Most of the potentially potash-bearing salt in this evaporite sequence lies far below the 3-km assessment depth limit, but a few diapirs or fault blocks may have raised potash to the surface or near surface in the extreme eastern and southeastern parts of the tract. It is also possible that, locally, some potash-bearing Jurassic evaporites lie in shallow areas near the crests of large regional anticlines (Bekker, 1996) or in areas uplifted by block tectonics (Klett and others, 2006).

Salt

Nikolaev (2002) reported that Jurassic salt beds extend under most of the Afghan-Tajik Basin. Most Jurassic sedimentary rocks that include the salt and potash units in the Afghan-Tajik tract lie at depths of 4–7 km (fig. 4-3*B*; Bekker, 1996; Nikolaev, 2002). However, the depth of salt burial and tectonic movement along basement and other faults has caused halokinesis within the tract, and has brought some Jurassic evaporites to the surface, or at least above the 3-km assessment depth limit. There are several exposures of probable Upper Jurassic (to Lower Cretaceous?) salt in the Afghan-Tajik Basin, most notably in salt domes west of Kulyab, Tajikistan, and in three domes 50–75 km east-southeast of Konduz in northern Afghanistan (fig. 1-2).

[1]U.S. Geological Survey, Vancouver, Washington, United States.

[2]U.S. Geological Survey, Tucson, Arizona, United States.

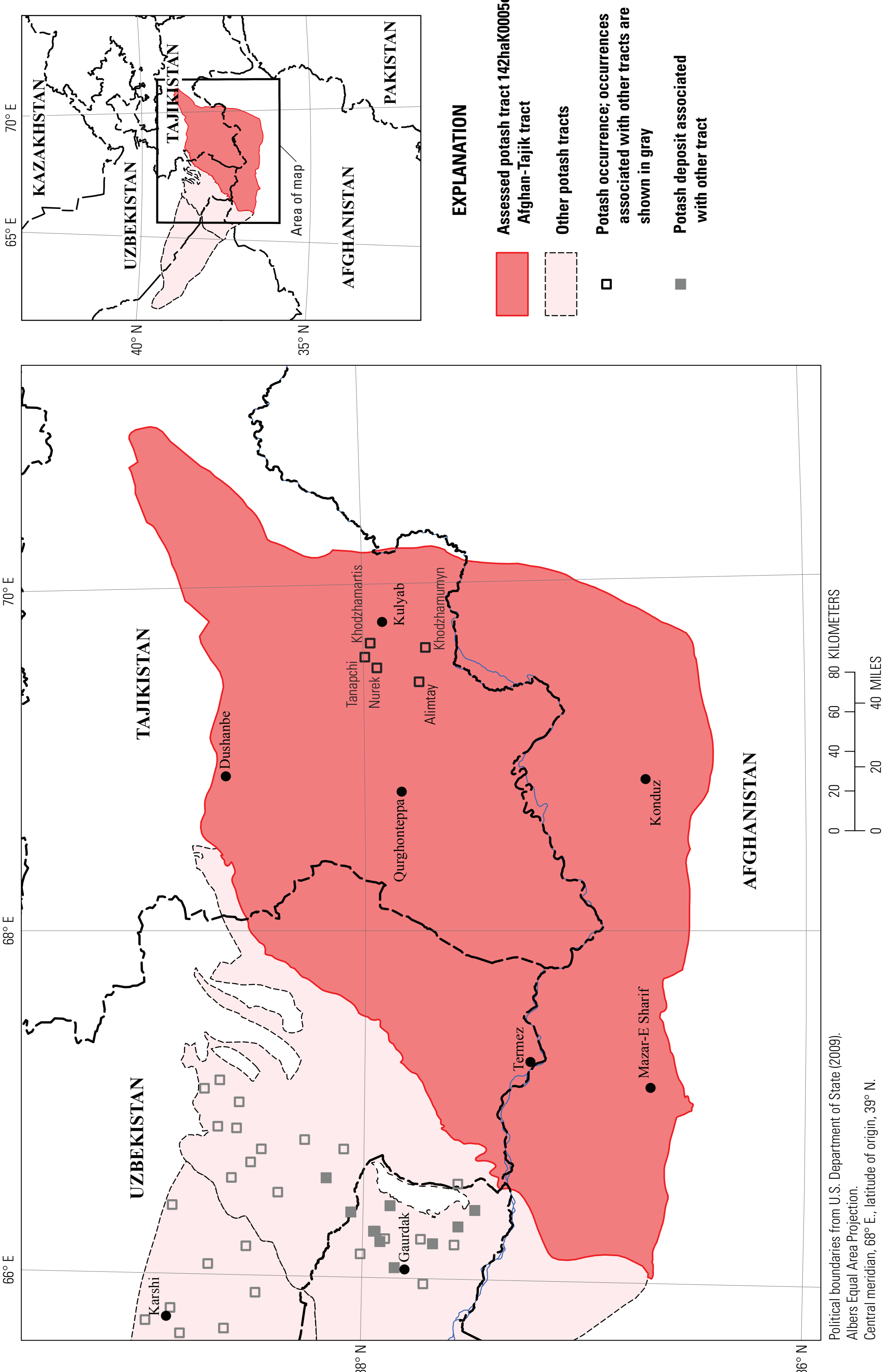

Figure 4-1. Map showing location of the Afghan-Tajik tract (142haK0005c), Uzbekistan, Tajikistan, and Afghanistan and and potash occurrences.

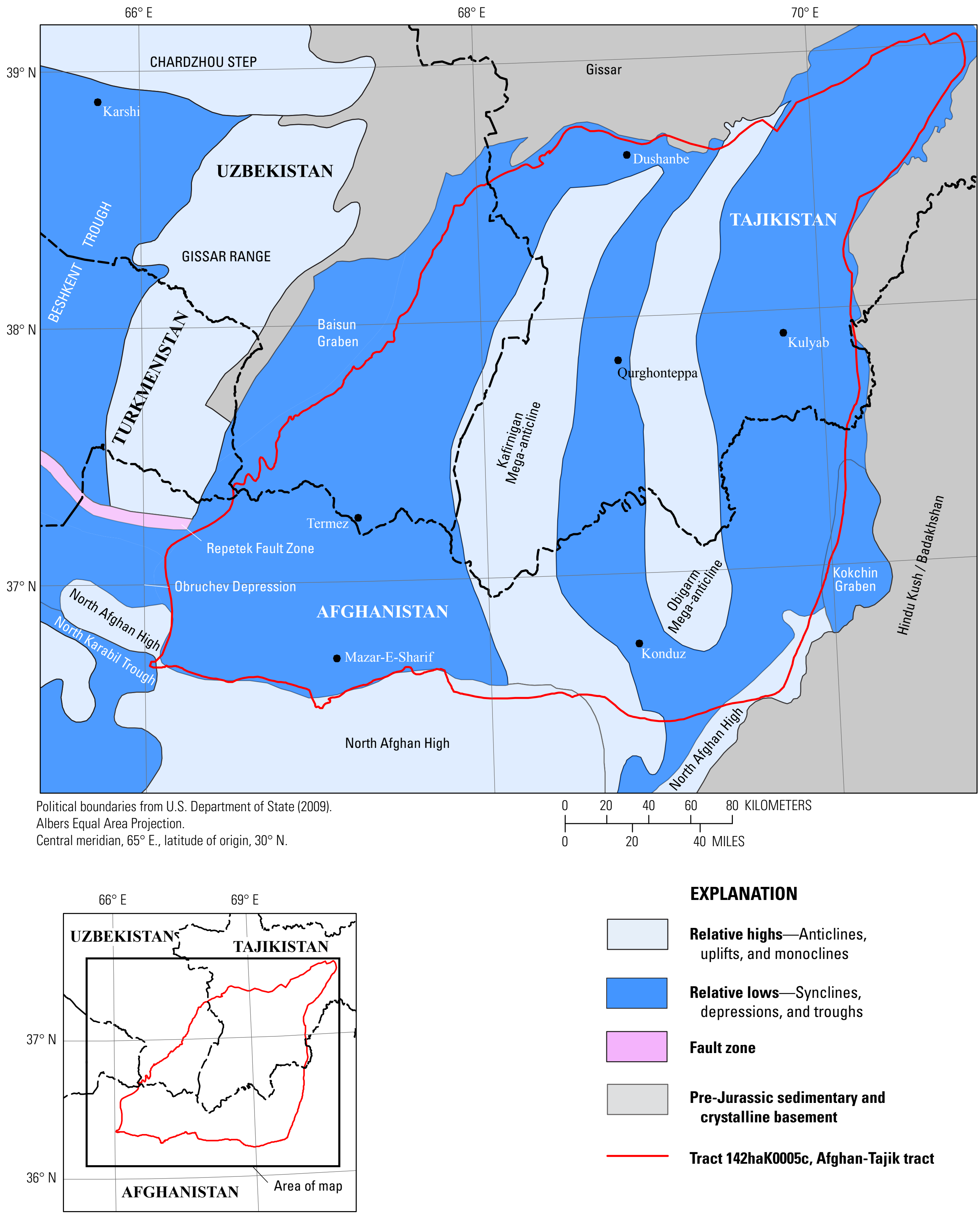

Figure 4-2. Map showing structural features in and near the Afghan-Tajik tract, Uzbekistan, Tajikistan, and Afghanistan, adapted from Steinshouer and others (2006).

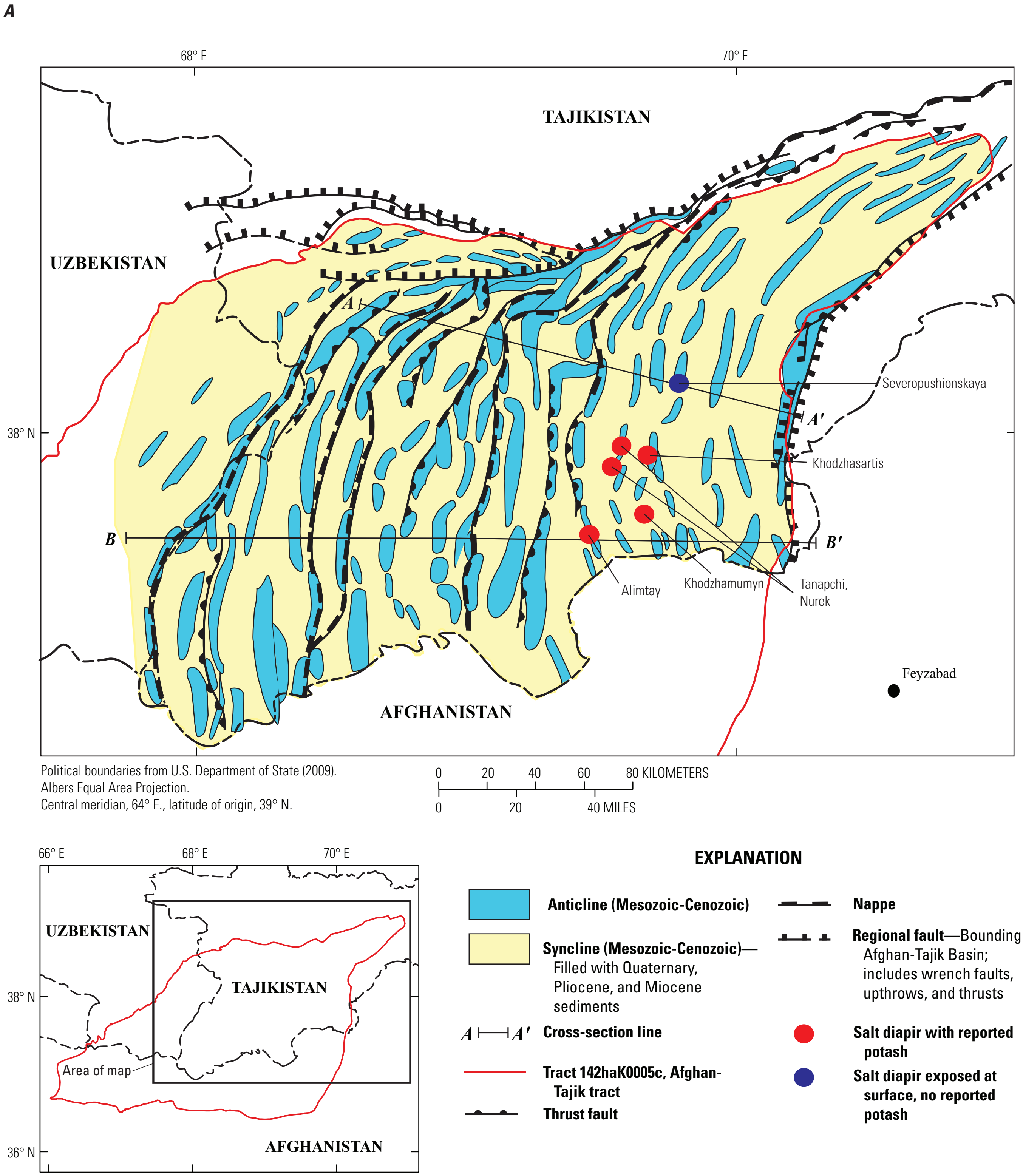

Figure 4-3. *A*, Map showing Mesozoic-Cenozoic structures and locations of cross sections shown on fig. 4-3*B*, and the Afghan-Tajik tract, Uzbekistan, Tajikistan, and Afghanistan, adapted from Bekker, 1996. *B*, Cross-sections showing depths to salt for the central and northeastern parts of the Afghan-Tajik tract (see fig. 4-3*A* for locations), adapted from Bekker (1996).

B

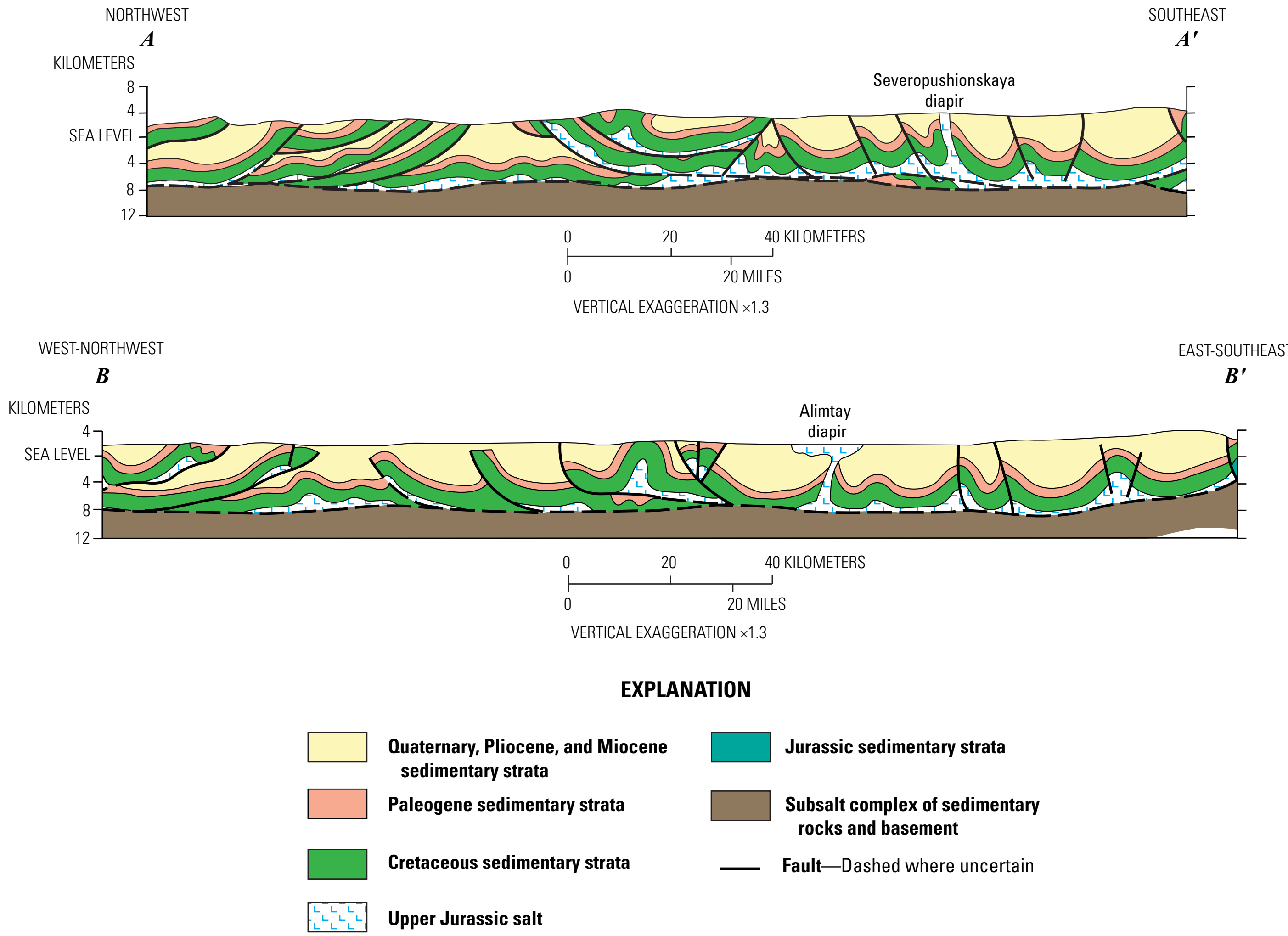

Figure 4-3.—Continued

Cross sections in Bekker (1996) suggest that any Jurassic salt above the 3-km assessment depth is rare (fig. 4-3*B*). Salt diapirs near Kulyab are found along anticlines associated with major faults (Leith and Simpson, 1986; see cross section *A*–*A*' on fig. 4-3). These salt structures are narrow, several kilometers high, and pierce the entire postsalt sequence. The Khodzamumyn dome (fig. 4-3*A*) forms a mountain that rises 880 m above the river valley, and the Khodzasartis dome rises 400 m above the adjacent plain (Baikov and Sedletskiy, 1992); both have reported occurrences of potash. Potash has been reported in the cupola of the Alimtay diapir (fig. 4-3*A*).

Several salt diapirs of probable Upper Jurassic or possibly Lower Cretaceous age are exposed approximately 60 km west-southwest of Konduz in northern Afghanistan (fig. 1-2). The Taqcha Khana salt dome (also known locally as Namakab, after the local river that cuts it and makes the downstream water too salty to drink; fig. 1-2) is several kilometers in diameter (Kulke, 1972). This salt deposit is currently being mined for rock salt by using primitive (hand) mining methods. The rock salt is finely crystalline and light-gray to red-brown (Mennessier, 1963). Rock salt of the Chal-I and Chal-II occurrences (fig 1-2) has been mined in the past and workings extend to depths of about 20 m (Mikhalov and others, 1967; Abdullah and others, 1977).

Assessment

The modest amount of specific information available for the Afghan-Tajik tract is not sufficient to conduct a quantitative estimate of undiscovered potash resources in halokinetic potash-bearing salt deposits (appendix B).

Russian seismic data (fig 4-3*B*; Bekker, 1996) suggest that virtually all Jurassic salt lies well below the 3-km assessment depth limit, notably excepting diapirs and fault blocks raised closer to the surface by halokinesis and tectonics. While the assessment team was able to identify areas where tectonics and halokinesis could have resulted in potash-bearing salt above the assessment depth limit, no further refinement of the tract was possible.

Delineation of the Permissive Tract

The boundary of the Afghan-Tajik tract represents our best estimate of the extent of Upper Jurassic salt within the Afghan-Tajik Basin. We know that the Upper Jurassic salt hosts significant potash deposits in the Gissar tract immediately to the west, and that potash occurs in salt diapirs in at least six locations within this basin (table 4-1). Potash is most likely to occur within salt structures in this tract, but the total number of salt structures is unknown; therefore, we used the probable extent of Upper Jurassic salt as the main limit of potash-bearing salt structures of that age. The Afghan-Tajik tract boundaries (fig. 4-1) were thus determined by contacts or faults dividing Upper Jurassic and younger rocks from Middle Jurassic and older rocks. This approach implicitly accepts Nikolaev's (2002) assertion that Jurassic salt underlies most of the basin.

The western boundary of the Afghan-Tajik tract shares the eastern boundary of the Gissar tract and is roughly coincident with the eastern boundary of the Baisun Graben (fig. 4-2). Northern, northeastern, and eastern tract boundaries are defined by the extent of Upper Jurassic sedimentary rock map units as shown on the Central Asia geologic map of Seltmann and others (2005). The southern boundary in Afghanistan was inferred from the geologic map of Afghanistan by Doebrich and Wahl (2006) to be the edge of the North Afghan High (fig. 4-2).

Mineral Occurrences

There is no historic production of potash in the Afghan-Tajik tract, and there are no known potash deposits. Six occurrences have been reported (table 4-1); only one is specifically located (fig. 4-1). Vysotskiy and others (1988) report that three horizons of rock salt in the cupola of the Alimtay salt dome contain sylvite. Concentrations of as much as 10.4 percent are reported, but it is not clear if this percentage represents the sylvite-carnallite content or the concentration of potash as K_2O or KCl. In addition, Mineral Mining plc has reported potash at an undisclosed location in the western part of the Afghan-Tajik tract (Newswire Today, 2011) and stringers of potash have been reported in some salt domes in the eastern part of the tract (Sedletskiy, 1969). Potash deposits with known reserves and (or) resources have been reported in several locations in the adjacent Gissar tract to the west where there is one mine in production and at least one additional mine being developed.

Exploration History

There was no reported exploration for potash within the Afghan-Tajik tract through 2010; available information on halokinetic salt structures is largely a product of Soviet-era oil exploration and the few surface salt exposures in this arid environment. Several structures have been mined for salt by using primitive (hand) mining methods.

In 2011, Mineral Mining plc was reported to be exploring a potash prospect in Tajikistan "90 km southeast of the Uzbekistan border" (Newswire Today, 2011). Exploration has included "geophysical work" and a single 1,065-m-deep drill hole that encountered several 3–6-m-thick intervals containing 40–60 percent potash salts, apparently disrupted by postdepositional faulting. Although no age or specific location was given in the report, the described location of this prospect

Table 4-1. Known potash occurrences within the Afghan-Tajik tract, Uzbekistan, Tajikistan, and Afghanistan.

Name	Latitude	Longitude	Comments	Reference
Alimtay	37.749	69.432	Sylvite reported in three horizons of this salt structure	Vysotsky and others (1988); Bekker (1996)
Khodzhasartis	37.946	69.662	Dispersed impregnations and very fine intercalations of sylvite in rock salt	Sedletsky (1969); Rundkvist (2001)
Khodzhamumyn	37.729	69.637	Dispersed impregnations and very fine intercalations of sylvite in rock salt	Sedletsky (1969); Rundkvist (2001)
Nurek	37.937	69.530	Small amounts of potash minerals reported; potash averages less than 1 percent	Sedletsky (1969); Rundkvist (2001)
Tanapchi	37.916	69.503	Dispersed impregnations and very fine intercalations of sylvite in rock salt	Sedletsky (1969); Rundkvist (2001)
Unnamed occurrence[1]			"Several" intervals containing 40–60 percent potash salts	Newswire Today (2011)

[1]Location is described as "90 km southeast of the Uzbekistan border."

is within the area included in this tract. Plans to continue exploration with an additional drill hole were mentioned in the short report, but no other information on the occurrence was provided.

Data Availability

Most data for the Afghan-Tajik tract (table 4-2) were acquired in the 1970s and 1980s incidental to oil and gas exploration. The authors believe that cross sections (fig. 4-3*B*) showing depth to Jurassic salt along with subsurface structure, are largely derived from seismic and gravity profiling and well logs (generally these are referred to as “geophysical data” or “геофизическим данным”). Two 1:500,000-scale geologic maps (Seltmann and others, 2005) were available to the authors to use as a base, but only very coarse-resolution magnetic and gravity data were accessible. Original seismic data and well logs were not available. In these older Russian reports, figures were crudely sketched with little to register them against, and text was often abstracted from earlier, apparently unpublished, reports.

Discussion

Based on seismic-reflection data, most of the Jurassic salt in the Afghan-Tajik tract lies below the 3-km assessment depth limit (Bekker, 1996; figs. 4-3*A*,*B*). Although only six occurrences of potash are known within the tract, there is still the possibility that significant deposits of potash might exist. The Gissar tract to the west includes all known potash deposits in the CASB. They are Jurassic in age and were uplifted in the Miocene during the formation of the Gissar Flank Mega Anticline (Fedin, 1981; Vysotskiy and others, 1988; Seltmann and others, 2005; see fig. 4-2). Continuation of this Jurassic mineralized salt, albeit at greater depth, into the Afghan-Tajik tract is geologically reasonable. There is no information to judge how far east any potash extends, though the reported occurrence of sylvite at Alimtay (fig. 4-1) indicates potential to at least that longitude. No significant potash mineralization has been reported in the Jurassic salt diapirs being worked for salt in Tajikistan and Afghanistan, although the occurrence of potash has been reported at a handful of sites. Areas of potash deposition can be very large, such as the potash mineralization in the Elk Point Basin of Canada, where potash in the Patience Lake Member of the Prairie Formation occurs over an area larger than 125,000 km^2. Alternatively, areas of mineralization can be small; potash in the Mulhouse Basin of France and Germany only occupies an area of about 438 km^2.

The assessment team felt that one or more deposits exist within 3 km of the surface, especially in shallow areas resulting from the Gissar uplift on the west. However, based on the lack of data and exploration, the complexities of potash deposits hosted by halokinetic salt, and the relative inaccessibility of the area, it is unlikely that potash deposits within this tract will be discovered and developed in the short to medium term.

Table 4-2. Principal sources of information for the Afghan-Tajik tract, Uzbekistan, Tajikistan, and Afghanistan.

[GIS, geographic information system; NA, not applicable]

Theme	Name or title	Scale	Citation
Geology	Jurassic Basins	Unknown	Vysotskiy and others (1988)
	Some aspects of the genesis of halogenic sequences	Unknown	Baikov and Sedletskiy (2001)
	Tectonics of the Afghan-Tajik depression	Varies	Bekker (1996)
	Afghan-Tajik Depression	Unknown	Nikolaev (2002)
	Tellus sedimentary basins of the world	Varies	Fugro-Robertson, Ltd. (2010)
	Mineral deposits map of Central Asia	1:500,000	Seltmann and others (2005)
	Geologic and mineral resource map of Afghanistan	1:850,000	Doebrich and Wahl (2006)
	Geologic map of Turkmenistan	1:500,000	Mirzakhanov (1989)
Subsurface geology	Petroleum resource potential GIS of northern Afghanistan	Varies	Steinshouer and others (2006)
	Petroleum geology and resources of the Amu-Darya Basin	Varies	Ulmishek (2004)
Geophysics	Petroleum resource potential GIS of northern Afghanistan	Various	Steinshouer and others (2006)
Exploration	Lithofacies and potassium potential of Upper Jurassic halogen deposits in Central Asia	Unknown	Sedletskiy and Fedin (1981)
	Potassium-bearing basins of the world	Unknown	Vysotskiy and others (1988)
	World survey of potash resources	Unknown	British Sulphur Corporation (1979)
	Mineral Mining PLC—Research continues at Tajikistan potash deposit	NA	Newswire Today (2011)
Mineral occurrences	Jurassic Basins	NA	Vysotskiy and others (1988)
	Potash salts of Central Asia	NA	Sedletskiy (1969)
	Mineragenetic map of Russian Federation and adjacent states	1:2,500,000	Rundkvist (2001)

This page intentionally left blank

Chapter 5. Spatial Databases for Resource Assessments

By Pamela Dunlap[1]

Introduction

Spatially referenced data for the distribution of mineral deposits and areas permissive for undiscovered deposits are important elements of mineral resource assessments. When used in conjunction with a common set of descriptive data and a variety of other types of spatial data, this information can be used to conduct detailed resource assessments to understand the likely distribution and availability of potash resources to meet future needs and to help inform resource policy.

The datasets and documentation presented in this report were developed primarily for use with Esri software, in particular ArcGIS version 10 or higher. Geographic information system (GIS) terminology specific to Esri software is used throughout this report; definitions of GIS-related terms and concepts are available online at http://support.esri.com/en/knowledgebase/Gisdictionary/browse [last accessed December 3, 2015].

Overview of Spatial Databases

The spatial databases (digital data files) released in this report are listed and briefly described in table 5-1. Each spatial database is provided in vector format as a feature class in the Esri file geodatabase (FGDB) **CentralAsia_potash.gdb**. The geodatabase is packaged with metadata files and a brief descriptive ASCII text file in the compressed archive file **sir20105090aa_gis.zip**, available at http://dx.doi.org/10.3133/sir20105090AA.

FGDC-compliant (Federal Geographic Data Committee; www.fgdc.gov) metadata provides information about the spatial databases. Embedded metadata in extensible markup language (XML) format can be viewed in ArcGIS 10. Metadata are also provided in standalone XML and Adobe PDF (portable document file) format files (table 5-1).

CentralAsia_deposits Spatial Database

The deposits spatial database, the FGDB feature class CentralAsia_deposits, contains vector (point features) and descriptive data for 66 potash sites representing areas, leases/concessions/permits, mines, mineral occurrences, and salt structures in the Central Asia Salt Basin. Brief descriptions of fields and values in this spatial database are provided in table 5-2; a "<NULL>" entry in any field indicates that the value is not known.

CentralAsia_thickness Spatial Database

The regional thickness spatial database, the FGDB feature class CentralAsia_thickness, contains vector information (point features) for thickness of the potash-bearing intercepts in drill holes and at mineral occurrence sites as compiled from Rayevskiy and Fiveg (1973), Sedletskiy and Derevyagin (1980), Fedin (1981), Sedletskiy and Fedin (1981), Zharkov and others (1982a, 1982b), Khudaikuliev (1986), and Vysotskiy and others (1988). Brief descriptions of fields and values in this spatial database are provided in table 5-3.

CentralAsia_tracts Spatial Database

The permissive tracts spatial database, the FGDB feature class CentralAsia_tracts, contains vector information (polygon features) for each tract, in addition to descriptive data used in the mineral resource assessment and the quantitative calculations (table 2-1). Brief descriptions of fields and values in the spatial database are provided in table 5-4.

[1]U.S. Geological Survey, Tucson, Arizona, United States.

Table 5-1. List and description of spatial databases (digital data files) in this report.

File name	File description
Compressed archive file containing spatial databases, associated metadata files, and readme.txt	
sir20105090aa_gis.zip	Geographic information system (GIS) and associated files: Esri file geodatabase (FGDB), metadata (*.pdf and *.xml), and readme.txt (ASCII text).
File geodatabase (FGDB) (located in folder \CentralAsia)	
CentralAsia_potash.gdb	FGDB (ArcGIS 10) contains spatial databases prepared for and used in the mineral resource assessment for undiscovered potash in the Central Asia Jurassic Salt Basin, Turkmenistan, Uzbekistan, Tajikistan, and Afghanistan.
FGDB feature classes in CentralAsia_potash.gdb	
CentralAsia_deposits	FGDB feature class (points) for sixty-two potash deposits (includes areas, leases/concessions/permits, mines, mineral occurrences, and salt structures).
CentralAsia_thickness	FGDB feature class (points) of thickness data for potash-bearing intercepts in drill holes and at mineral occurrence sites.
CentralAsia_tracts	FGDB feature class (polygons) of assessment data and results for three tracts permissive for undiscovered potash.
Metadata—Adobe Acrobat PDF (*.pdf) and extensible markup language (XML) format (*.xml) files (located in subfolder \CentralAsia\Metadata)	
CentralAsia_deposits_metadata.pdf/.xml	Metadata for spatial database for deposits.
CentralAsia_thickness_metadata.pdf/.xml	Metadata for spatial database for thickness of potash mineralization.
CentralAsia_tracts_metadata.pdf/.xml	Metadata for spatial database of tract assessment data and results.
ASCII text file (located in subfolder \CentralAsia)	
readme.txt	Brief description of report and associated digital data.

Table 5-2. User-defined fields in the feature attribute table for CentralAsia_deposits.

Field	Description
ID_NO	Unique numeric identifier.
SITE_NAME	Mineralized feature.
ALT_NAMES	Known synonym.
TYPE_REC	Site type.
COUNTRY	Country.
LATITUDE	Positive number represents latitude north of the equator.
LONGITUDE	Positive number represents longitude east of the Greenwich meridian.
BASIN	Evaporite basin.
BASIN_TYPE	Type of basin.
TRACT_NAME	Informal name of permissive area for undiscovered potash.
DEP_TYPE	Type of mineralization style.
COMMODS	Significant commodities; multiple commodities are listed in approximate order of significance.
K_MINERALS	Potash mineral(s) known to be present.
OTHER_MINS	Other mineral(s) of significance or interest.
AGE	Age of evaporite sequence, as taken from source(s).
UNIT	Formal and (or) informal name of stratigraphic rock unit(s) that contain mineralization (as derived from sources).
LITH	Lithology and (or) composition of the host rock and (or) unconsolidated sediment.
SALT_STR	Name of salt structure, if any, associated with mineralized site (where DEP_TYPE is 'evaporite-halokinetic').
K_THK_M	Reported thickness of potash horizon(s).
K_DEPTH_M	Reported depth to top of potash.
GEOL_NOTES	Additional geologic information.
AV_K2O_PCT	Reported average potash (K2O) not associated with reported production or reserve information, in percent.
FIGURES	Image(s) portraying representative geology, in PDF format; includes name of folder where file is stored (no figures were available/included for technical review).
P_STATUS	Production and (or) development status, queried where uncertain, year included when known.
P_FIRST_YR	Year(s) of first known production.
P_LAST_YR	Year(s) of last known production.
COMPANY	Last known owner and (or) operator; may include year for which owner or operator was confirmed.
P_ORE_MT	Reported production of ore, in million metric tons; numbered entries correspond to those in P_REFS.
P_K2O_MT	Reported production of potash, in million metric tons; numbered entries correspond to those in P_REFS.
P_K2O_PCT	Grade of reported production of potash (K2O), in percent; numbered entries correspond to those in P_REFS.
P_REFS	Abbreviated citation(s) for source reference(s) for production data; full citations are provided in report; numbered entries correspond to numbered entries in P_ORE_MT, P_K2O_MT, P_K2O_PCT, and P_YEARS.
P_YEARS	Year(s) for which production data were reported; numbered entries correspond to those in P_REFS.
MEAS_INV	Categorical field denoting if reserves or resources were reported.
RR_ORE_MT	Reported reserves and (or) resources of ore, in million metric tons; modifying abbreviations are listed in table 4 in report; numbered entries correspond to numbered entries in RR_REFS.
RR_K2O_MT	Reported reserves and (or) resources of potash (K2O), in million metric tons; modifying abbreviations are listed in table 4 in report; numbered entries correspond to numbered entries in RR_REFS.
RR_K2O_PCT	Reported reserves and (or) resources of potash (K2O), in percent; numbered entries correspond to numbered entries in RR_REFS.
RR_REFS	Abbreviated citation(s) for source reference(s) for resource and (or) reserve data; full citations are provided in report; numbered entries correspond to numbered entries in RR_ORE_MT, RR_K2O_MT, RR_K2O_PCT, and RR_YEARS.
RR_YEARS	Year(s) for which resource and (or) reserve data were reported, if known; numbered entries correspond to those in RR_REFS.
MISC_NOTES	Additional information.
SHORT_REFS	Abbreviated citation(s) for source reference(s).

Table 5-3. User-defined fields in the feature attribute table for Central Asia_thickness.

Field	Description
LATITUDE	Positive number represents latitude north of the equator.
LONGITUDE	Positive number represents longitude east of the Greenwich meridian.
THICK_M	Total thickness of potash-bearing intercept, in meters.
REFERENCES	Short citation (author, year) for reference.
SITE_NAME	Identifier for site.
SITE_TYPE	Type of site (drill hole or occurrence).

Table 5-4. User-defined fields in the feature attribute table for CentralAsia_tracts.

Field	Description
Coded_ID	Coded, unique identifier assigned to permissive tract.
Tract_name	Informal name of permissive tract.
Unregcode	Three digit United Nations code for the region that underlies most of the permissive tract.
Country	Country(ies) in which permissive tract is located, hyphen-delimited.
Commodity	Primary commodity being assessed.
Dep_type	Name of the deposit type assessed.
Age	Age of geologic feature assessed.
Unit	Rock unit in which potash mineralization occurs.
Geology	Geologic feature assessed.
Asmt_date	Year assessment was conducted.
Asmt_methd	Assessment method used.
Asmt_depth	Maximum depth beneath the Earth's surface used for the assessment, in kilometers.
Thickness	How thickness variation was determined for the assessment.
Volume_km3	Volume of tract (in cubic kilometers) for areas of carnallite and areas of non carnallite in the format TRRN(min,max,mode) where TRRN is SYSTAT code for triangular distribution, min = minimum value, max = maximum value, mode = mode or average value.
Density	Specific gravity used in assessment calculations.
Tonnage	Tonnage of mineralized rock, in billions of tons (gigatons), in the format TRRN(min,max,mode) where TRRN is SYSTAT code for triangular distribution; min = minimum value, max = maximum value, mode = mode or average value.
K2O grade	K_2O grade (as percent K_2O) for areas of carnallite and areas of non-carnallite; distribution specified in the format ZRN(mean,s.d.) where ZRN is SYSTAT code for normal distribution and s.d. = standard deviation.
Embayments	Embayments (as percent of area); distribution specified in the format TRRN(min,max,mode) where TRRN is SYSTAT code for triangular distribution, min = minimum value, max = maximum value, mode = mode or average value.
Anomalies	Anomalies (as percent of area); distribution specified in the format TRRN(min,max,mode) where TRRN is SYSTAT code for triangular distribution, min = minimum value, max = maximum value, mode = mode or average value.
Other_adj	Other needed adjustments.
K2O_known	Known resources of potash, in billion metric tons (gigatons).
K2O_median	Median of undiscovered resources of contained potash, in billion metric tons (gigatons).
K2O_mean	Mean of undiscovered resources of contained potash, in billion metric tons (gigatons).
K2O_densit	Mean of undiscovered resources of contained potash divided by area of permissive tract, in million metric tons K_2O per square kilometer.
Estimators	Names of people on the estimation team (listed alphabetically).
Area_km2	Area of permissive tract, to three significant figures, in square kilometers.

References Cited

Abdullah, S., Chmiriov, V.M., Stazhilo-Alekseev, K.F., Dronov, V.I., Kofarsky, A.K., and Malyarov, E.P., 1977, Mineral resources of Afghanistan: Kabul, Afghanistan Geological and Mines Survey, 419 p.

Agapito Associates, Inc., 2011, Satimola, Ltd.—Kazakhstan; potash and borate mine planning: Agapito Associates, Inc. Web page, accessed April 4, 2011, at http://www.agapito.com/2010/12/satimola-potash-and-borate-mine-planning E2, 80-94 kazakhstan/.

Ansher Holding Limited, 2010, Uzbekistan develops potash fertilizer industry: News Release 8 January 2010, accessed May 14, 2010, at http://www.ansherholding.com/we/news/73854.

Anthony, J.W., Bideaux, R.A., Bladh, K.W., and Nichols, M.C., 1997, Handbook of mineralogy, Volume III—Halides, hydroxides, oxides: Tucson, Ariz., Mineral Data Publishing, 628 p.

Anthony, J.W., Bideaux, R.A., Bladh, K.W., and Nichols, M.C., 2003, Handbook of mineralogy, Volume V—Borates, carbonates, sulfates: Tucson, Ariz., Mineral Data Publishing, 813 p.

Ashurmatov, D., 2006, Uzbekistan to extend its chemical industry: Uzbekistan Today, December 8, 2006, 2 p., accessed January 7, 2009, at http://www.ut.uz/eng/business/uzbekistan_to_extend_its_chemical_industry.mgr.

Back, M.E., and Mandarino, J.A., 2008, Fleischer's glossary of mineral species 2008: Tucson, Ariz., The Mineralogical Record Inc., 344 p.

Baikov, A.A., and Sedletskiy, V.I., 1992, Growth rate of salt structures: Lithology and Mineral Resources, v. 27, no. 3, p. 262–268.

Baikov, A.A., and Sedletskiy, V.I., 2001, Some aspects of the genesis of halogenic sequences—Evidence from the Central Asia halogenic basin: Lithology and Mineral Resources v. 36, no. 6, p. 582–593.

Bawiec, W.J., and Spanski, G.T., 2012, Quick-start guide for version 3.0 of EMINERS—Economic Mineral Resource Simulator: U.S. Geological Survey Open-File Report 2009–1057, 26 p., accessed June 30, 2012, at http://pubs.usgs.gov/of/2009/1057/. [This report supplements USGS OFR 2004–1344.]

Bekker, Y.A., 1996, Tectonics of the Afghan-Tajik Depression: Geotectonics, v. 30, no. 1, p. 64–70.

Belarusian Telegraph Agency, 2010, Belarus' geologists start exploring Garlyk deposit in Turkmenistan: Belarusian Telegraph Agency Web page, accessed October 27, 2011, at http://news.belta.by/en/news/econom?id=541134.

Belelovskiy, M.L., Sedletskiy, V.I., and Korobka, V.S., 1971, Salt tectonics of the southwestern Gissar meganticline and the Afghan-Tadzhik Trough: Geotectonics, v. 2, p. 116–122.

Belenitskaya, G.A., 2000, Distribution pattern of hydrogen sulphide-bearing gas in the former Soviet Union: Petroleum Geoscience, v. 6, p. 175–187.

Blackbourn, Graham, 2008, Enclosure 2—Amu Dar'ya Basin and surrounding areas—Generalized location map showing major structural elements, hydrocarbon provinces, hydrocarbon fields and well locations: Blackbourn Geoconsulting, scale 1:1,350,000, accessed January 7, 2009, at http://www.blackbourn.co.uk/downloads/Amu-Darya-Enclosure-2.pdf.

British Sulphur Corporation Limited, 1979, World survey of potash resources (3rd ed.): London, British Sulphur Corporation Limited, 138 p.

British Sulphur Corporation Limited, 1984, World survey of potash resources (4th ed.): London, British Sulphur Corporation Limited, 145 p.

Canadian Institute of Mining, Metallurgy and Petroleum (CIM), 2005, CIM definition standards—For mineral resources and mineral reserves: Canadian Institute of Mining, Metallurgy and Petroleum Web page, accessed February 3, 2015, at http://web.cim.org/UserFiles/File/CIM_DEFINITON_STANDARDS_Nov_2010.pdf.

Canadian Institute of Mining, Metallurgy and Petroleum (CIM), 2012, Potash: Canadian Institute of Mining, Metallurgy and Petroleum Web page, accessed February 3, 2015, at http://web.cim.org/UserFiles/File/Potash-Estimation-Guidelines.pdf.

Cassard, D., 2006, Tethyan Plate Tectonics: Lausanne University and (French) Bureau de Recherches Géologiques et Minières Web page, accessed February 3, 2015, at http://giseurope.brgm.fr/Tethyan/Permian-Triassic_boundary_-_248_Ma.gif.

Chinese Academy of Sciences, 2010, ISL expands technological shares in China-Laos Minerals Development and Investment Corp.: Chinese Academy of Sciences Web page, accessed June 28, 2011, at http://english.cas.cn/Ne/ICN/201002/t20100206_50775.shtml.

Clarke, J.W., 1986, Petroleum geology of the Amu-Dar'ya province of Soviet Central Asia: American Association of Petroleum Geologists Bulletin, v. 70, no. 5, p. 573–574.

Clarke, J.W., 1988, Petroleum geology of the Amu-Dar'ya gas-oil province of Soviet Central Asia: U.S. Geological Survey Open-File Report 88-272, 59 p. [Also available at http://pubs.usgs.gov/of/1988/0272/report.pdf.]

Cohen, K.M, Finney, S.C., Gibbard, P.L., and Fan, J., 2013, The ICS International Stratigraphic Chart: International Committee on Stratigraphy, accessed February 1, 2016, at http://www.stratigraphy.org/ICSchart/ChronostratChart2015-01.jpg.

Doebrich, J.L., and Wahl, R.R., 2006, Geologic and mineral resource map of Afghanistan: U.S. Geological Survey Open-File Report 2006-1038, scale 1:850,000. [Also available at http://pubs.usgs.gov/of/2006/1038/.]

Duval, J.S., 2012, Version 3.0 of EMINERS—Economic Mineral Resource Simulator: U.S. Geological Survey Open-File Report 2004–1344, accessed June 30, 2012, at http://pubs.usgs.gov/of/2004/1344/.

Environmental Resources Management, 2009, Independent environmental and social due diligence assessment, Gremyachinskoye potash mine and processing plant, Volgograd, Russian Federation—Non-technical summary: Moscow, Environmental Resources Management, 32 p.

Fedin, O.V., 1981, Otsenka perspektiv kaliyenosnosti verkhneyurskikh solyanykh otlozheniy yuga Sredney Azii [An evaluation of the prospects for potash-bearing capabilities in the Upper Jurassic salt deposits in southern Central Asia], *in* Yanshin, A.L., and Zharkov, M.A., eds., Stroyeniye i usloviya formirovaniya mestorozhdeniy kaliynykh soley [The structure and formation conditions of potash salt deposits]: Novosibirsk, USSR, Izd. Nauka, p. 171–176.

Fugro-Robertson, Ltd., 2005, Fugro Tellus sedimentary basins of the world map: Fugro Robertson, Ltd. Web page, accessed June 7, 2010, at http://gisudril.aapg.org/gisdemo/FugroTellus.html.

Garrett, D.E., 1996, Potash—Deposits, processing, properties, and uses: New York, Chapman and Hall, 734 p.

Gavril'cheva, L.G., 1981, Fatsial'naya zonal'nost' i usloviya osadkonakopleniya solenosnoy formatsii verkhney yury na territorii Vostochnogo Turkmenistana [Facies zoning and conditions of sediment accumulation of Upper Jurassic salt-bearing formations in the territories of eastern Turkmenia], *in* Yanshin, A.L., and Zharkov, M.A., eds., Stroyeniye i usloviya formirovaniya mestorozhdeniy kaliynykh soley [Structure and formation conditions of salt-bearing horizons]: Novosibirsk, USSR, Izd. Nauka, Sibirsk. Otdel., p. 120–127.

Gavril'cheva, L.G., and Pashaev, M.S., 1993, Stroyeniye verkhneyurskikh otlozheniy i proslezhivayemost' otrazhayushchikh seysmicheskikh gorizontov v amudar'inskoy sineklize [Structure of Upper Jurassic deposits and traces of seismic reflection of horizons at Amu-Darya syneclise]: Geologiya Nefti i Gaza, v. 11, p. 15–19.

General Mining Corporation Ltd., 2009, 2009 prospectus: Perth, Western Australia, General Mining Corporation Ltd., 13 p., accessed September 28, 2010, at www.generalmining.com.

Hammarstrom, J.M., Zientek, M.L., Orris, G.J., and Taylor, C.D., 2010, Global Mineral Resource Assessment—Challenges and opportunities for developing and refining assessment methods [abs.]: Geological Society of America Denver 2010 Annual Meeting Final Program Web page, accessed November 22, 2010, at http://gsa.confex.com/gsa/2010AM/finalprogram/abstract_178026.htm.

Harben, P.W., and Kuzvart, M., 1996, Industrial minerals—A global geology: London, Industrial Minerals Information Ltd., 462 p.

Harris, D.P., 1984, Mineral resources appraisal—Mineral endowment, resources and potential supply—Concepts, methods, and cases: New York, Oxford University Press, 445 p.

Henley, Stephen, 2004, Russian mineral reporting: Mining Journal, August 20, p. 18–21.

Henley, Stephen, and Allington, Ruth, 2010, Reserves classification systems around the world: Pan-European Reserves Reporting Committee, 51 p., accessed August 21, 2015, at http://www.vmine.net/PERC/documents/reserves-classification-systems-around-the-world-FINAL.pdf.

ITE Gulf FZ LLC, 2010, Uzbekistan develops potash fertilizer industry: Dubai, ITE Gulf FZ LLC Web page, accessed January 7, 2009, at http://ww.itegulf.com/index.php?part=newsandnews_id=70.
[NOTE: This webpage no longer available as of September 7, 2015; authors have PDF copy.]

Jasinski, S.M., 2015, Potash [advance release], in Metals and minerals: U.S. Geological Survey Minerals Yearbook 2013, v. I, p. 58.1–58.6. [Also available at http://minerals.usgs.gov/minerals/pubs/commodity/potash/myb1-2013-potas.pdf.]

Khudaikuliev, Kh., 1986, Osnovniye chyerti stroyeniya vyerhnyeyoorskoy galogyennoy formatsii i yeye rol' v prognozirovanii po gryebyennih rifov v amudar'inskoy [Main structural features of the Upper Jurassic halogenous formation and its role in forecasting buried reefs in the Amu Darya syneclise], *in* Yanshin, A.L., and Merzlyakov, G.A., eds., Novye dannye po geologii solenosnykh basseinov Sovetskogo Soyuza [New data on the geology of saliferous basins of the Soviet Union]: Moscow, Nauka, p. 101–115.

Khudaikuliev, Kh., 1989, Structure of the Upper Jurassic halogen complex and its role in predicting buried reefs in the Amu-Dar'ya regional low: Petroleum Geology, v. 23, no. 7–8, p. 247–252.

Klett, T.R., Ulmishek, G.F., Wandrey, C.J., Agena, W.F., and The U.S. Geological Survey-Afghanistan Ministry of Mines and Industry Joint Oil and Gas Resource Assessment Team, 2006, Assessment of undiscovered technically recoverable conventional petroleum resources of northern Afghanistan: U.S. Geological Survey Open-File Report 2006–1253, 237 p. [Also available at http://pubs.usgs.gov/of/2006/1253/of2006-1253.pdf.]

Kulke, H., 1972, Zur Petrographie des Steinsalzes der Diapire von Taqca Khana und Kalafgan (Nordost-Afghanistan) [Petrography of halite from the Taqca Khana and Kalafgan diapirs, northeastern Afghanistan]: Der Aufschluss, v. 23, no. 5, p. 145–154.

Kutuzov, A.P., and Popov, V.S., 1976, Novyye dannyye po geologii Donguzsyrta (Yugo-Vostochnaya Turkmeniya) [New data on the geology of Donguzsyrt, Southeast Turkmenia]: Sovetskaya Geologiya, v. 1976, no. 9, p. 137–142.

Lefond, S.J., 1969, Handbook of world salt resources: New York, Plenum Press, 384 p.

Leith, W., and Simpson, D.W., 1986, Earthquakes related to active salt doming near Kulyab, Tadjikistan, USSR: Geophysical Research Letters, v. 13, no. 10, p. 1019–1022.

Levine, R.M, and Wallace, G.J., 2001, The mineral industries of the Commonwealth of Independent States; Armenia, Azerbaijan, Belarus, Georgia, Kazakhstan, Kyrsyzstan, Moldova, Russia, Tajikistan, Turkmenistan, Ukraine, and Uzbekistan: U.S. Geological Survey Minerals Yearbook, 66 p.

Lomas, Susan, 2002, Technical report for the Udon North Deposit, Udon Thani Concession, Thailand, prepared for Asia Pacific Potash Corporation: Vancouver, British Columbia, MRDI Canada [variously paged.]

Luchnikov, V.S., 1981, O genezise solyanykh tel solyanokupol'noy oblasti Yugo-Zapadnogo Tadzhikistana [The genesis of salt bodies in the salt dome region of southwestern Tadzhikistan], *in* Yanshin, A.L., and Zharkov, M.A., eds., Stroyeniye i usloviya formirovaniya mestorozhdeniy kaliynykh soley [The structure and formation conditions of potash salt deposits]: Novosibirsk, USSR, Izd. Nauka, p. 182–186.

Luchnikov, V.S., 1982, Upper Jurassic halogen deposits of southeast Central Asia: Petroleum Geology, v. 20, no. 7, p. 296–298. [Also see Trudy Inst. Geol. i Geofiz. 1982, v. 535, p. 19–33.]

Magen, H., 2010, Current world potash situation and future outlook, AFA International Annual Fertilizers Forum and Exhibition: Cairo, Egypt, International Potash Institute Web page, accessed August 25, 2011, at http://www.ipipotash.org/udocs/Current_World_Potash_Situation_and_Future_Outlook_paper.pdf.

Mennessier, G., 1963, Sur l'âge de la série salifère de Namakab en Afghanistan [On the age of the Namakab salt series in Afghanistan]: Comptes Rendus Hebdomadaires des Seances de l'Academie des Sciences, v. 256, no. 6, p. 1319–1320.

Mikhalov, K.Y., Kolchanov, V.P., Kulakov, V.V., Pashkov, B.R., Androsov, M.A., and Chalyan, M.A., 1967, Report on geological surveying and prospecting for coal at scale 1:200,000 (sheets 222–C, 502–D, 503–B; part of sheets 221–F, 222–D, 222–F, 502–C, 502–F, 503–C, 503–D, 503–E, 504): Afghanistan Department of Geological and Mineral Survey, scale 1:200,000.

Mirzakhanov, M.K., ed., 1989, Gyeologichyeskaya karta Toorkmyenskoy SSR [Geologic map of Turkmenistan]: Ministry of Geology of USSR and Turkmengeologiya, 1 map on 12 sheets, scale 1:500,000.

Neuendorf, K.K.E., Mehl, Jr., J.P., and Jackson, J.A., 2005, Glossary of geology (5th ed.): Alexandria, Virginia, American Geological Institute, 799 p.

Newswire Today, 2011, Mineral Mining plc—Research continues at Tajikistan potash deposit: San Francisco, Limelon Advertising and Communications Newswire Today Web page, accessed February 16, 2011, at http://www.newswiretoday.com/news/85532.

Nikolaev, V.G., 2002, Afghan-Tajik Depression, architecture of sedimentary cover and evolution: Russian Journal of Earth Sciences, v. 4, no. 6, p. 399–421.

Orris, G.J., Cocker, M.D., Dunlap, P., Wynn, J.C., Spanski, G.T., Briggs, D.A., and Gass, L., with contributions from Bliss, J.D., Bolm, K.S., Yang, C., Lipin, B.R., Ludington, S., Miller, R.J., and Slowakiewicz, M., 2014, Potash—A global overview of evaporite-related potash resources, including spatial databases of deposits, occurrences, and permissive tracts: US Geological Survey Scientific Investigations Report 2010–5090–S, 76 p., and spatial data, http://dx.doi.org/10.3133/sir20105090S.

Osichkina, R.G., 1978, Geochemical features and development conditions of salt deposits in Upper Jurassic halogen formation of South-central Asia: Lithology and Mineral Resources, v. 13, no. 4, p. 467–474.

Osichkina, R.G., 2006, Regularities of trace element distribution in water–salt systems as indicators of the genesis of potassium salt rocks—An example from the Upper Jurassic halogen formation of Central Asia: Geochemistry International, v. 44, no. 2, p. 164–174.

Ourchemical, 2011, Found in western Qaidam salt and brines: Shenzhen, China, Ourchemical Web page, accessed August 16, 2011, at http://www.ourchemical.com/catalogs_14/145398-73-8.html.

Pebble Creek Mining Ltd., 2008, Pebble Creek applies for permits to explore potash on 6,000 square kilometers in Rajasthan, India: Vancouver, British Columbia, Pebble Creek Mining Ltd. Web page, accessed July 29, 2008, at http://www.pebcreek.com/pr_072908.pdf.

Petrov, N.P., and Chistyakov, P.A., 1964, Lithologia solvevykh I krasnocvetnykh otljzenij yugo-eapadnykh otrogov gissara [Lithology salt and red deposits southwestern Gissar spurs]: Tashkent, Uzbekistan, Izdatelstvo “Nauka” Uzbekskoy SSR, 221 p.

Popov, V.S., 1968, Upper Jurassic evaporites of intracontinental marine saline basins of Central Asia: Lithology and Mineral Resources, v. 1968, no. 1, p. 45–55.

Popov, V.S., 1988, Potassium and sulfur contents of Late Jurassic halogenic rocks in Central Asia: Tashkent, Fan. [In Russian.]

Popov, V.S., Mirakhmedov, M. and Rubanov, I.V., 1984, Karakalpakiya; novyy perspektivnyy rayon po proizvodstvu beskhlornykh kaliynykh udobreniy [Karakalpakaya—A new prospective region for the production of non-chloride potash fertilizers]: Zapiski Uzbekistanskogo Otdeleniya V’sesoyuznogo Mineralogicheskogo Obshchestva, v. 37, p. 135–137.

Popov, V.S., and Osichkina, R.G., 1973, On the behavior of bromine during halogenesis in the Upper Jurassic Saline Basin of Middle Asia: Geochemistry International, v. 10, p. 294–305.

Rayevskiy, V.I., and Fiveg, M.P., 1973, Mestorozhdeniya kaliynykh soley SSSR; metody ikh poiskov i razvedki [Deposits of potassium salts in the USSR; methods of exploration and surveying]: Leningrad, Izd. Nedra, Leningr. Otd., 344 p.

Rodnov, Y.N., Belkina, I.L., Bystrova, G.P., Zabotkin, L.V., Larin, A.M., Sviridov, A.P., Simonova, L.S., and Smolenkov, V.I., 2001, *in* Rundkvist, D.V., ed., Mineragenetic map of Russian Federation and adjacent states (within the boundaries of former USSR): Ministry of Natural Resources of Russian Federation, State Research and Development Enterprise AEROGEOLOGIA, scale 1:2,500,000, one map on 18 sheets.

Root, D.H., Menzie, W.D., and Scott, W.A., 1992, Computer Monte Carlo simulation in quantitative resource estimation: Nonrenewable Resources, v. 1, no. 2, p. 125–138.

Roskill Information Services, 1989, The economics of potash (2d ed.): London, Roskill Information Services Ltd., 121 p.

Rundkvist, D.V., 2001 Metallogenic belts, provinces, and epochs of the U.S.S.R.: Episodes, v. 7, p. 28–32.

Schultz, H., Bauer, G., Schachl, E., Hagedorn, F., and Schmittinger, P., 2000, Potassium compounds, *in* Ullmann’s Encyclopedia of Industrial Compounds (7th ed.): New York, Wiley-VCH, 30,000 p.

Schulz, K.J., and Briskey, J.A., 2003, The Global Mineral Resource Assessment Project: U.S. Geological Survey Fact Sheet 053-03. [Also available at http://pubs.usgs.gov/fs/fs053-03/.]

Sedletskiy, V.I., 1969, Potash salts of Central Asia: Lithology and Mineral Resources, v. 1969, no. 5, p. 625–633.

Sedletskiy, V.I., Baykov, A.A., and Semenov, G.A., 2000, Tectonics and Late Jurassic halogenesis on Scythian-Turanian Platform: Petroleum Geology, v. 34, p. 43–46.

Sedletskiy, V.I., and Fedin, O.V., 1981, Lithofacies and potassium potential of Upper Jurassic halogen deposits in Central Asia: Lithology and Mineral Resources, v. 16, p. 83–92.

Seltmann, R., Shatov, V., and Yakubchuk, A., 2005, Mineral deposits map of central Asia: London, Natural History Museum, Centre for Russian and Central Asia Mineral Studies [CERCAMS], scale 1:1,500,000 [digital map distributed as Corel Draw file on CD-ROM; dated June 11, 2007].

Semashev, R.G., 1983, O gidrogeologicheskikh usloviyakh gazonakopleniya v Murgabskoy vpadine [Hydrogeologic conditions of gas reservoirs in Murgab Basin]: Geologiya Nefti i Gaza v. 1983, no. 10, p. 43–49.

Shanghai Cooperation Organization for Economic Cooperation, 2006, Construction of Dehkanabad plant of potassium fertilizers on the base of Tyubegatan potash deposit: Shanghai Cooperation Organization for Economic Cooperation [Powerpoint presentation of March 20, 2006], accessed December 23, 2008, at http://www.sco-ec.gov.cn/crweb/scor/upload/4034dehk.ppt.

Singer, D.A., 1993, Basic concepts in three-part quantitative assessments of undiscovered mineral resources: Nonrenewable Resources, v. 2, no. 2, p. 69–81.

Singer, D.A., and Menzie, W.D., 2005, Statistical guides to estimating the number of undiscovered mineral deposits—An example with porphyry copper deposits, *in* Cheng, Qiuming, and Bonham-Carter, Graeme, eds., Proceedings of IAMG—The annual conference of the International Association for Mathematical Geology: Geomatics Research Laboratory, York University, Toronto, Canada, p. 1028–1033.

Singer, D.A., and Menzie, W.D., 2010, Quantitative mineral resource assessment—An integrated approach: New York, Oxford University Press, 219 p.

Steinshouer, D.W., Klett, T.R., Ulmishek, G.F., Wandrey, C.J., Wahl, R.R., Hill, R.J., Pribil, M., Pawlewicz, M.J., King, J.D., Agena, W.F., Taylor, D.J., Amirzada, A., Selab, A.M., Mutteh, A.-S., Haidari, G.N., and Wardak, M.G., 2006, Petroleum resource potential GIS of northern Afghanistan: U.S. Geological Survey Open-File Report 2006-1179. [Also available at http://pubs.usgs.gov/of/2006/1179/.]

Troitskiy, V., Petrov, I., and Grishaev, S., 1998, Industrial minerals of the CIS: Worcester Park, Surrey, England, Industrial Minerals Information Ltd., 135 p.

Ulmishek, G.F., 2004, Petroleum geology and resources of the Amu-Darya Basin, Turkmenistan, Uzbekistan, Afghanistan, and Iran: U.S. Geological Survey Bulletin 2201-H, 38 p. [Also available at http://pubs.usgs.gov/bul/2201/H/.]

U.S. Geological Survey World Energy Assessment Team, 2000, U.S. Geological Survey World Petroleum Assessment 2000—Description and results: U.S. Geological Survey Digital Data Series DDS-60, version 1.1, scale 1:5,000,000, CD-ROM.

Uzbekistan Daily, 2006, Industry and company news: Tashkent, Ansher Capital Web page, accessed December 28, 2007, at http://www.anshergroup.com.

Vakhabov, A., 1986, Osobennosti geologicheskogo stroyeniya nizhney chasti evaporitov verkhney yury v Zapadnom Uzbekistane (na primere Alanskogo rifa) [Characteristics of the geologic structure in the lower part of the Upper Jurassic evaporites in western Uzbekistan; for example, the Alan Reef cap]: Uzbekskiy Geologicheskiy Zhurnal, no. 2, p. 29–34.

Vysotskiy, E.A., Garetskiy, R.G., and Kislik, V.Z., 1988, Yurskiye bassyeyni [Jurassic basins], *in* Kalienosnye basseiny mira [Potassium-bearing basins of the world]: Minsk, Izd. Nauka i Tekhnika, Byelorussian SSR, p. 232–247.

Xi'an Center of Geolgical Survey, 2008, The scientists from China and German associated drilled to obtain the rock core in Qaidam Basin: Xi-an Geological Survey Center Web page, accessed February 26, 2011, at http://www.xian.cgs.gov.cn/english/2008/1124/article_187.html.

Zhang Yongsheng, Zheng Mianping, Qi Wen, Li Hao, and Xiang Renjie, 2005, Investigation of potassium resource, exploitation and utilization in Turkmenistan: Kuangchuang Dishi [Mineral Deposits], v. 24, no. 6, p. 692–696.

Zharkov, M.A., Blagovidov, V.V., Zharkova, T.M., and Merzlyakov, G.A., 1982a, Kvoprosu o stroyenii pozdnyeyoorskih solyenosnih otlozhyeniy Sryednyey Azii [The problem of the structure of Late Jurassic saliferrous sediments of Central Asia], *in* Yanshin, A.L., ed., Osobennosti stroenya osadocgnikh formatsiy [Structural characteristics of sedimentary formations]: Novosibirsk, Trudy Instituta Geologii i Geofiziki, p. 3–18.

Zharkov, M.A., Blagovidov, V.V., Zharkova, T.M., and Merzlyakov, G.A., 1982b, Verkhneyurskiye solenosnye otlozheniya Sredney Azii [Salt deposits of the Upper Jurassic in Central Asia]: Sovetskaya Geologiya, v. 1982, no. 7, p. 58–65.

Zharkov, M.A., Blagovidov, V.V., Zharkova, T.M., and Merzlyakov, G.A., 1982c, Upper Jurassic salt deposits of Central Asia: Petroleum Geology, v. 20, no. 7, p. 291–295.

Additional References

Azimov, P.K., Lebzin, Ye.V., and Ovchinnikov, Yu.M., 1983, Deep structure and problems of completion of the sub-salt sediments of southwest Tajikistan: Petroleum Geology, v. 19, no. 9, p. 426–428.

Baikov, A.A., Berkeliev, K.P., and Zhdanov, B.P., 1974, Geologiya I poleznye iskopaemye Gaurdak-Kugitangskogo raiona Turkmenskoi SSR (Geology and Mineral Deposits of the Gaurdak-Kugitang Region, Turkmen Republic), Rostov-on-Don: Rostov University.

Belopolsky, A.V., and M. Talwani, 1999, Assessment of the greater Caspian region petroleum reserves and their role in the world energy: Houston, Texas, Center for International Political Economy and James Baker III Institute for Public Policy, 3 p.

Brookfield, M.E., and Hashmat, A., 2001, The geology and petroleum potential of the North Afghan platform and adjacent areas in northern Afghanistan, with parts of southern Turkmenistan, Uzbekistan and Tajikistan: Earth-Science Reviews, v. 55, p. 41–71.

Derevyagin, V.S., and Sedletskiy, V.I., 1977, Upper Jurassic evaporites of Ciscaucasia: Lithology and Mineral Resources, v. 12, no. 4, p. 483–490.

Dyman, T.S., Litinsky, V.S., and Ulmishek, G.F., 1999, Geology and natural gas potential of deep sedimentary basins in the former Soviet Union: U.S. Geological Survey Open-File Report 99-381, 36 p. [Also available at http://pubs.usgs.gov/of/1999/0381/report.pdf.]

Kahle, K., and Scherzberg, H., 2000, New potassium-projects as a source for sodium chloride products with a high purity, *in* Geertman, R.M., ed., 8th World Salt Symposium: New York, Elsevier, v. 1, p. 583–588.

Kovin, O.N., Ph.D. Research Proposal—GPR Investigations in Upper Kama potash mines: Rolla, Missouri, University of Missouri Geology and Geophysics Web page, accessed March 20, 2009, at http://gse.mst.edu/.

Lefond, S.J., 1969, Handbook of world salt resources: New York, Plenum Press, 384 p.

Linn, K.O., and Adams, S.S., 1966, Barren halite zones in potash deposits, Carlsbad, New Mexico, *in* Rau, J.L., ed., Second symposium on salt: Cleveland, Ohio, The Northern Ohio Geological Society, Inc., p. 59–69.

Luppov, N.P., 1972, Geology of the USSR, v. 22, Turkmen SSR: Moscow, Nedra, 768 p. [In Russian.]

Mirakhmedov, M., 1968, Ob usloviyakh obrazovaniya kaliyenosnykh gorizontov Lyalimkanskogo mestorozhdeniya [Genetic environment of potassium-bearing horizons in the Lyalimkan deposit]: Uzbekiston Geologiya Zhurnali, v. 3, p. 30–35.

Obukhov, A.N., 1994, Gravitational geodynamics in the intermontane basins of central Asia: Geotectonics, v. 28, no. 3, p. 254–266.

Pashayev, M.S., Gavril'cheva, L.G., and Redzhepov, K.A., 1993, Stroyeniye i fatsial'naya zonal'nost nizhnemelovoy soli (formirovaniye lovushek neantiklainal'nogo tipa na yugo-vostoke Turkmenistana) [Structure and facies zonality of Lower Cretaceous salt—Formation of non-anticlinal traps in southeastern Turkmenistan]: Geologiya Nefti i Gaza, v. 5, p. 15–18.

Pashayev, M.S., Gavril'cheva, L.G., and Redzhepov, K.A., 1993, Structure and facies zonality of Lower Cretaceous salt, formation of non-anticlinal traps in southeast Turkmenistan: Petroleum Geology, v. 28, p. 263–266.

Petrov, N.P., Ishniyazov, D.P., Mirakhmedov, M.M., and Yuldashev, E.L., 1973, Novyye dannyye o stroyenii i sostave galogennoy formatsii Khodzhaikanskoy kaliyenosnoy ploshchadi [New data concerning structure and composition of evaporates in the Khodzhaikan potassium ore field]: Uzbekiskiy Geologicheskiy Zhurnal, v, 3, p. 73–74.

Rempel, Hilmar, 2002, The Caspian Region—Source for oil supply to Europe and Asia: AAPG Annual Meeting, Houston, Texas, March 10–13, 2002, 6 p.

Roskill Information Services, 1989, The economics of potash (2d ed.): London, Roskill Information Services Ltd., 121 p.

Sadikov, T.S., 1981, Galogyennaya formatsiya yugo-zapadnogo tajikistana [Halogenic formations of southwest Tadjikistan], *in* Yanshin, A.L., and Zharkov, M.A., eds., Stroyeniye i usloviya formirovaniya mestorozhdeniy kaliynykh soley [Structure and condition of formation of salt formations]: Novosibirsk, Nauka, p. 137–143.

Sedletskiy, V.I., 1970, Litologo-fatsial'nyye osobennosti i usloviya kaliyenosnosti mezozoyskikh otlozheniy yuga Sredney Azii [Lithofacies features and conditions of potassium mineralization in Mesozoic sediments of southern central Asia], *in* Sostoyanie i zadachi sovetskoi litologii [State and problems of Soviet lithology]: Moscow, Nauka, p. 49–57.

Sheikh-Zade, E.R., 1996, Results of seismic reflection profiling in the Turanian Platform: Tectonophysics, v. 264. p. 123–135.

Sokolovskaya, L.G., and Sedletskiy, V.I., 1989, The hydrogeological significance of salt beds in southern Central Asia: International Geology Review, v. 31, p. 806–814.

Talwani, Manik, Belopolsky, Andrei, and Berry, D.L., 1998, Unlocking the assets—Energy and the future of central Asia and the Caucasus, geology and petroleum potential of central Asia: Houston, The James Baker III Institute for Public Policy, Rice University, 25 p., accessed March 5, 2010, at http://bakerinstitute.org/files/2682/.

Thomas, J.C., Cobbold, P.R., Shein, V.S., and Le Douaran, S., 1999, Sedimentary record of late Paleozoic to Recent tectonism in central Asia—Analysis of subsurface data from the Turan and south Kazak domains: Tectonophysics, v. 313, p. 243–263.

Troitskiy, V.I., 1967, Upper Triassic and Jurassic sedimentary deposits in southern Uzbekistan: Nedra, Leningrad. [In Russian.]

Yermolkin, V.I., 1986, Zonalnost neftegazionakopleniya na platformennykh territoriyakh [Zonality of oil and gas accumulation on platforms]: Moscow, Nedra, 185 p.

Zharkov, M.A., 1984, Paleozoic salt bearing formations of the world: New York, Springer-Verlag, 427 p.

This page intentionally left blank

Appendixes A–H

Appendix A. Summary Descriptive Model of Stratabound Potash-Bearing Salt Deposits

By Mark D. Cocker[1] and Greta J. Orris[1]

Introduction

Stratabound potash-bearing salt is associated with thick sections of evaporitic salt (halite) that form laterally continuous strata in marine evaporite basins. Deposits are extremely soluble and thus are easily altered or destroyed over geologic time. Stratabound potash deposits range in size from several tens of millions to more than 30 billion metric tons (Bt) of potassium oxide (K_2O). Most of the world's potash resources are associated with this deposit type.

Representative Deposits

Examples of stratabound potash-bearing salt deposits include those in the Givetian (Middle Devonian) Elk Point Basin in Canada, the Frasnian and Famennian (Upper Devonian) Pripyat Basin in Belarus, and the Lopingian (upper Permian) Solikamsk Basin in Russia (fig. A-1). Some larger basins, such as the Lopingian Zechstein Basin in Europe and the Central Asia Salt Basin (fig. A-1), contain potash-bearing salt in both stratabound and halokinetic (appendix B) forms.

Brief Description

Synonyms

Synonyms for this type of deposit include potash deposits, potash-bearing salt deposits, bedded potash, and marine potash.

Principal Commodities and Byproducts

The principal products of potash mining are potassium chloride (KCl), which is referred to as muriate of potash (MOP), and potassium sulfate (K_2SO_4), which is referred to as sulfate of potash (SOP). Where carnallite ($KMgCl_3{\bullet}6H_2O$) constitutes a major part of a deposit, magnesium may be recovered. The main byproduct commodity is halite or rock salt.

[1]U.S. Geological Survey, Tucson, Arizona, United States.

Relative Importance of the Deposit Type

Stratabound potash-bearing salt deposits may contain billions to trillions of tons of mineralized rock and are amenable to low-cost, bulk underground mining methods. Approximately 75 percent of the world's potash production is from stratabound potash-bearing salt deposits, and more than 25 percent of that production is from the Middle Devonian Prairie Evaporite Formation of the Elk Point Basin in Saskatchewan, Canada.

Global Distribution

The largest and economically most important deposits of potash are found in North America, Europe, and Asia. Newly explored deposits in Africa and South America are increasingly important.

Associated and Related Deposit Types

Stratabound potash-bearing salt deposits are associated with stratabound and bedded gypsum, anhydrite, halite, and sulfur deposits (Long, 1992). Halokinetic potash-bearing salt deposits (see appendix B, this report) originally formed in the same manner as stratabound deposits but deformation of salt resulted in grade and tonnage differences between these two end-member deposit types. Stratabound and halokinetic potash-bearing salt may occur concurrently in some larger basins.

Descriptive and Genetic Synopsis

Potash-bearing salt is a chemically deposited sedimentary rock made up of fine- to coarse-grained, potassium- and magnesium-chloride and sulfate minerals intergrown with halite. Beds of laterally continuous stratabound potash-bearing salt occur within thick sections of halite-dominant evaporite deposits. Potash-bearing strata range from centimeters to meters in thickness, and potash-bearing intervals may consist of one bed or numerous thin layers. These deposits are commonly attributed to evaporation of large volumes of seawater in hydrographically restricted or isolated basins under hyperarid climatic conditions (Warren, 2006, 2010; Kendall, 2010). Progressive evaporation of saline water, usually seawater, and salt

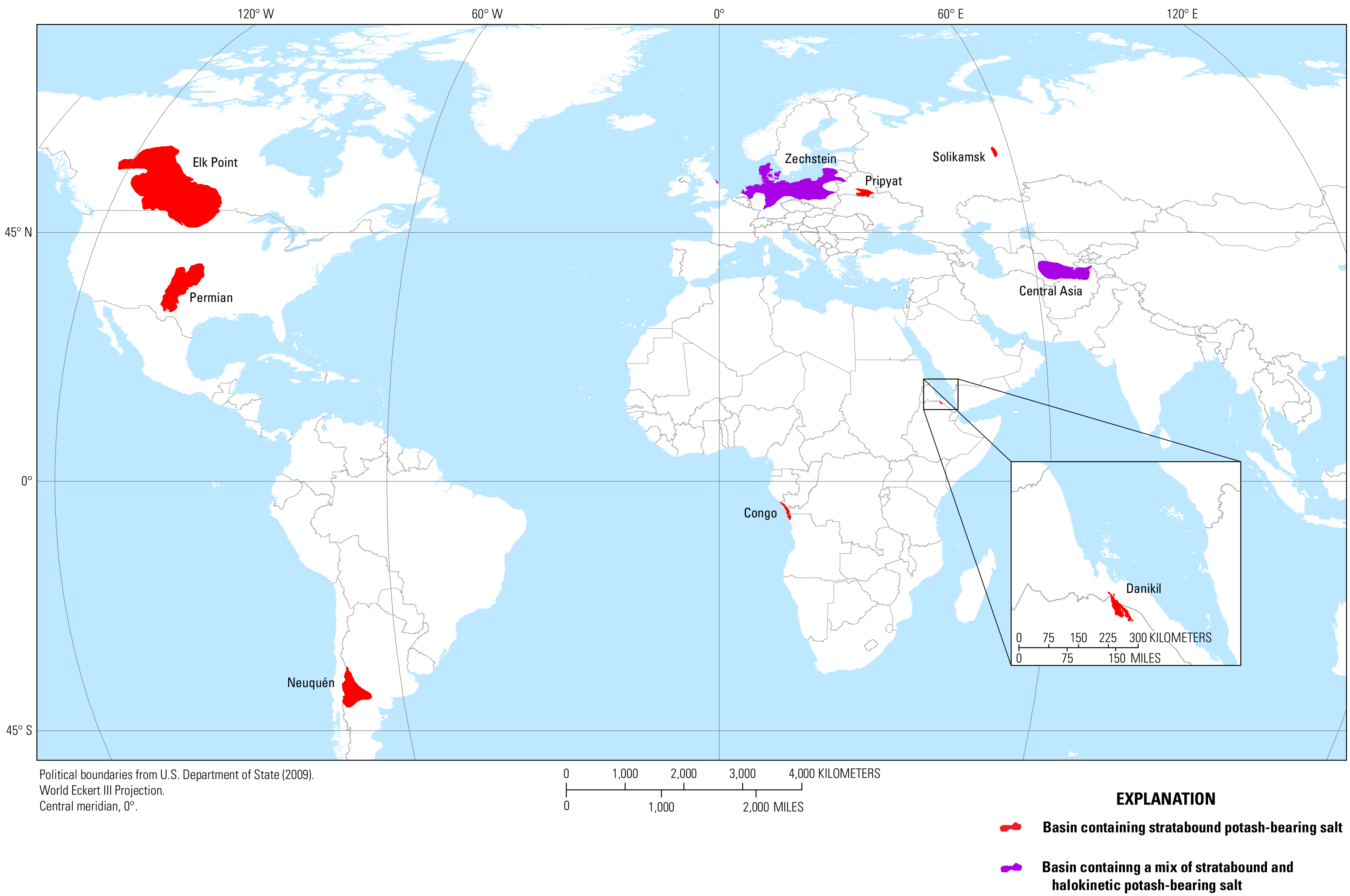

Figure A-1. Map showing basins containing stratabound potash-bearing salt and those containing a mix of stratabound and halokinetic potash-bearing salt from Orris and others (2014).

precipitation contribute to increasingly hypersaline conditions, formation of bitterns, and eventual deposition of potassium- and magnesium-bearing minerals. Multiple episodes of saline water inflow can result in cyclic deposition of potash minerals and yield deposits that are many tens of meters thick.

Permissive Tract Delineation

The fundamental geologic feature used to delineate of tracts permissive for stratabound potash-bearing salt is an evaporite- bearing sedimentary basin that contains halite-dominated areas and evidence that evaporation reached the bittern stage. Evidence of potash mineralization includes reports of the presence of sylvite, carnallite, polyhalite, or other potassium saline minerals, or indirect evidence from downhole geophysical surveys.

Permissive tracts are outlined by selecting basins with known evaporites, restricting tract boundaries to areas likely underlain by salt at depths of 3 kilometers (km) or less, and if possible, using drill hole or other information to limit tracts to areas underlain by potash-bearing salt. Halite-rich layers are preferably many tens to hundreds of meters thick and (or) areally extensive.

Regional Geologic Attributes

Tectonic Setting of Basin

Stratabound potash-bearing salt is found in sedimentary basins that formed in regions of arid climate. Tectonic plate interactions formed basins between 15° and 45° north and south of the equator that were likely places for stratabound potash-bearing salt deposition. Deposits have been described in continental and oceanic rift basins, foreland basins, intracontinental sag basins, and in transform basins that are products of the breakup (or failed breakup) of continents, convergence or collision of continental plates, or intraplate thinning and weakening (Warren, 2010). Basin type is less critical than climatic conditions at the time of deposition. Hot, hyperarid climatic conditions are necessary to form brines from saline waters and deposit evaporites. These conditions may result from global scale atmospheric wind circulation patterns (Warren, 2010). Many of the world's deserts are near latitudes of 30° N and 30° S, which correspond to the boundary between atmospheric circulation cells.

Depositional Systems

In an evaporite basin, nearshore, shallow clastic facies rocks grade to carbonate-, then sulfate-, then halide-rich rocks towards the central part of a basin or parts more distal from the point of seawater influx. Central parts of an evaporite basin may have facies representing shallow to deep water (Schmalz, 1969; Warren, 2006; Kendall, 2010). The resulting stratigraphic sequence begins with minor clastic red beds, followed by carbonate rocks, anhydrite or gypsum, salt, and ends with potash-bearing salt. Multiple episodes of evaporite mineral precipitation may be recorded in cyclic sequences of rock layers, with individual cyclic units ranging from a few centimeters to hundreds of meters thick.

Age Range and Age-Related Features

Potash-bearing salt deposits are found in basins that are Neoproterozoic in age or younger (Goncharenko, 2006; Kovalevych and others, 2006; Warren, 2006, 2008; Zharkov, 1984, 2005). Half of the world's known potash-containing basins are Middle and Late Devonian, Permian, or Paleogene-Neogene in age (Goncharenko, 2006).

Differences in deposit mineralogy likely reflect temporal changes in global seawater chemistry. During the Phanerozoic, marine brine chemistry appears to have oscillated between Na-K-Mg-Ca-Cl and Na-K-Mg-Cl-SO_4 types (Hardie, 1990, 1996; Holland and others, 1996; Kovalevych and others, 1998; Horita and others, 2002; Warren, 2006; Ries, 2010). Magnesium sulfate- poor deposits dominated by sylvite and carnallite are derived from the Na-K-Mg-Ca-Cl brines. Magnesium-rich sulfate type deposits, with variable amounts of K- and Mg-sulfate minerals, may form from Na-K-Mg-Cl-SO_4 brines. Local environmental conditions may be significant factors in basin brine geochemistry.

Local Geologic Attributes and Deposit Characteristics

Host Rocks

Host rocks are evaporitic sedimentary rocks, such as rock salt, sylvinite, carnallitite, kainitite, hartsalz, anhydrite, and gypsum. The mineralized rock strata consist of potash salt minerals, including chlorides, sulfates, and halite, in evaporite sequences.

Deposit Characteristics

Deposit Form and Dimensions

Stratabound potash-bearing salt deposits are composed of one or more layers or beds of potash-bearing salt. The beds or layers or groups of layers are commonly laterally continuous across large areas of a basin. Individual potash beds or layers range in thickness from less than a meter to several tens of meters, to almost a hundred meters (rare). A sequence of potash-bearing salt beds may range from tens of meters to a few hundred meters thick. The areal extent of potash mineralization is ultimately limited by the basin size at time of deposition. Typical volumes of stratabound potash-bearing salt can be hundreds to thousands of cubic kilometers.

Mineralogy

Potash Ore Mineralogy

Primary potash ore minerals include sylvite, carnallite, kainite, polyhalite, and langbeinite (table A-1). These minerals occur most commonly as intergrowths with halite.

Potash Ore Assemblages

The dominant potash ore assemblages contain sylvite and halite with minor (<6 weight percent) carnallite or carnallite plus halite with negligible amounts of sylvite. Some deposits may contain ore assemblages of kainite, langbeinite, polyhalite, kieserite, and (or) bischofite mixed with halite and gypsum or anhydrite.

Gangue Mineralogy

Gangue minerals include halite, clay minerals, dolomite, anhydrite, gypsum, bischofite, epsomite, tachyhydrite, leonite, blödite, hexahydrite, vanthoffite, löweite, aphthitalite, picromerite, and borate minerals (table A-1). Sonnenfeld (1991) noted the presence of halloysites, kaolinite, iron-chlorite, magnesium-chlorites, montmorillonite, palygorskite, illite, sepiolite, and muscovite in evaporite basins.

Primary mineral zoning may consist of an outer or stratigraphically lower zone dominated by sulfates such as anhydrite or gypsum, changing to a halite-dominated zone, and culminating with an inner or upper zone containing halite plus potassium chloride or potassium sulfate minerals.

Table A-1. Ore minerals and common accessory and gangue minerals in stratabound potash-bearing salt deposits from Orris and others (2014).

[Composition formulas from Back and Mandarino (2008)]

Ore minerals	Composition	Other minerals	Composition
Carnallite	$KMgCl_3•6H_2O$	Aphthitalite	$(K,Na)_3Na(SO_4)_2$
Kainite	$MgSO_4•KCl•3H_2O$	Anhydrite	$CaSO_4$
Langbeinite	$K_2Mg_2(SO_4)_3$	Bischofite	$MgCl•6H_2O$
Polyhalite	$K_2Ca_2Mg(SO_4)_4•2H_2O$	Blödite	$Na_2Mg(SO_4)_2•4H_2O$
Sylvite	KCl	Boracite	$Mg_7B_7O_{13}Cl$
		Dolomite	$CaMg(CO_3)_2$
		Epsomite	$MgSO_4•7H_2O$
		Gypsum	$CaSO_4•2H_2O$
		Halloysite	$Al_2Si_2O_5(OH)_4$
		Halite	NaCl
		Hexahydrite	$MgSO_4•6H_2O$
		Kaolinite	$MgSO_4•H_2O$
		Kieserite	$MgSO_4•H_2O$
		Kurnakovite	$K_2Mg(SO_4)_2•4H_2O$
		Leonite	$Na_{12}Mg_7(SO_4)_{13}•15H_2O$
		Löweite	$(Na,Ca)_{0.3}(Al,Mg)_2Si_4O_{10}(OH)_2•nH_2O$
		Lüneburgite	$Mg_3B_2(PO_4)_2(OH)_6•6H_2O$
		Montmorillonite	$(Mg,Al)_2Si_4O_{10}(OH)•4H_2O$
		Palygorskite	$K_2Mg(SO_4)_2•6H_2O$
		Picromerite	$Mg_4Si_6O_{15}(OH)_2•6H_2O$
		Sepiolite	$CaMgCl_6•12H_2O$
		Tachyhydrite	$Na_6Mg(SO_4)_4$
		Vanthoffite	$Na_6Mg(SO_4)_4$
		Volkovskite	$KCa_4B_{22}O_{32}(OH)10Cl•4H_2O$

Under certain conditions at the end of an evaporation sequence, some other bittern minerals such as tachyhydrite or bischofite may also be present and preserved. These minerals are highly soluble and are commonly no longer present in most of these deposits.

Effects of Alteration

Potash-bearing salt is highly soluble and susceptible to alteration, recrystallization, and dissolution by surface water, less saline brine, and groundwater (Warren, 2010). Groundwater dissolution can modify the mineralogy, layering, grain size, or porosity, or it can totally destroy a deposit. Increased pressure and temperature related to burial metamorphism can also lead to recrystallization and destruction of primary textures and changes in grain size.

Exploration Guides

Geochemical Signature(s)

In many primary deposits, brines in boreholes may be anomalous in potassium, sodium, magnesium, bromine, chlorine, and sulfur (Rogers, 2011). Exceptionally saline wells and saline spring water are indicative of an evaporite sequence, and have historically led to discoveries of concealed salt and potash deposits.

Bromine content of halite increases as the salinity of the brine increases; bromine profiles show increasing upwards trends in unaltered evaporite cycles. Residual brines at this stage may contain hundreds of parts per million (ppm) bromine, and on the order of a thousand parts per million or more bromine during precipitation of potash minerals, although reported values are typically much lower due to dilution and dissolution, diagenesis, and brine fluctuations (Webb and Stewart, 2011).

Geophysical Signature(s)

Radiometric Signatures

High gamma radiation signatures from the natural isotope potassium-40 (^{40}K) are used to map potassium content of salt in downhole geophysical surveys (Garrett, 1996).

Seismic Signatures

Reflection seismic methods are used to delineate salt structures and layers (Fox, 1987; Simeonova and Iasky, 2005).

Other Exploration Guides

Except for drilling confirmation of potash, there are few sure indications of the presence of potash-bearing salt. Thick sections of halite, usually greater than 100 meters (m), are believed to be necessary prior to potash deposition (Harben and Kužvart, 1996), and this could be used in conjunction with other data to identify or rank the potash potential of basins with little exploration history.

Typical Grade and Tonnage

Average reported potash grades in explored deposits of this type may range from 5.3 to 38 percent K_2O (de Ruiter, 1979; Kumar and Bakliwal, 2005). Most reported grades in operating mines range from 11 to 25 percent K_2O. In general, the lowest average grade that is currently being mined is in the range of 8–10 percent K_2O, with the lowest associated cutoff grade less than 4 percent K_2O.

The minimum thickness of a potash layer that is currently being mined is about 1 m. In Saskatchewan, minimal mining thicknesses range from 2.44 to 3.35 m because of the mining equipment used and the thickness of the highest grade ore in different mines (Moore and others, 2010a,b,c,d, 2011).

Reported tonnages for potash deposits range from a few tens of millions to 30 Bt (British Sulphur Corporation Limited, 1984; Hardy and others, 2009). Tonnages since 2000 for greenfield potash projects that reported NI 43-101-compatible reserves and resources largely exceed 500 million metric tons, and commonly, 1 Bt of potash ore (Rauche and van der Klauw, 2009, 2012; BHP Billiton, 2010; Western Potash, 2010; South Boulder Mines, 2012).

References Cited

Back, Malcolm, and Mandarino, J.A., 2008, Fleischers glossary of mineral species 2008: Mineralogical Record, Inc., 346 p.

BHP Billiton, 2010, BHP Billiton announces mineral resource estimate for its Jansen potash project: BHP Billiton news release, June 7, 2010, 2 p., accessed June 26, 2010, at http://www.bhpbilliton.com/bb/investorsMedia/news/2010/bhpBillitonAnnouncesMineralResourceEstimateForItsJansenPotash-Project.jsp.

British Sulphur Corporation Limited, 1984, World survey of potash resources (4th ed.): London, British Sulphur Corporation Limited, 145 p.

de Ruiter, P.A.C., 1979, The Gabon and Congo Basins salt deposits: Economic Geology, v. 74, no. 2, p. 419–431.

Fox, James, 1987, Seismic interpretation in salt-controlled basins: The Leading Edge, v. 6, no. 3, p. 11–18.

Garrett, D.E., 1996, Potash—Deposits, processing, properties and uses: New York, Chapman & Hall, 734 p.

Goncharenko, O.P., 2006, Potassic salts in Phanerozoic evaporite basins and specific features of salt deposition at the final stages of halogenesis: Lithology and Mineral Resources, v. 41, no. 4, p. 378–388.

Harben, P.W., and Kužvart, M., 1996, Industrial minerals—A global geology: London, Industrial Minerals Information Ltd., 462 p.

Hardie, L.A., 1990, The roles of rifting and hydrothermal CaCl2 brines in the origin of potash evaporites—An hypothesis: American Journal of Science, v. 290, no. 1, p. 43–106.

Hardie, L.A., 1996, Secular variation in seawater chemistry—An explanation for the coupled secular variation in the mineralogies of marine limestones and potash evaporites over the past 600 m.y.: Geology, v. 24, p. 279–283.

Hardy, M., Halabura, S.P., and Shewfelt, D., 2009, Technical Report—2009 potash resource assessment for Subsurface Mineral Permit KP 289, Saskatchewan: Agapito Associates, Inc., North Rim Exploration Ltd., 163 p.

Holland, H.D., Horita, Juske, and Seyfried, W.E., Jr., 1996, On the secular variation in the composition of marine potash evaporates: Geology, v. 24, no. 11, p. 993–996.

Horita, Juske, Zimmerman, Heide, and Holland, H.D., 2002, Chemical evolution of seawater during the Phanerozoic—Implications from the record of marine evaporites: Geochimica et Cosmochimica Acta, v. 66, no. 21, p. 3733–3756.

Kendall, A.C., 2010, Marine evaporites, in James, N.P., and Dalrymple, R.W., eds., Facies models 4: Geological Association of Canada, GEOtext 6, p. 505–540.

Kovalevych, V.M., Peryt, T.M., and Petrychenko, O.Y., 1998, Secular variation in seawater chemistry during the Phanerozoic as indicated by brine inclusions in halite: Journal of Geology, v. 106, p. 695–712.

Kovalevych, V.M., Marshall, T., Peryt, T.M., Petrychenko, O.Y., and Zhukova, S.A., 2006, Chemical composition of seawater in Neoproterozoic—Results of fluid inclusion study of halite from Salt Range (Pakistan) and Amadeus Basin (Australia): Precambrian Research, v. 144, p. 39–51.

Kumar, V., and Bakliwal, P.C., 2005, Potash in India: Geological Survey of India Miscellaneous Publication 65, 131 p.

Long, K.R., 1992, Descriptive model of stratabound sulfur and contained-sulfur model of stratabound sulfur: U.S. Geological Survey Open-File Report 92–0705, 8 p. [Also available at http://pubs.er.usgs.gov/publication/ofr92705.]

Moore, G., Danyluk, T.K., Franklin, B., Prugger, A., and Vander Most, A., 2010a, National Instrument 43–101 technical report on Allan potash deposit (KL–112R), Saskatchewan, Canada: Saskatoon, Sask., Potash Corporation of Saskatchewan Inc., 62 p.

Moore, G., Danyluk, T.K., Franklin, B., Prugger, A., and Vander Most, A., 2010b, National Instrument 43–101 technical report on Cory potash deposit (KL–103R), Saskatchewan, Canada: Saskatoon, Sask., Potash Corporation of Saskatchewan Inc., 63 p.

Moore, G., Danyluk, T.K., Franklin, B., Prugger, A., and Vander Most, A., 2010c, National Instrument 43–101 technical report on Lanigan potash deposit (KLSA–001), Saskatchewan, Canada: Saskatoon, Sask., Potash Corporation of Saskatchewan Inc., 65 p.

Moore, G., Danyluk, T.K., Franklin, B., Prugger, A., and Vander Most, A., 2010d, National Instrument 43–101 technical report on Rocanville potash deposit (KLSA–002), Saskatchewan, Canada: Saskatoon, Sask., Potash Corporation of Saskatchewan Inc., 68 p.

Moore, Garth, Danyluk, T.K., Franklin, Bob, Prugger, Arnfinn, and Vander Most, Anastasia, 2011, National Instrument 43–101 technical report on Rocanville potash deposit (KLSA–002) Saskatchewan, Canada: Saskatoon, Sask. Potash Corporation of Saskatchewan, Inc., 68 p.

Orris, G.J., Cocker, M.D., Dunlap, P., Wynn, J.C., Spanski, G.T., Briggs, D.A., and Gass, L., with contributions from Bliss, J.D., Bolm, K.S., Yang, C., Lipin, B.R., Ludington, S., Miller, R.J., and Slowakiewicz, M., 2014, Potash—A global overview of evaporite-related potash resources, including spatial databases of deposits, occurrences, and permissive tracts: US Geological Survey Scientific Investigations Report 2010–5090–S, 76 p., and spatial data, http://dx.doi.org/10.3133/sir20105090S.

Rauche, Henry, and van der Klauw, S.N.G.C., 2009, Updated reserve and resource estimate for MagMinerals Kouilou potash project, Republic of Congo: Technical report prepared for MagMinerals Inc., 209 p., accessed August 15, 2011, at http://www.magindustries.com/cmsdocs/Technical%20Reports/08-016_NI-43-101_Updated_Reserve-Report_June_2009_rev01.pdf.

Rauche, Henry, and Van der Klauw, S.N.G.C., 2012, Preliminary economic assessment, sylvinite mining in the Danakhil potash deposit, Afar State, Ethiopia—Preliminary economic assessment study: Erfurt, Germany, ERCOPSPLAN Ingenieurgesellschaft, 131 p. [plus appendixes.]

Ries, J.B., 2010, Review—Geological and experimental evidence for secular variation in seawater Mg/Ca (calcite-aragonite seas) and its effect on marine biological calcification: Biogeosciences, v. 7, p. 2795–2849.

Rogers, M.C., 2011, Saskatchewan descriptive mineral deposit models: Saskatchewan Ministry of Energy and Resources Open File Report 2011–57, 112 p.

Schmalz, R.F., 1969, Deep-water evaporite deposition—A genetic model: American Association of Petroleum Geologists Bulletin, v. 53, no. 4, p. 798–823.

Simeonova, A.P., and Iasky, R.P., 2005, Seismic mapping, salt deformation, and hydrocarbon potential of the central western Officer Basin, Western Australia: Western Australia Geological Survey Report 98, 49 p. [plus appendixes.]

Sonnenfeld, P., 1991, Evaporite basin analysis, in Force, E.R., Eidel, J.J., and Maynard, J.B., Sedimentary and diagenetic mineral deposits—A basin analysis approach to exploration: Reviews in Economic Geology Volume 5, p. 159–169.

South Boulder Mines, 2012, Colluli potash project, Web site, accessed April 17, 2012, at http://www.southbouldermines.com.au/projects/colluli-potash-project/.

U.S. Department of State, 2009, Small-scale digital international land boundaries (SSIB)—Lines, edition 10, and polygons, beta edition 1, *in* Boundaries and Sovereignty Encyclopedia (B.A.S.E.): U.S. Department of State, Office of the Geographer and Global Issues.

Warren, J.K., 2006, Evaporites—Sediments, resources and hydrocarbons: Berlin, Springer-Verlag, 1,035 p.

Warren, J.K., 2008, Salt as sediment in the Central European Basin system as seen from a deep time perspective, *in* Littke, Ralf, Bayer, Ulf, and Gajewski, Dirk, eds., Dynamics of complex intracontinental basins: Berlin, Springer-Verlag, p. 249–276.

Warren, J.K., 2010, Evaporites through time—Tectonic, climatic, and eustatic controls in marine and nonmarine deposits: Earth-Science Reviews, v. 98, issues 3–4, p. 217–268.

Webb, T.C., and Stewart, H.J., 2011, Bromine as an indicator of potash mineralization in Carboniferous marine evaporites, Sackville Subbasin, southeastern New Brunswick: New Brunswick Department of Natural Resources, Lands, Minerals and Petroleum Division Mineral Resource Report 2011-1, 40 p.

Western Potash, 2010, Western Potash Corp. updates measured and indicated potash resource to 174 million tonnes: Western Potash Corp Web page, accessed July 5, 2010, at http://www.westernpotash.com/.

Zharkov, M.A., 1984, Paleozoic salt bearing formations of the world: New York, Springer-Verlag, 427 p.

Zharkov, M.A., 2005, Evolyutsiya evaporitov v dokembrii v svyazi s preobrazovaniyami biosfery i khimicheskogo sostava mirovogo okeana; Stat’ya 1, Evapority arkheya i rannego proterozoya [Evolution of Precambrian evaporites, transformation of biosphere and the world oceans’ chemical composition—Paper 1, Archean and Paleoproterozoic evaporites]: Stratigrafiya, Geologicheskaya Korrelyatsiya, v. 13, no. 2, p. 19–29.

Appendix B. Summary Descriptive Model of Halokinetic Potash-Bearing Salt Deposits

By Mark D. Cocker[1] and Greta J. Orris[1]

Introduction

Halokinetic potash-bearing salt occurs in salt structures developed from stratabound potash-bearing salt deposits where differential loading by thick overlying sediments initiated and drove upward movement of low-density potash-bearing salt. The original stratabound salt beds are disrupted during halokinesis, resulting in complexly deformed lenses and beds of potash-bearing salt. Potash deposits within salt structures range in size from 1 million to more than 1,000 million metric tons. Most mined halokinetic potash deposits are from 50 million to several hundred million metric tons in size.

Representative Deposits

Some of the best known halokinetic potash-bearing salt deposits occur in the evaporites of the Lopingian (upper Permian) Zechstein Basin of Germany, Poland, The Netherlands, and Denmark; the Cisuralian (lower Permian) Pricaspian Basin of Kazakhstan and Russia; the Middle Pennsylvanian of the Paradox Basin in the United States; and the Miocene Carpathian Basin of Romania and Ukraine (fig. B-1). Some larger basins, such as the Zechstein Basin (fig. B-1) and the Central Asia Salt Basin (fig. B-1), contain potash-bearing salt in both halokinetic and stratabound (appendix A) forms.

Brief Description

Synonyms

Synonyms for this type of deposit include potash deposits, potash-bearing salt deposits, diapiric potash, marine potash, and halokinetic potash-bearing salt deposits.

[1]U.S. Geological Survey, Tucson, Arizona, United States.

Principal Commodities and Byproducts

The principal products of potash mining are potassium chloride (KCl), which is referred to as muriate of potash (MOP), and potassium sulfate (K_2SO_4), which is referred to as sulfate of potash (SOP). Where carnallite ($KMgCl_3 \bullet 6H_2O$) constitutes a major part of a deposit, magnesium may be recovered. The main byproduct commodity is halite or salt.

Relative Importance of the Deposit Type

An estimated 10–15 percent of the world's potash production is from halokinetic potash-bearing salt deposits.

Global Distribution

The largest known deposits are found in Europe and Central Asia.

Associated and Related Deposit Types

Some salt structures may contain associated gypsum, sulfur, iodine, bromine, or borate deposits (Raup, 1991; Long, 1992). Salt structures and associated fault-related features commonly form hydrocarbon traps (Kyle and Posey, 1991; Long, 1992). Because stratabound potash-bearing salt deposits have not suffered the deformation characteristic of halokinetic potash-bearing salt deposits, there are important differences in grades and tonnages between these two end member deposit types. Stratabound and halokinetic potash-bearing salt may both be found in some larger basins.

Descriptive and Genetic Synopsis

Halokinetic potash-bearing salt deposits are the layers or beds of stratabound potash-bearing salt deposits that have moved by plastic flow into a salt structure along with the enclosing sedimentary rock, most of which is salt. The internal structure of the salt layers, and hence the potash-bearing salt layers, can be simple to complex, and the original continuity and thickness of the potash-rich layers may be altered considerably by the internal deformation.

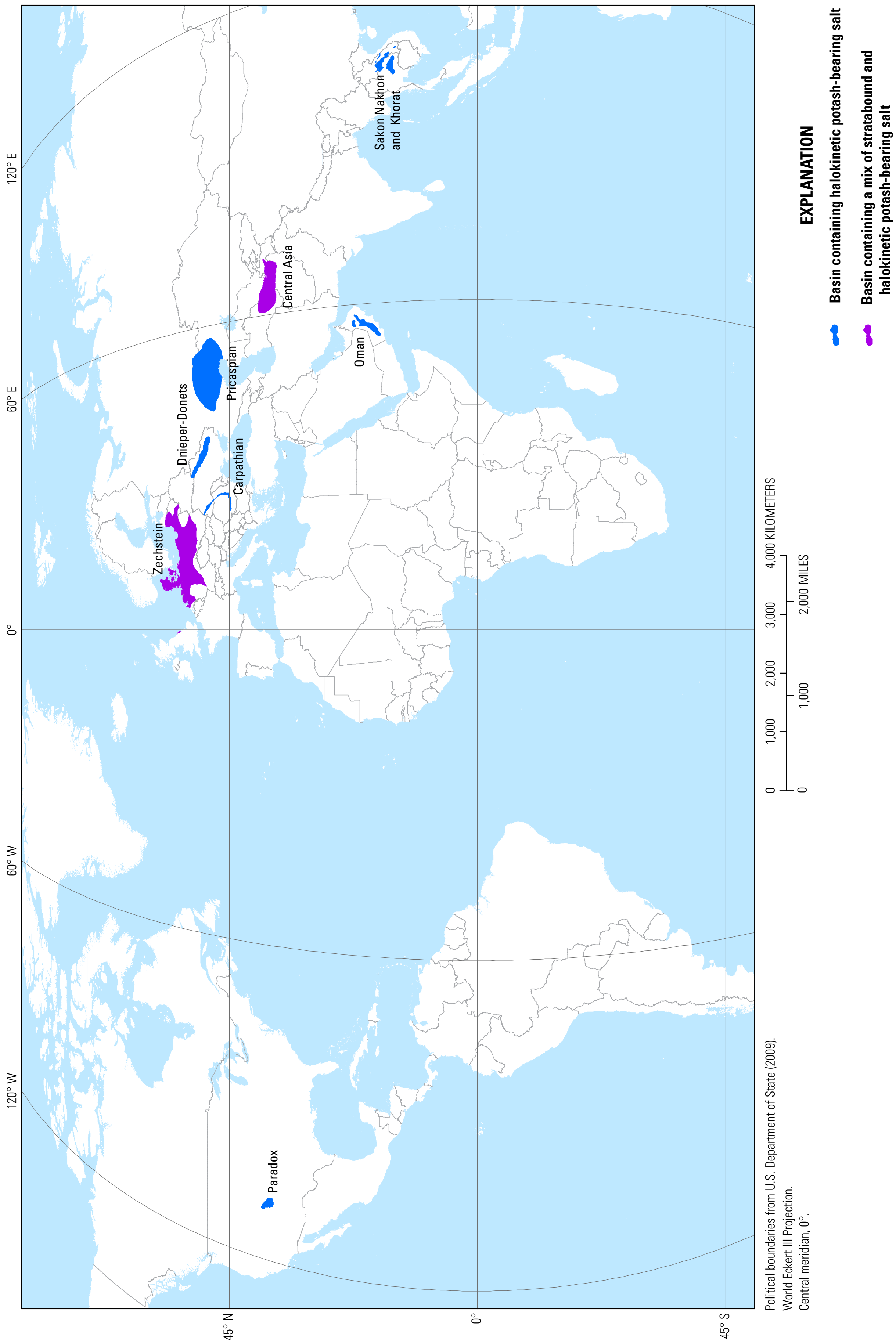

Figure B-1. Map showing basins containing halokinetic potash-bearing salt and those containing a mix of stratabound and halokinetic potash-bearing salt from Orris and others (2014).

Structural deformation of low-density salt may be related to differential loading or unloading of the sedimentary sequence and local or regional tectonic activity. Halokinetic salt structures are generally developed in tectonically active salt basins such as rift or foreland basins.

Permissive Tract Delineation

The fundamental unit for delineation of tracts permissive for potash-bearing bedded salt is an evaporite-bearing sedimentary basin that contains halite-dominated areas and evidence that evaporation reached the bittern stage. Evidence of potash mineralization includes reports of the presence of sylvite, carnallite, polyhalite, other potassium saline minerals or indirect evidence from downhole geophysical surveys.

Permissive tracts for halokinetic potash-bearing salt deposits are outlined by (1) selecting basins with known halokinetic salt; (2) restricting tract boundaries to areas likely underlain by halokinetic salt at depths of 3 kilometers (km) or less; (3) if possible, using drill hole or other information to limit tracts to areas underlain by potash-bearing salt; and (4) delineating specific salt structures likely to contain potash-bearing salt.

Regional Geologic Attributes

Halokinesis is most common in continental and oceanic rift basins, foreland basins, convergent basins, and transform basins where lateral compression or extension is active. Halokinesis may be initiated by such factors as (1) differential loading through rapid deposition of thick, overlying clastic sediments; (2) differential unloading resulting from listric block faulting during extensional rifting; (3) differential erosion of overlying sedimentary rocks; (4) rift basement block faulting; and (5) compressional or extensional regional tectonic activity (Kityk, 1970; Amor, 1999; Al-Zoubi and ten Brink, 2001; Jarhani and others, 2007).

Depositional Systems

In an evaporite basin, near-shore, shallow clastic facies rocks grade to carbonate-, then sulfate-, then halide-rich rocks towards the deep, central parts of a basin. Central parts of an evaporite basin may have facies representing shallow to deep water (Schmalz, 1969; Warren, 2006; Kendall, 2010). The resulting stratigraphic sequence begins with minor clastic red beds, followed by carbonate rocks, anhydrite or gypsum, salt, and ends with potash-bearing salt. Multiple episodes of evaporite mineral precipitation may be recorded in cyclic sequences of rock layers, with individual cyclic units ranging in thickness from a few centimeters to hundreds of meters. During halokinesis, the original depositional layering is partly to wholly disrupted by plastic flow, which may result in complex folding, discontinuous mineralization, or even loss of mineralization.

Age Range and Age-Related Features

Potash-bearing salt deposits are found in basins that are Neoproterozoic in age or younger (Zharkov, 1984, 2005; Goncharenko, 2006; Kovalevych and others, 2006; Warren, 2006, 2008). Half the world's known potash-containing basins are Middle and Late Devonian, Permian, or Paleogene-Neogene in age (Goncharenko, 2006).

Differences in deposit mineralogy likely reflect temporal changes in global seawater chemistry. During the Phanerozoic, marine brine chemistry oscillated between Na-K-Mg-Ca-Cl and Na-K-Mg-Cl-SO_4 types (Hardie, 1990, 1996; Holland and others, 1996; Kovalevych and others, 1998; Horita and others, 2002; Warren, 2006; Ries, 2010). Magnesium sulfate- poor deposits dominated by sylvite and carnallite are derived from Na-K-Mg-Ca-Cl brines. Magnesium-rich sulfate type deposits, with variable amounts of K- and Mg-sulfate minerals, may form from Na-K-Mg-Cl-SO_4 brines. Local environmental conditions may be a significant factor in basin brine geochemistry.

Local Geologic Attributes and Deposit Characteristics

Host Rocks

Host rocks are evaporitic sedimentary rocks, such as rock salt, sylvinite, carnallitite, kainitite, hartsalz, anhydrite, and gypsum. Diapiric structures pierce overlying sediments, so any younger, originally overlying sedimentary rocks may appear to host salt and potash mineralization.

Impacts of Local Structures

Halokinetic salt structures are commonly aligned over basement faults.

Deposit Characteristics

Deposit Form and Dimensions

The areal extent of salt diapirs ranges from a few to several hundred square kilometers. With a vertical extent ranging from a few hundred meters to more than 10 kilometers, salt volumes of diapirs are on the order of tens to hundreds of cubic kilometers. Potash forms only a small part of an individual salt diapir.

Mineralogy

Potash Ore Mineralogy

Primary ore minerals include sylvite, carnallite, kainite, polyhalite, and langbeinite (table B-1). These minerals occur most commonly as intergrowths with halite.

Table B-1. Ore minerals and common accessory and gangue minerals in halokinetic potash-bearing salt deposits from Orris and others (2014).

[Composition formulas from Back and Mandarino (2008)]

Ore minerals	Composition	Other minerals	Composition
Carnallite	$KMgCl_3•6H_2O$	Aphthitalite	$(K,Na)_3Na(SO_4)_2$
Kainite	$MgSO_4•KCl•3H_2O$	Anhydrite	$CaSO_4$
Langbeinite	$K_2Mg_2(SO_4)_3$	Bischofite	$MgCl•6H_2O$
Polyhalite	$K_2Ca_2Mg(SO_4)_4•2H_2O$	Blödite	$Na_2Mg(SO_4)_2•4H_2O$
Sylvite	KCl	Boracite	$Mg_7B_7O_{13}Cl$
		Dolomite	$CaMg(CO_3)_2$
		Epsomite	$MgSO_4•7H_2O$
		Gypsum	$CaSO_4•2H_2O$
		Halloysite	$Al_2Si_2O_5(OH)_4$
		Halite	NaCl
		Hexahydrite	$MgSO_4•6H_2O$
		Hydroboracite	$CaMgB_6O_8(OH)_6•3H_2O$
		Inderite	$Al_2Si_2O_5(OH)_4$
		Kaolinite	$MgSO_4•H_2O$
		Kieserite	$MgSO_4•H_2O$
		Kurnakovite	$K_2Mg(SO_4)_2•4H_2O$
		Leonite	$Na_{12}Mg_7(SO_4)_{13}•15H_2O$
		Löweite	$(Na,Ca)_{0.3}(Al,Mg)_2Si_4O_{10}(OH)_2•nH_2O$
		Lüneburgite	$Mg_3B_2(PO_4)_2(OH)_6•6H_2O$
		Montmorillonite	$(Mg,Al)_2Si_4O_{10}(OH)•4H_2O$
		Palygorskite	$K_2Mg(SO_4)_2•6H_2O$
		Picromerite	$Mg_4Si_6O_{15}(OH)_2•6H_2O$
		Sepiolite	$CaMgCl_6•12H_2O$
		Tachyhydrite	$Na_6Mg(SO_4)_4$
		Vanthoffite	$Na_6Mg(SO_4)_4$
		Volkovskite	$KCa_4B_{22}O_{32}(OH)10Cl•4H_2O$

Potash Ore Assemblages

The dominant ore assemblages contain sylvite and halite with minor (<6 weight percent) carnallite or carnallite plus halite and negligible amounts of sylvite. Some deposits may contain ore assemblages of kainite, langbeinite, polyhalite, kieserite and (or) bischofite mixed with halite and gypsum or anhydrite.

Gangue Mineralogy

Gangue minerals include halite, clay minerals, dolomite, anhydrite, gypsum, bischofite, epsomite, tachyhydrite, leonite, blödite, hexahydrite, vanthoffite, löweite, aphthitalite, picromerite, and borate minerals (table B-1). Sonnenfeld (1991) noted the presence of halloysites, kaolinite, iron-chlorite, magnesium-chlorites, montmorillonite, palygorskite, illite, sepiolite, and muscovite in evaporite basins.

Primary mineral zoning may consist of (1) an outer or stratigraphically lower zone dominated by sulfates such as anhydrite or gypsum, changing to (2) a halite-dominated zone, and culminating with (3) an inner or upper zone containing halite plus potassium chloride or potassium sulfate minerals. Under certain conditions at the end of an evaporation sequence, some other bittern minerals, such as tachyhydrite or bischofite, may also be present and preserved. These minerals are highly soluble and are commonly no longer present in most of these deposits.

Mineral Zoning

Secondary zoning caused by alteration may be pronounced along the flanks and apexes of salt structures.

Ore Controls

Ore controls peculiar to potash-bearing halokinetic salt structures include (1) zones of primary and secondary potash mineralization, (2) internal structure of the salt structures that affects thickness and location of the potash beds, and (3) depth to the potash ore. Halokinesis may move potash-bearing salt to shallower depths, where the potash is more amenable to discovery and mining.

Effects of Alteration

As they rise to the surface, halokinetic potash-bearing salt structures interact with less saline brine and groundwater. Surface and groundwater may partially dissolve carnallite, removing magnesium chloride and leaving potassium chloride to form sylvite. In the upper part of a salt structure, dissolution of salt minerals leaves insoluble materials such as gypsum, anhydrite, and clay that form a caprock that may be may be on the order of tens to a thousand meters thick (Warren, 2006).

Halokinesis can bring potash-bearing salt to the Earth's surface or close to it, exposing the salt to surface weathering. In areas of extreme aridity, such as the Middle East, surface weathering is minimal and salt and potash-bearing salt can exist on the surface.

Exploration Guides

Geochemical Signature(s)

Primary indicator elements of potash mineralization in rocks and groundwater include potassium, sodium, magnesium, bromine, chlorine, and sulfur as sulfate (Rogers, 2011). Exceptionally saline wells and saline spring water may be indicative of an evaporite sequence at depth, and have historically led to discoveries of concealed salt and potash deposits.

Geophysical Signature(s)

Seismic, gravity, and downhole gamma radiation surveys may be useful in the delineation of potash-bearing salt. The velocity contrast between salt and most other sedimentary rocks is sufficient that reflection seismic methods are used extensively to delineate salt structures and beds (Ratcliff and others, 1992; Ezersky, 2005). Salt is less dense than most enclosing sediments, so gravity surveys work well to identify and define salt structures (Nettleton, 1968; Benassi and others, 2006). High gamma radiation from the natural isotope ^{40}K provides a measure of the potassium content of salt in drill-hole logs (Garrett, 1996). In underground mines, ground penetrating radar may be used to define the structure of the salt diapir (Behlau and Mingerzahn, 2001; Kovin, 2011).

Geomorphic and Physiographic Features

Near-surface diapirs may be expressed as domal or collapse structures that are roughly circular topographic highs or lows. Lakes may form at the crest of near-surface salt structures owing to dissolution of the underlying evaporites.

Other Exploration Guides

The most readily detectable features of concealed salt structures that may contain potash include saline wells and springs. Except for drilling confirmation of potash, there are few sure indications of the presence of potash-bearing salt. Thick sections of halite, usually greater than 100 m, are believed to be necessary prior to potash deposition (Harben and Kužvart, 1996), and this feature could be used in conjunction with other data to identify or rank the potash potential of basins with little exploration history.

Typical Grade and Tonnage

Tonnages of these deposits are smaller on average than stratabound potash-bearing salt deposits. However, some of the deposits have reported resources of as much as 6–10 billion metric tons in some unusually large and complex salt structures. Grades are highly variable, but commonly average less than 20 percent K_2O.

References Cited

Al-Zoubi, Abdallah, and ten Brink, U.S., 2001, Salt diapirs in the Dead Sea basin and their relationship to Quaternary extensional tectonics: Marine and Petroleum Geology, v. 18, no. 7, p. 779–797.

Amor, H., 1999, Halokinesis and structural evolution of the major features in eastern and southern Tunisian Atlas: Tectonophysics, v. 306, no. 1, p. 79–95.

Back, Malcolm, and Mandarino, J.A., 2008, Fleischers glossary of mineral species 2008: Mineralogical Record, Inc., 346 p.

Behlau, J., and Minzerzahn, G., 2001, Geological and tectonic investigations in the former Morsleben salt mine (Germany) as a basis for the safety assessment of a radioactive waste repository: Engineering Geology, v. 61, p. 83–97.

Benassi, R., Jallouli, C., Hammami, M., and Turki, M.M., 2006, The structure of Jebel El Mourra, Tunisia—A diapiric structure causing a positive gravity anomaly: Terra Nova, v. 18, p. 432–439.

Ezersky, M., 2005, The seismic velocities of the Dead Sea salt applied to the sinkhole problem: Journal of Applied Geophysics, v. 58, no. 1, p. 45–58.

Garrett, D.E., 1996, Potash—Deposits, processing, properties and uses: New York, Chapman & Hall, 734 p.

Goncharenko, O.P., 2006, Potassic salts in Phanerozoic evaporite basins and specific features of salt deposition at the final stages of halogenesis: Lithology and Mineral Resources, v. 41, no. 4, p. 378–388.

Harben, P.W., and Kužvart, M., 1996, Industrial minerals—A global geology: London, Industrial Minerals Information Ltd., 462 p.

Hardie, L.A., 1990, The roles of rifting and hydrothermal CaCl2 brines in the origin of potash evaporites—An hypothesis: American Journal of Science, v. 290, no. 1, p. 43–106.

Hardie, L.A., 1996, Secular variation in seawater chemistry—An explanation for the coupled secular variation in the mineralogies of marine limestones and potash evaporites over the past 600 m.y.: Geology, v. 24, p. 279–283.

Holland, H.D., Horita, Juske, and Seyfried, W.E., Jr., 1996, On the secular variation in the composition of marine potash evaporates: Geology, v. 24, no. 11, p. 993–996.

Horita, Juske, Zimmerman, Heide, and Holland, H.D., 2002, Chemical evolution of seawater during the Phanerozoic—Implications from the record of marine evaporites: Geochimica et Cosmochimica Acta, v. 66, no. 21, p. 3733–3756.

Jarhani, S., Callot, J.-P., Frizon de Lamotte, D., Letouzey, J., and Leturmy, P., 2007, The salt diapirs of the eastern Fars Province (Zagros, Iran)—A brief outline of their past and present, *in* Lacombe, O., Lavé, J., Roure, F., and Vergés, J., eds., Thrust belts and foreland basins: Berlin, Springer, p. 289–308.

Kendall, A.C., 2010, Marine evaporites, *in* James, N.P., and Dalrymple, R.W., eds., Facies models 4: Geological Association of Canada, GEOtext 6, p. 505–540.

Kityk, V.I., 1970, Solianaia tektonika Dneprovsksko-Donetskoi vpadiny [Salt tectonics of the Dnieper-Donets Depression]: Kiev, Akad. Nauk Ukrain. SSR, Inst. Geol. Nauk, 201 p.

Kovalevych, V.M., Marshall, T., Peryt, T.M., Petrychenko, O.Y., and Zhukova, S.A., 2006, Chemical composition of seawater in Neoproterozoic—Results of fluid inclusion study of halite from Salt Range (Pakistan) and Amadeus Basin (Australia): Precambrian Research, v. 144, p. 39–51.

Kovalevych, V.M., Peryt, T.M., and Petrychenko, O.Y., 1998, Secular variation in seawater chemistry during the Phanerozoic as indicated by brine inclusions in halite: Journal of Geology, v. 106, p. 695–712.

Kovin, O., 2011, Mapping of evaporite deformation in a potash mine using ground penetration radar—Upper Kama deposit, Russia: Journal of Applied Geophysics, v. 74, p. 131–141.

Kyle, J.R., and Posey, H.H., 1991, Halokinesis, cap rock development, and salt dome mineral resources, *in* Melvin, J.L., ed., Evaporites, petroleum and mineral resources: New York, Elsevier, p. 413–474.

Long, K.R., 1992, Descriptive model of salt-dome sulfur and contained-sulfur model for salt-dome sulfur: U.S. Geological Survey Open-File Report 92–403, 8 p. [Also available at http://pubs.er.usgs.gov/publication/ofr92705.]

Nettleton, L.L., 1968, Gravity anomalies over salt diapirs, northern Spain, *in* Mattox, R.B., Holser, W.T., Odé, H., McIntire, W.L., Short, N.M., Taylor, R.E., and Van Siclen, D.C., eds., Saline deposits: Geological Society of America Special Paper 88, p. 75–82.

Orris, G.J., Cocker, M.D., Dunlap, P., Wynn, J.C., Spanski, G.T., Briggs, D.A., and Gass, L., with contributions from Bliss, J.D., Bolm, K.S., Yang, C., Lipin, B.R., Ludington, S., Miller, R.J., and Slowakiewicz, M., 2014, Potash—A global overview of evaporite-related potash resources, including spatial databases of deposits, occurrences, and permissive tracts: U.S. Geological Survey Scientific Investigations Report 2010–5090–S, 76 p., and spatial data, http://dx.doi.org/10.3133/sir20105090S.

Ratcliff, D.W., Gray, S.H., and Whitmore, N.D., Jr., 1992, Seismic imaging of salt structures in the Gulf of Mexico: The Leading Edge, v. 11, p. 15–31.

Raup, O.B., 1991, Descriptive model of salt domes; Deposit subtype—Diapiric salt structures, *in* Orris, G.J., and Bliss, J.D., Some industrial mineral deposit models—Descriptive deposit models: U.S. Geological Survey Open-File Report 91–11A, 73 p.

Ries, J.B., 2010, Review—Geological and experimental evidence for secular variation in seawater Mg/Ca (calcite-aragonite seas) and its effect on marine biological calcification: Biogeosciences, v. 7, p. 2795–2849.

Rogers, M.C., 2011, Saskatchewan descriptive mineral deposit models: Saskatchewan Ministry of Energy and Resources Open File Report 2011–57, 112 p.

Schmalz, R.F., 1969, Deep-water evaporite deposition—A genetic model: American Association of Petroleum Geologists Bulletin, v. 53, no. 4, p. 798–823.

Sonnenfeld, P., 1991, Evaporite basin analysis, *in* Force, E.R., Eidel, J.J., and Maynard, J.B., Sedimentary and diagenetic mineral deposits—A basin analysis approach to exploration: Reviews in Economic Geology Volume 5, p. 159–169.

U.S. Department of State, 2009, Small-scale digital international land boundaries (SSIB)—Lines, edition 10, and polygons, beta edition 1, *in* Boundaries and Sovereignty Encyclopedia (B.A.S.E.): U.S. Department of State, Office of the Geographer and Global Issues.

Warren, J.K., 2006, Evaporites—Sediments, resources and hydrocarbons: Berlin, Springer-Verlag, 1,035 p.

Warren, J.K., 2008, Salt as sediment in the Central European Basin system as seen from a deep time perspective, *in* Littke, Ralf, Bayer, Ulf, and Gajewski, Dirk, eds., Dynamics of Complex Intracontinental Basins: Berlin, Springer-Verlag, p. 249–276.

Zharkov, M.A., 1984, Paleozoic salt bearing formations of the world: New York, Springer-Verlag, 427 p.

Zharkov, M.A., 2005, Evolyutsiya evaporitov v dokembrii v svyazi s preobrazovaniyami biosfery i khimicheskogo sostava mirovogo okeana; Stat'ya 1, Evapority arkheya i rannego proterozoya [Evolution of Precambrian evaporites, transformation of biosphere and the world oceans' chemical composition—Paper 1, Archean and Paleoproterozoic evaporites]: Stratigrafiya, Geologicheskaya Korrelyatsiya, v. 13, no. 2, p. 19–29.

Appendix C. Adaptive Geometric Estimation for Stratabound Potash-Bearing Salt Deposits—Summary

By Greta J. Orris,[1] James D. Bliss,[1] Pamela Dunlap,[1] and Mark D. Cocker[1]

This summary describes a geometric estimation approach for assessment of areally extensive bedded or stratiform mineral deposits and the use of this approach to estimate undiscovered potash in stratabound potash-bearing salt deposits. This methodology is adaptable to varied types of data inputs and the resulting estimate is in a format compatible with results from the U.S. Geological Survey (USGS) three-part form of assessment (Singer and Menzie, 2010).

Requirements for Methodology

An assessment methodology for stratabound deposits must meet several criteria:

- The process must produce a probabilistic estimate of undiscovered resources as a distribution of expected grades and tonnages of the contained mineral or commodity (for example, K_2O for potash). A probabilistic distribution is compatible with outputs from areas assessed using the traditional USGS three-part form of assessment (Singer and Menzie, 2010) and indicates not only the best estimate, but also the uncertainty of the estimate. A single number conveys a level of certainty unlikely to be achievable in this type of exercise.
- The methodology must be appropriate for a stratabound deposit type; it should be based on volume (area multiplied by thickness) with appropriate adjustments for unmineralized areas, uncertainties and variability in input, and other factors that affect the estimate of the amount of mineralization.
- The methodology must be adaptable to large variations in basin size and to highly variable input data volumes, formats, and densities across a tract.
- The output must be adjustable for known reserves and resources.
- The methodology needs to be easily implemented with readily available hardware and software, as well as be adaptable to new and (or) different software, hardware, and estimation techniques.

These requirements led to development of a methodology that can be adapted to highly variable inputs on a basin-by-basin basis, yet still provides a common underlying approach and results in a format that allows for comparison between areas.

General Approach

A simplified description of ore reserve estimates that meet the Canadian Securities Administrators National Instrument 43-101 report standards for potash (Canadian Institute of Mining, Metallurgy and Petroleum, 2003), starts with a volume estimate of mineralized material that is converted to ore tonnage using an appropriate density (table C-1). The estimated ore tonnage is then adjusted for unmineralized areas contained within the area estimated. An overview of mineral reserve and resource estimation standards for these reports, as well as some potash specific guidelines, are available from the Canadian Institute of Mining, Metallurgy and Petroleum (2003, 2004). The adaptive geometric estimation (AGE) methodology takes a similar approach to estimating undiscovered resources with the less robust data inputs to be expected from poorly-explored areas and with an additional correction for known reserves and resources.

Table C-1. Densities used in calculating tonnage.

[g/cm^3, grams per cubic centimeter]

	Formula	Density (g/cm^3)
Carnallite	$KMgCl_3 \cdot 6H_2O$	1.6
Halite	NaCl	2.17
Sylvite	KCl	1.99
Elk Point sylvinite		2

[1]U.S. Geological Survey, Tucson, Arizona, United States.

Overall, the approach can be most simply stated as:

$$T = (VOL \times DENS) - NOMIN - RR,$$

where

T = "undiscovered" in-place tonnage,
VOL = volume,
$DENS$ = density of ore,
$NOMIN$ = correction for unmineralized areas, and
RR = known reserves and resources.

It follows that the tonnage of the commodity of interest, potash (K_2O), is

$$KT = T \times GRD,$$

where

KT = tonnage of contained potash as K_2O, and
GRD = potash grade as percent K_2O.

Adaption of Reserves Estimation to Undiscovered Resources Estimation

The AGE methodology for assessing stratabound potash deposits consists of several steps. First, the tract area for potash is identified and delineated using geologic maps, deposit models, and other data. Second, the volume of this area is calculated using known and (or) estimated thickness data. Third, a potash grade is selected from an appropriate grade distribution model. If the dominant ore mineral is not known, then an assumption is made about the probable ore mineral based on the selected grade. The grade and ore mineral are used to determine an appropriate density to convert the volume estimate to an in-place tonnage for the delineated area. Fourth, the tonnage estimate is adjusted for unmineralized areas within the tract (anomalies) and along its edges (embayments) and for known mineralization, as appropriate. Finally, the contained potash in the ore (as metric tons of K_2O) is determined from the tonnage and grade. The process is repeated for 5,000 iterations to produce a probabilistic estimate of contained potash. A flow chart of this process is shown in figure C-1.

Although this approach is conceptually simple, implementation in areas with undiscovered resources is complicated by incomplete data. The extent of mineralization, in terms of area and thickness, is usually not well-defined and reported grade, density, and similar data may not represent the entire assessment area. It is inevitable in areas with undiscovered resources that one or more data inputs will be unknown and must be estimated. These estimates can be based on analogy with similar, better explored areas, or models can be constructed based on incomplete data from the area being studied.

This is a largely stochastic approach that requires simplifying assumptions along with estimates of missing data. Most estimates of missing data are not single numbers, but are distributions of possible values. These distributions are randomly sampled using Monte Carlo simulation(s) in the AGE methodology. For potash, 5,000 iterations were typically used. This process produces stable or repeatable distributions of estimated undiscovered ore and the contained commodity, with the medians of those distributions representing the most likely values.

Implementation of this methodology for the potash assessment requires a geographic information system (GIS) or other system to calculate areas and volumes, as well as statistical and modeling software. For this study, ArcGIS was used to map data and estimate volumes. Data distributions were constructed and (or) tested using JMP 8 data analysis software. More complex statistical procedures, simulations and estimations were programmed and executed using SYSTAT 12 software (appendix F). Individual steps and some of the alternate estimation procedures are discussed more completely in the following sections.

Tract Delineation and Volume

The first step in an assessment process is to delineate a tract, the area containing the mineralization of interest. Tract delineation is commonly done using a mix of geologic and other maps, geophysical data, and point data, such as drill holes and mineral occurrences. In addition, tract delineation may be constrained by criteria such as minimum thickness, grade, or maximum levels of deleterious materials or contaminants. At an assessment scale of 1:1,000,000, uncertainties in potash tract boundaries, caused by lack of detail in source materials used to delineate the mineralized areas, can be significant and assessors should account for this in their estimates. An Albers Equal Area or other equal area projection of the tract boundaries should be used for accurate area and volume calculations.

In well-explored areas, thickness values can be extracted from drill-hole data and the information contoured. In less-explored areas, thickness data might be a mix of drill-hole and other point data on thickness. For these latter cases, a single volume can be calculated using a continuous raster surface of the total potash thickness and the lateral tract boundaries. Most tracts have multiple sources for thickness estimates, including drill-hole and isopach data, and these data are commonly unevenly distributed. In these tracts, thickness isopachs can be constructed for the entire tract using the available data and informed judgment. Volumes can then be calculated using the isopachs.

In some areas, thickness data are not available as either point data or isopachs to allow calculation of volume. In these areas, an "average" thickness can be estimated and used.

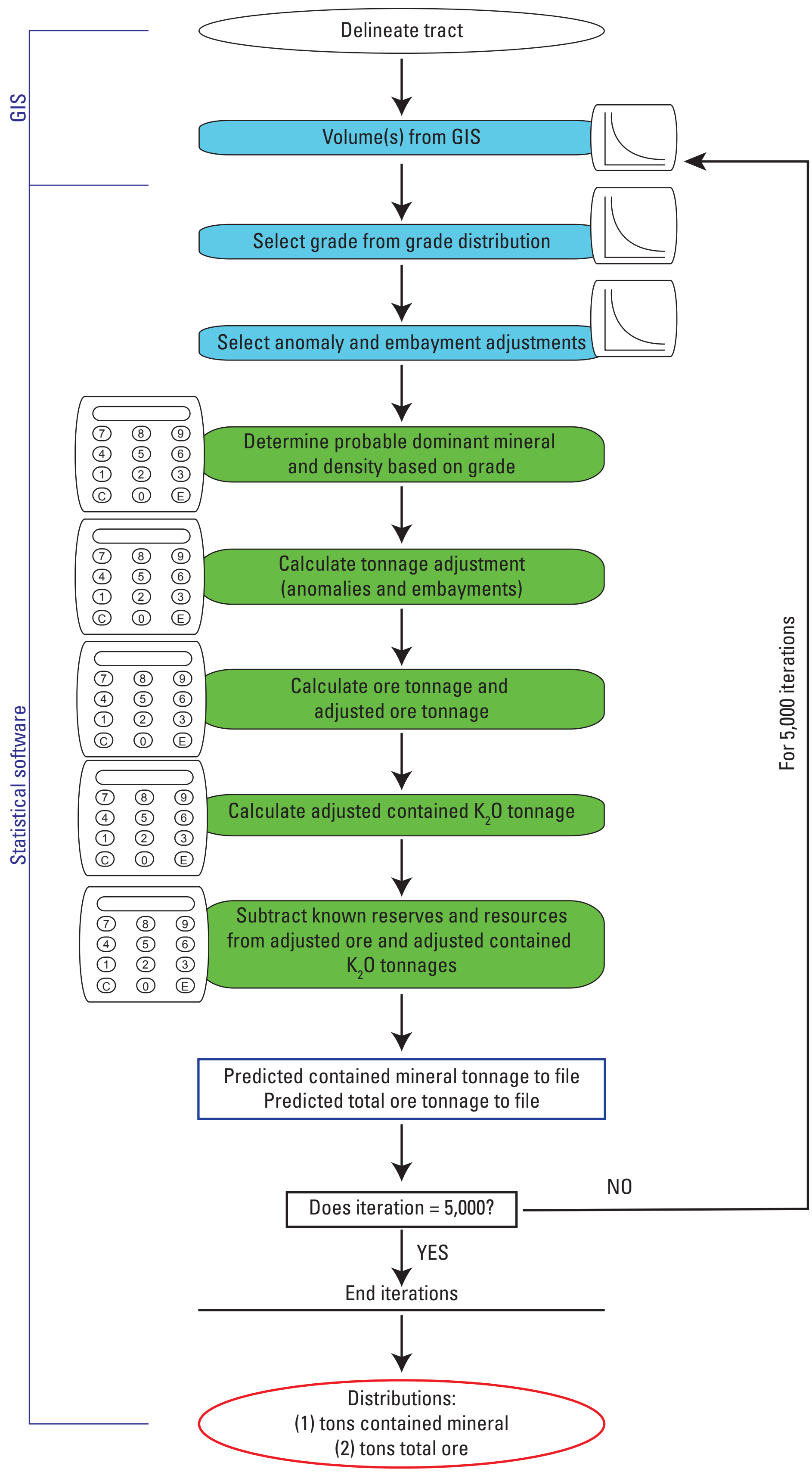

Figure C-1. Flow chart showing generalized approach for assessing stratabound industrial mineral deposits.

If possible, a maximum, minimum, and mode estimate of thickness should be made. These values allow construction of a triangular distribution (Kotz and van Dorp, 2004). Use of triangular distributions is not an optimal choice because the tails of the distribution tend to be overestimated and the relationship between the maximum and minimum values and the mode are assumed to be linear (fig. C-2). However, the triangular distribution is widely used in risk assessment and other areas where the underlying distribution is not known, and this distribution is commonly available in statistical software packages. The advantage of this distribution is that most scientists understand what the input values mean and can estimate these values consistently when provided with a given level of geologic information. However, the use of the triangular distribution is not considered to be as statistically rigorous by some statisticians as other distributions. In the case of potash thickness, we do not know the underlying distribution (normal, lognormal, exponential, or other) and published studies for thickness distributions for other lithologies are not in agreement. Therefore, use of the triangular distribution is often the best available option.

In assessment of undiscovered potash resources, the exact method of calculating the volumes is not considered to be a significant issue compared to other uncertainties, and the assessor should use the tools available. Testing of calculated differences in volumes, such as comparing the outcomes of kriging and nearest neighbor in this study, showed maximum differences of 3–11 percent where the data points were unevenly distributed and data point density was low. In most calculations, the potential error from incomplete, missing, and widely and unevenly spaced data is significantly larger than differences arising from the volume calculation technique.

Grade and Density

For most potash tracts, grade was modeled using available grade data for thickness intervals of 1 m or greater. Grades of rock-forming commodities such as potash are normally distributed (as opposed to the lognormal distribution of commodities such as Cu, Au, Pb, and so on; see Harris, 1984). Grade models were constructed by USGS staff from published potash horizon thicknesses and grades taken from well log data. Grades and thicknesses determined by the USGS from well logs met the following criteria: (1) contiguous extent of potash and halite mineralization with minimum thickness of 1 meter and no maximum thickness; (2) average grade within selected thickness greater than 4 percent K_2O equivalent; and (3) potash horizons divided by “unmineralized” halite. Note that “unmineralized” halite consists of (1) halite horizons that were not sampled and analyzed by drillers because of assumed low grade, (2) 1 meter or more of halite that would drop potash grade below the minimum grade if included in the potash horizon, and (3) halite outside of geophysically-determined potash horizons. Most of the grade models constructed for potash tracts are distributed normally if $n>30$, where n is the number of data points. For very small datasets, the mean of the documented data and other information was used to create a normal distribution of K_2O grade. For tracts with little data where correlation between potash horizons in different parts of the tract could not be determined and for tracts where reported data consisted of the aggregate thickness of all potash horizons and the average grade across all the horizons, potash resources were estimated as total potash without consideration of intervening halite.

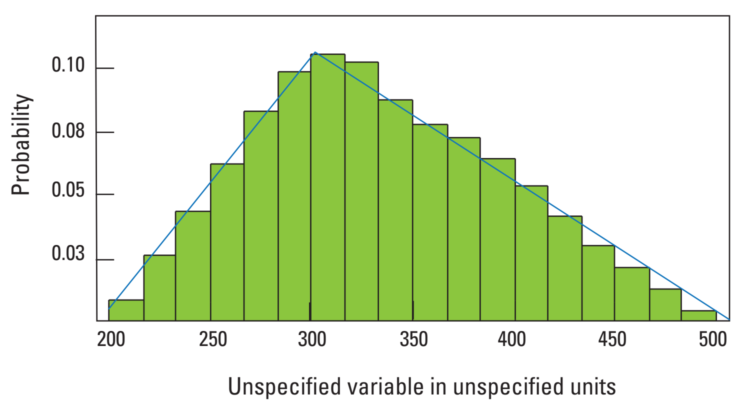

Figure C-2. Graph showing example of a triangular distribution of an unspecified variable with a mode value of 300, a maximum of 500, and a minimum of 200.

To convert estimated volume(s) of potash mineralization to tonnage(s) requires a known or estimated density. In some areas, such as Saskatchewan, many companies use a standard average density for conversion for sylvite ore based on knowledge or assumptions about the ore composition. For most potash tracts evaluated by the USGS, we estimate density based on grade distributions constructed for each tract and modeled sylvinite or carnallitite grade and density relationships (see appendix F). Data released by Rauche and others (2013) allowed relationships between carnallite and sylvinite grades and measured density to be modeled using linear regression. A Monte Carlo simulation was used to sample the grade distribution and that grade was substituted in one of the following formulas based on regression of the Rauche and others Congo data to determine the density:

- Sylvinite—density = 2.177–0.003×grade, or
- Carnallite—density = 2.044 – 0.027×grade.

These formulas are considered appropriate because the mean of the density response for sylvinite in that regression is 2.08, a common average density used for sylvinite ore tonnage calculations in Saskatchewan. Also, the carnallitite grade and density relationship provides densities similar to a scattered handful of carnallitite grade and density reports. Although region-specific relationships would be preferred if the data were available, grade and measured density are rarely reported together.

A major simplifying assumption is made in the absence of specific data on the type of potash mineralization. The resource is considered to be a mix of the potash mineral carnallite and halite (carnallitite) if the selected grade in an iteration is less than 16.9 percent K_2O (the maximum K_2O content of carnallite). For grades of 16.9 percent K_2O or greater, the ore is considered to be a mix of sylvite and halite (sylvinite).

Tonnage and Adjustments to Tonnage

Once density is determined, in-place ore tonnage can be calculated by multiplying ore volume by density. Estimators need to ensure that the volume units and density units are compatible.

There may be large unmineralized areas within the tract boundaries. For potash, these areas may result from non-deposition, dissolution, erosion, remineralization, or other factors that significantly decrease the size of the potential resource. Therefore, once a gross tonnage is determined for the potash mineralized area, the tonnage needs to be adjusted for what the potash assessment team has classified as anomalies and embayments (fig. C-3), as well as known reserves and resources.

Anomalies are defined as any barren areas inside the tract other than rocks that are too old to host mineralization and that should be excluded from the tract during the initial delineation process. Anomalies include depletion zones, replacement zones, and halite zones, washout and leach or “salt horst” anomalies, or salt dissolution and collapse anomalies (Baar, 1974; Korenevskiy, 1989; Boys, 1990; Filippov, 1990; Kopnin, 1995; Abbott and Kuchling, 2009). Anomalies are interruptions in the normal continuity of potash-bearing beds and may range in size from less than a meter to tens of square kilometers or larger. The lack of potash mineralization may result from dissolution, non-deposition, erosion, or another cause; halite is typically encountered in these areas rather than potash. Anomalies may occupy as much as 40 percent or more of the mineralized area (Linn and Adams, 1966; Boys, 1990) or as little as 5 percent (Kopnin, 1995). The reported average seems to be in the range of 20 to 25 percent (Halabura and Hardy, 2007; Hardy and others, 2009). For most tracts, this variable needs to be estimated, and there is commonly at least some information specific to each tract on which to base the estimate.

Embayments are a correction for actual edge irregularities in the mineralization not represented in the tract boundaries. These irregularities may be in part caused by dissolution, but largely result from non-deposition because of topography, facies change, water or sediment incursion from the basin edges, or mechanical weathering. This correction is added because the effect on volume and tonnage may be large; it is determined and estimated where appropriate on a tract-by-tract basis and considers how the tract boundary was delineated and the scale of the most detailed information. Potash-bearing tracts may show effects of just anomalies or just embayments, but at common assessment scales such as 1:1,000,000, effects of both need to be considered. In places, the cumulative area of potash loss due to embayments and anomalies may be a significant percentage of the overall potash mineralized area and leads to a “Swiss cheese” pattern of potash distribution, such as in the Krasnyi IIIB horizon of the Permian Solikamsk deposit, Russia (fig. C-3; Zharkov, 1984).

The last adjustment to tonnage is to subtract known reserves and resources. For the potash assessment, this includes all proven, measured, recoverable, indicated, and inferred reserves and resources, as well as those classified as A, B, C1, and C2 under the Russian resource/reserve reporting system (Henley, 2004). All known reserve and resource figures are converted to in-place ore and contained potash (as K_2O) before being subtracted from the estimate.

Constructing a Probabilistic Distribution

The process outlined above is repeated for 5,000 iterations to create a probabilistic distribution of estimates of contained potash. This was done using the Monte Carlo simulation function of the SYSTAT 12 software and tract-specific tracts.

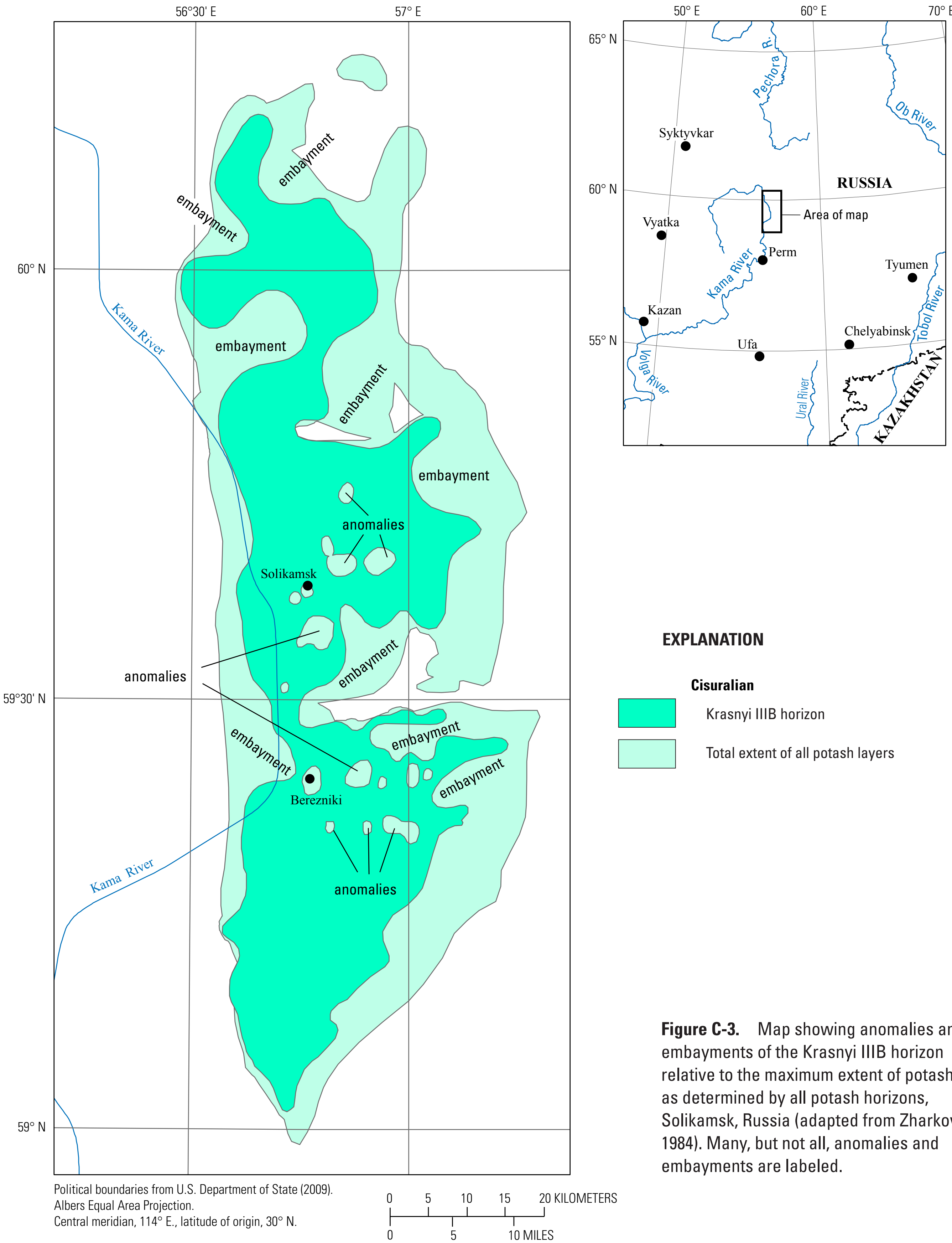

Political boundaries from U.S. Department of State (2009).
Albers Equal Area Projection.
Central meridian, 114° E., latitude of origin, 30° N.

Figure C-3. Map showing anomalies and embayments of the Krasnyi IIIB horizon relative to the maximum extent of potash as determined by all potash horizons, Solikamsk, Russia (adapted from Zharkov, 1984). Many, but not all, anomalies and embayments are labeled.

Summary

The AGE methodology produces a distribution of in-place ore tonnage and contained K_2O tonnage for the assessed potash tracts. This approach also provides an estimation of the uncertainty in the assessment. Input variables for estimates that form distributions are sampled using successive Monte Carlo simulations; for most tracts, 5,000 iterations were performed to produce stable distributions of estimated ore and contained K_2O tonnages. The most probable ore tonnage and contained K_2O estimates are centered near the mean; the values in the tails of these distributions are considered unlikely but help quantify the uncertainty.

References Cited

Abbott, D.M., and Kuchling, K.J., 2009, Encanto Potash Corp. and Angus Ventures Corp., Technical report for Saskatchewan potash properties—Ochapowace/Chacachas prospect, T29, R5-6W2 latitude 50.48°N longitude 102.38°W; Piapot/Muscowpetung prospect, T21, R17-18W2 latitude 50.76°N longitude 104.27°W; Day Star prospect, T29, R16W2 latitude 51.55°N longitude W104.27°W: Toronto, Behre Dolbear and Company, Ltd., 47 p.

Baar, C.A., 1974, Geological problems in Saskatchewan potash mining due to peculiar conditions during deposition of Potash Beds, *in* Coogan, A.H., ed., Fourth Symposium on Salt: Cleveland, Ohio, Northern Ohio Geological Society, p. 101–118.

Boys, C., 1990, The geology of potash deposits at PCS Cory Mine, Saskatchewan: Saskatoon, Saskatchewan, Canada, University of Saskatchewan, Master's thesis, 225 p.

Canadian Institute of Mining, Metallurgy and Petroleum, 2003, Estimation of mineral resources and mineral reserves—Best practice guidelines: Canadian Institute of Mining, Metallurgy and Petroleum Web page, accessed June 23, 2013, at http://web.cim.org/UserFiles/File/Estimation-Mineral-Resources-Mineral-Reserves-11-23-2003.pdf.

Canadian Institute of Mining, Metallurgy and Petroleum, 2004, Potash: Canadian Institute of Mining, Metallurgy and Petroleum Web page, accessed June 23, 2013, at http://web.cim.org/UserFiles/File/Potash-Estimation-Guidelines.pdf.

Filippov, S.A., 1990, Morfogeneticheskiye raznovidnosti zon razubozhivaniya i zameshcheniya produktivnykh plastov kaliynykh mestorozhdeniy i ikh klassifikatsiya [Morphogenetic variation of impoverished zones and localization of potash deposits and their classification], *in* Merzlyakov, G.A., and Zharkov, M.A., eds., Usloviya obrazovaniya mestorozhdenii kaliinykh solei [The conditions of the formation of potash salt deposits]: Novosibirsk, Nauka, p. 41–47.

Halabura, S.P., and Hardy, M.P., 2007, An overview of the geology of solution mining of potash in Saskatchewan, *in* Solution Mining Research Institute Fall Conference: Halifax, Nova Scotia, Canada, Solution Mining Research Institute Technical Conference Paper, 17 p.

Hardy, M., Halabura, S.P., and Shewfelt, D., 2009, Technical report—2009 potash resource assessment for subsurface mineral permit KP 289, Saskatchewan: Grand Junction, Colo., and Saskatoon, Saskatchewan, Agapito Associates, Inc. and North Rim Exploration Ltd., 163 p.

Harris, D.P., 1984, Mineral resources appraisal—Mineral endowment, resources and potential—Concepts, methods and cases: Oxford, Clarendon Press, 445 p.

Henley, S., 2004, Russian mineral reporting: Mining Journal, London, no. August 20, p. 18–21.

Henley, Stephen, and Allington, Ruth, 2010, Reserves classification systems around the world: Pan-European Reserves Reporting Committee, 51 p., accessed August 21, 2015, at http://www.vmine.net/PERC/documents/reserves-classification-systems-around-the-world-FINAL.pdf.

Kopnin, V.I., 1995, Halite anomalies in potash-bearing beds in the southern part of the Verkhnekama potash salt deposit: Structure and genesis: Lithology and Mineral Resources, v. 30, no. 5, p. 453–464.

Korenevskiy, S.M., 1989, Substitution and depletion zones of potash and potassium-magnesium salt deposits: Lithology and Mineral Resources, v. 24, no. 1, p. 50–63.

Kotz, S., and van Dorp, J.R., 2004, Beyond Beta—Other continuous families of distributions with bounded support and applications: Hackensack, New Jersey, World Scientific Publishing Company, 308 p.

Linn, K.O., and Adams, S.S., 1966, Barren halite zones in potash deposits, Carlsbad, New Mexico, *in* Rau, J.L., ed., Second symposium on salt: Cleveland, Ohio, The Northern Ohio Geological Society, Inc., p. 59–69.

Rauche, Henry, van der Klauw, Sebastiaan, and Linsenbarth, Ralf, 2013, Summary of the Feasibility Study for a Solution Mine on the ALLANA Potash Project, Danakhil Depression, Afar State, Ethiopia: Technical Report NI 43-101, February 4, 2013 news release, Allana Potash Corp., accessed August 21, 2015, at http://www.allanapotash.com/news/2013/index.php?&content_id=33.

Singer, D.A., and Menzie, W.D., 2010, Quantitative mineral resource assessment—An integrated approach: New York, Oxford University Press, 219 p.

Zharkov, M.A., 1984, Paleozoic salt bearing formations of the world: New York, Springer-Verlag, 427 p.

Appendix D. Grade Data for Gissar and Amu Darya Tracts

By Greta J. Orris,[1] Mark D. Cocker,[1] and Jeff Wynn[2]

Table D-1. Grade data for the Central Asia Salt Basin.

[U., upper; Mid., middle; %, percent; m, meter; —, no data]

Well or site	Orebody or layer	K_2O (%)	Thickness (m)	Reference
2	Lower II	17.79	2	Petrov and Chistakov (1964)
5	Lower II	13.6	3.5	Petrov and Chistakov (1964)
6	Lower II	20.44	1.5	Petrov and Chistakov (1964)
7	Lower II	16.49	1.5	Petrov and Chistakov (1964)
8	Lower II	19.53	5.03	Petrov and Chistakov (1964)
11	Lower II	11.62	1.5	Petrov and Chistakov (1964)
14	Lower II	26.61	1.5	Petrov and Chistakov (1964)
15	Lower II	26.09	2	Petrov and Chistakov (1964)
17	Lower II	16.13	1.5	Petrov and Chistakov (1964)
18	Lower II	16.09	2	Petrov and Chistakov (1964)
26	Lower II	15.17	2.5	Petrov and Chistakov (1964)
35	Lower II	17.24	1.5	Petrov and Chistakov (1964)
36	Lower II	17.77	4.5	Petrov and Chistakov (1964)
44	Lower II	16.84	2	Petrov and Chistakov (1964)
45	Lower II	18.45	8	Petrov and Chistakov (1964)
46	Lower II	10.39	2.5	Petrov and Chistakov (1964)
47	Lower II	9.64	1	Petrov and Chistakov (1964)
49	Lower II	20.72	3	Petrov and Chistakov (1964)
51	Lower II	14.38	3.5	Petrov and Chistakov (1964)
54	Lower II	15.41	1.5	Petrov and Chistakov (1964)
55	Lower II	13.01	1.2	Petrov and Chistakov (1964)
1	Lower II	12.3	1.55	Petrov and Chistakov (1964)
2	Lower II	19.28	6	Petrov and Chistakov (1964)
3	Lower II	23.96	4.4	Petrov and Chistakov (1964)
46	Lower II	18.05	1.5	Petrov and Chistakov (1964)
47	Lower II	10.84	1	Petrov and Chistakov (1964)
48	Lower II	18.06	1.5	Petrov and Chistakov (1964)
50	Lower II	17.43	1.5	Petrov and Chistakov (1964)
51	Lower II	19.33	2	Petrov and Chistakov (1964)
1	Blue	17.17	3.15	Petrov and Chistakov (1964)
5	Blue	18.79	2	Petrov and Chistakov (1964)
6	Blue	14.6	1.5	Petrov and Chistakov (1964)
7	Blue	16.23	3	Petrov and Chistakov (1964)
11	Blue	19.81	2.2	Petrov and Chistakov (1964)
14	Blue	23.41	4	Petrov and Chistakov (1964)

[1]U.S. Geological Survey, Tucson, Arizona, United States.

[2]U.S. Geological Survey, Vancouver, Washington, United States.

Table D-1. Grade data for the Central Asia Salt Basin.—Continued

Well or site	Orebody or layer	K_2O (%)	Thickness (m)	Reference
15	Blue	19.61	3.72	Petrov and Chistakov (1964)
16	Blue	7.95	1.5	Petrov and Chistakov (1964)
19	Blue	13.85	2.5	Petrov and Chistakov (1964)
20	Blue	13.01	1.5	Petrov and Chistakov (1964)
21	Blue	21.89	1.6	Petrov and Chistakov (1964)
22	Blue	12.63	2.5	Petrov and Chistakov (1964)
23	Blue	14.98	2.5	Petrov and Chistakov (1964)
24	Blue	16.48	3.5	Petrov and Chistakov (1964)
25	Blue	15.35	3.59	Petrov and Chistakov (1964)
26	Blue	14.24	5.5	Petrov and Chistakov (1964)
28	Blue	23.71	2.5	Petrov and Chistakov (1964)
29	Blue	14.24	1.5	Petrov and Chistakov (1964)
30	Blue	22.35	2	Petrov and Chistakov (1964)
32	Blue	17.56	1.5	Petrov and Chistakov (1964)
35	Blue	15.75	2.5	Petrov and Chistakov (1964)
36	Blue	10.18	1.5	Petrov and Chistakov (1964)
38	Blue	13.35	3	Petrov and Chistakov (1964)
40	Blue	16.69	5	Petrov and Chistakov (1964)
44	Blue	14.16	4	Petrov and Chistakov (1964)
45	Blue	24.5	3	Petrov and Chistakov (1964)
46	Blue	15.7	2	Petrov and Chistakov (1964)
47	Blue	13.19	2	Petrov and Chistakov (1964)
48	Blue	26.19	2	Petrov and Chistakov (1964)
49	Blue	19.07	2.6	Petrov and Chistakov (1964)
51	Blue	10.74	1.5	Petrov and Chistakov (1964)
53	Blue	16.01	1.5	Petrov and Chistakov (1964)
55	Blue	15.09	1.5	Petrov and Chistakov (1964)
56	Blue	17.12	3.5	Petrov and Chistakov (1964)
Tyubegatan	—	22.51	Not specified	Fedin (1981)
Gaurdak	—	18.91	Not specified	Fedin (1981)
Karlyuk	—	20.13	Not specified	Fedin (1981)
Okuzbulak	—	18.3	Not specified	Fedin (1981)
Akbash	—	12.02	Not specified	Fedin (1981)
Yuzhno-Lyalimkan	—	19.92	Not specified	Fedin (1981)
Kyzylmazar	—	9.93	Not specified	Fedin (1981)
North Gaurdak	—	19.52	Not specified	Fedin (1981)
Karlyuk horizon	U. Carnallite	7.79	5.63 ave (0.29–25.36)	Rayevskiy and Fiveg (1973)
Karlyuk horizon	Ia	12.48	5.83 (0.33–31.2	Rayevskiy and Fiveg (1973)
Karlyuk horizon	II	13.22	3.53 (0.51–13.0)	Rayevskiy and Fiveg (1973)
Karlyuk horizon	III	13.04	4.2 (0.58–15.95)	Rayevskiy and Fiveg (1973)
Karlyuk horizon	Mid. Carnallite	13.93	4.02 (0.3–17.5)	Rayevskiy and Fiveg (1973)
Karlyuk horizon	IV	13.88	5.63 (1.37–46.75)	Rayevskiy and Fiveg (1973)
Karlyuk horizon	V	15.21	5.05 (1.0–22.1)	Rayevskiy and Fiveg (1973)
Karlyuk horizon	VI	16.71	5.67 (0.55–31.5)	Rayevskiy and Fiveg (1973)
Karlyuk horizon	VII	17.01	5.55 (1.06–18.6)	Rayevskiy and Fiveg (1973)
Karlyuk horizon	VIII	17.41	9.5 (1.45–28.2)	Rayevskiy and Fiveg (1973)
Karlyuk horizon	IX	12.44	4.9 (1.12–17.36)	Rayevskiy and Fiveg (1973)
Karlyuk	Upper lens	7.14	1.38	Rayevskiy and Fiveg (1973)
Karlyuk	Lower lens	16.63	2.94	Rayevskiy and Fiveg (1973)
Karlyuk	Lower lens	3.05	4.13	Rayevskiy and Fiveg (1973)
Karlyuk	U. Carnallite	11.41	5.15	Sedletskiy and Derevyagin (1980)
Karlyuk	I	12.76	3.71	Sedletskiy and Derevyagin (1980)
Karlyuk	II	11.36	3.4	Sedletskiy and Derevyagin (1980)

Table D-1. Grade data for the Central Asia Salt Basin.—Continued

Well or site	Orebody or layer	K_2O (%)	Thickness (m)	Reference
Karlyuk	III	13.36	3.75	Sedletskiy and Derevyagin (1980)
Karlyuk	Mid. Carnallite	8.92	1.47	Sedletskiy and Derevyagin (1980)
Karlyuk	IV	15.29	3.12	Sedletskiy and Derevyagin (1980)
Karlyuk	V	17.07	3.3	Sedletskiy and Derevyagin (1980)
Karlyuk	VI	15.7	3.34	Sedletskiy and Derevyagin (1980)
Karlyuk	VII	19	6.05	Sedletskiy and Derevyagin (1980)
Karlyuk	VIII	18.75	9.48	Sedletskiy and Derevyagin (1980)
Karlyuk	IX	17.1	3.52	Sedletskiy and Derevyagin (1980)
Dongusyrt 2D	—	14.51	3.35	Kutuzov and Popov (1976)
Karlyuk	VIII	17.41	>8	Vysotskiy and others (1988)
Karlyuk	VII	17.01	>3	Vysotskiy and others (1988)
Karlyuk	VI	16.71	>3	Vysotskiy and others (1988)
Karlyuk	—	5	>3	Vysotskiy and others (1988)
Karlyuk	—	7.02	>3	Vysotskiy and others (1988)
Karlyuk	I	12.48	>3	Vysotskiy and others (1988)
Karlyuk	II	13.22	>3	Vysotskiy and others (1988)
Karlyuk	III	13.04	>3	Vysotskiy and others (1988)
Tyubegatan	Lower II	22.5	5.1	Vysotskiy and others (1988)

References Cited

Fedin, O.V., 1981, Otsenka perspektiv kaliyenosnosti verkhneyurskikh solyanykh otlozheniy yuga Sredney Azii [An evaluation of the prospects for potash-bearing capabilities in the Upper Jurassic salt deposits in southern Central Asia], *in* Yanshin, A.L., and Zharkov, M.A., eds., Stroyeniye i usloviya formirovaniya mestorozhdeniy kaliynykh soley [The structure and formation conditions of potash salt deposits]: Novosibirsk, USSR, Izd. Nauka, Sibirsk. Otdel., p. 171–176.

Kutuzov, A.P., and Popov, V.S., 1976, Novyye dannyye po geologii Donguzsyrta (Yugo-Vostochnaya Turkmeniya) [New data on the geology of Donguzsyrt, Southeast Turkmenia]: Sovetskaya Geologiya, v. 1976, no. 9, p. 137–142.

Petrov, N.P., and Chistyakov, P.A., 1964, Lithologia solvevykh I krasnocvetnykh otljzenij yugo-eapadnykh otrogov gissara [Lithology salt and red deposits southwestern Gissar spurs]: Tashkent, Uzbekistan, Izdatelstvo Nauka Uzbekskoy SSR, 221 p.

Rayevskiy, V.I., and Fiveg, M.P., 1973, Mestorozhdeniya kaliynykh soley SSSR; metody ikh poiskov i razvedki [Deposits of potassium salts in the USSR; methods of exploration and surveying]: Leniingrad, Izd. Nedra, Leningr. Otd., 344 p.

Sedletskiy, V.I., and Derevyagin, V.S., 1980, Stroyeniye i sostav kaliyenosnih otlozhyeniy Karlyukskogo myestorozhdyeniya [The structure and composition of the potassium-bearing Karlyukskogo deposits], *in* Zharkov, M.A., ed., Osobennosti stroeniia zalezhei bishofita i kaliinykh solei [Structural features of bischofite and potassium salt deposits]: Novosibirsk, Academiia Nauk SSSR, Institut geologgi i geofiziki, p. 70–90.

Vysotskiy, E.A., Garetskiy, R.G., and Kislik, V.Z., 1988, Kalienosnye basseiny mira [Potassium-bearing basins of the world]: Minsk, Izd. Nauka i Tekhnika, Byelorussian SSR, 387 p.

Appendix E. Thickness Data for Gissar and Amu Darya Tracts

By Greta J. Orris,[1] Mark D. Cocker,[1] and Jeff Wynn[2]

Drill holes and occurrences with potash thickness information in the Amu Darya (142sbK0005b) and Gissar (142mxK0005a) tracts were obtained primarily from Russian publications (below). Evaporitic salt is not exposed at the surface in the Amu Darya tract, so this list includes aggregate potash thicknesses for discrete sylvite and carnallite layers encountered in drill holes in the tract. Potash entries with zero value were included from areas lying outside the tracts to constrain the minimum-curvature gridding effort, thus allowing us to obtain a reasonable thickness for potash over the entire area of the tracts. Sedletskiy and Fedin (1981, fig. 2) and Khudaikuliev (1986) show that potash in the tracts, with the exception of the bottom of a single drill hole in the Beshkent Trough, is shallower than 3 kilometers (km).

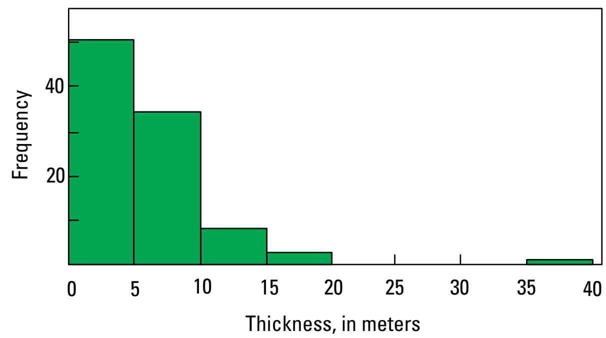

Figure E-1. Histogram showing potash thickness (in meters) in the Gissar and Amu Darya tracts.

Table E-1. Thickness data for Gissar and Amu Darya tracts, Central Asia.

[m, meter]

Name	Latitude	Longitude	Potash thickness (m)	Site type	Reference
Urtabulak	39.017	64.013	6	Occurrence	Fedin (1981)
Bagadzhin 10	39.217	62.667	2	Drill hole	Khudaikuliev (1986)
Donguzsyrt	37.495	65.080	10	Occurrence	Khudaikuliev (1986)
Gaurdak 560	37.877	66.026	>0	Drill hole	Khudaikuliev (1986)
Karabil 96	37.683	66.202	>0	Drill hole	Khudaikuliev (1986)
Khodzhambass 3	38.115	65.078	8	Drill hole	Khudaikuliev (1986)
Metedzhan 4	38.893	64.089	>0	Drill hole	Khudaikuliev (1986)
Okuzbulak 103	37.497	66.412	>0	Drill hole	Khudaikuliev (1986)
Sunduklu 3	38.365	64.451	8	Drill hole	Khudaikuliev (1986)
Akbash	38.172	66.584	9.5	Occurrence	Rayevskiy and Fiveg (1973)
Gaurdak	37.844	66.054	9	Occurrence	Rayevskiy and Fiveg (1973)
Khamkan	38.096	66.759	5	Occurrence	Rayevskiy and Fiveg (1973)
Kugitang	37.879	66.416	5	Occurrence	Rayevskiy and Fiveg (1973)
Skv. 72	37.564	66.320	5.5	Drill hole	Rayevskiy and Fiveg (1973)
Skv. 50	37.554	66.334	3.9	Drill hole	Rayevskiy and Fiveg (1973)
Karlyuk 87	37.533	66.373	0	Drill hole	Sedletskiy and Derevyagin (1980)
Skv. 70	37.575	66.294	38	Drill hole	Sedletskiy and Derevyagin (1980)
Skv. 110	37.615	66.344	0	Drill hole	Sedletskiy and Derevyagin (1980)
Skv. 123	37.623	66.353	0	Drill hole	Sedletskiy and Derevyagin (1980)

[1]U.S. Geological Survey, Tucson, Arizona, United States.

[2]U.S. Geological Survey, Vancouver, Washington, United States.

Table E-1. Thickness data for Gissar and Amu Darya tracts, Central Asia.—Continued

Name	Latitude	Longitude	Potash thickness (m)	Site type	Reference
Alyauduntau 2	38.411	65.608	10	Drill hole	Sedletskiy and Fedin (1981)
Beshkent 4	38.781	65.633	10	Drill hole	Sedletskiy and Fedin (1981)
Darbaz 1	39.183	64.834	5	Drill hole	Sedletskiy and Fedin (1981)
Dengizkul 7	39.098	63.840	3	Drill hole	Sedletskiy and Fedin (1981)
Karabai 1	38.600	66.565	7	Drill hole	Sedletskiy and Fedin (1981)
Kuruksai 2	38.402	65.913	17	Drill hole	Sedletskiy and Fedin (1981)
Metedzhan 2	38.893	64.089	10	Drill hole	Sedletskiy and Fedin (1981)
Metedzhan 5	38.894	64.090	5	Drill hole	Sedletskiy and Fedin (1981)
Pamuk 1	38.953	64.930	8	Drill hole	Sedletskiy and Fedin (1981)
Sakar 2	38.883	63.251	10	Drill hole	Sedletskiy and Fedin (1981)
Saman-Tepe 10	38.948	63.730	10	Drill hole	Sedletskiy and Fedin (1981)
Shurtan 7	38.529	66.169	15	Drill hole	Sedletskiy and Fedin (1981)
Urtabulak 2	39.017	64.013	10	Drill hole	Sedletskiy and Fedin (1981)
West Zevardy 1	38.874	64.500	2	Drill hole	Sedletskiy and Fedin (1981)
Zevardy 16	38.979	64.690	5	Drill hole	Sedletskiy and Fedin (1981)
Adamtash 5	38.658	67.132	8	Drill hole	Sedletskiy and Fedin (1981); Vysotskiy and others (1988)
Belesyainak	38.389	66.483	4.2	Occurrence	Sedletskiy and Fedin (1981); Vysotskiy and others (1988)
Girsan	38.617	65.167	3	Occurrence	Sedletskiy and Fedin (1981); Vysotskiy and others (1988)
Kamashi	38.733	65.427	3	Occurrence	Sedletskiy and Fedin (1981); Vysotskiy and others (1988)
Karabay	38.600	66.565	7	Occurrence	Sedletskiy and Fedin (1981); Vysotskiy and others (1988)
Karail	38.514	66.657	4.2	Occurrence	Sedletskiy and Fedin (1981); Vysotskiy and others (1988)
Kishtuvan	39.128	63.345	6.5	Occurrence	Sedletskiy and Fedin (1981); Vysotskiy and others (1988)
North Kamashi	38.978	65.725	3.5	Occurrence	Sedletskiy and Fedin (1981); Vysotskiy and others (1988)
Uzonshor	39.197	63.306	6.5	Occurrence	Sedletskiy and Fedin (1981); Vysotskiy and others (1988)
Aizovat	38.864	65.325	3.5	Occurrence	Vysotskiy and others (1988)
Chashtepe	39.199	63.584	6.5	Occurrence	Vysotskiy and others (1988)
Darbaza	39.218	64.838	6.5	Occurrence	Vysotskiy and others (1988)
Gumbulak	38.580	66.853	3.5	Occurrence	Vysotskiy and others (1988)
Khauzak	39.142	63.669	6.5	Occurrence	Vysotskiy and others (1988)
Kultak	38.75	64.883	3.5	Occurrence	Vysotskiy and others (1988)
Kyzylbayrak	38.570	67.005	3.5	Occurrence	Vysotskiy and others (1988)
Metedzhan	38.857	64.256	6.5	Occurrence	Vysotskiy and others (1988)
Mobik	38.665	66.862	3.5	Occurrence	Vysotskiy and others (1988)
Sakar	38.869	63.173	6.5	Occurrence	Vysotskiy and others (1988)
Saman-Tepe	38.953	63.705	6.5	Occurrence	Vysotskiy and others (1988)
Zevardy	38.975	64.713	3.5	Occurrence	Vysotskiy and others (1988)
Karaul-Kuiu 1	38.554	63.547	4	Drill hole	Zharkov and others (1982)
Severnyts Urtabulak 2	39.034	64.527	10	Drill hole	Zharkov and others (1982)
Zevarda 8	38.950	63.845	2	Drill hole	Zharkov and others (1982)
3	39.674	60.386	0	Drill hole	Zharkov and others (1982)
4	39.874	60.704	0	Drill hole	Zharkov and others (1982)
5	39.757	61.163	0	Drill hole	Zharkov and others (1982)
6	39.980	61.679	0	Drill hole	Zharkov and others (1982)
8	39.233	61.120	0	Drill hole	Zharkov and others (1982)
9	38.899	61.056	0	Drill hole	Zharkov and others (1982)
11	39.958	62.497	0	Drill hole	Zharkov and others (1982)
12	39.374	67.179	2	Drill hole	Zharkov and others (1982)
13	39.072	62.460	2	Drill hole	Zharkov and others (1982)
14	38.805	62.712	2	Drill hole	Zharkov and others (1982)
15	38.557	62.553	0	Drill hole	Zharkov and others (1982)
16	38.669	63.074	3	Drill hole	Zharkov and others (1982)
17	39.306	63.297	0	Drill hole	Zharkov and others (1982)
18	39.253	63.463	5	Drill hole	Zharkov and others (1982)

Table E-1. Thickness data for Gissar and Amu Darya tracts, Central Asia.—Continued

Name	Latitude	Longitude	Potash thickness (m)	Site type	Reference
19	39.077	63.632	8	Drill hole	Zharkov and others (1982)
22	38.862	64.009	5	Drill hole	Zharkov and others (1982)
23	38.971	64.067	6	Drill hole	Zharkov and others (1982)
25	38.945	64.340	7	Drill hole	Zharkov and others (1982)
26	39.064	64.466	8	Drill hole	Zharkov and others (1982)
29	38.946	64.982	7	Drill hole	Zharkov and others (1982)
30	38.752	64.802	5	Drill hole	Zharkov and others (1982)
31	38.741	64.617	6	Drill hole	Zharkov and others (1982)
32	38.430	64.649	8	Drill hole	Zharkov and others (1982)
33	38.717	65.323	3	Drill hole	Zharkov and others (1982)
34	38.778	65.493	4	Drill hole	Zharkov and others (1982)
36	38.413	65.864	16	Drill hole	Zharkov and others (1982)
38	38.349	61.737	0	Drill hole	Zharkov and others (1982)
39	37.940	61.574	0	Drill hole	Zharkov and others (1982)
40	37.276	60.817	0	Drill hole	Zharkov and others (1982)
41	37.328	61.631	0	Drill hole	Zharkov and others (1982)
42	38.132	62.423	0	Drill hole	Zharkov and others (1982)
43	37.060	61.896	0	Drill hole	Zharkov and others (1982)
45	36.499	62.822	0	Drill hole	Zharkov and others (1982)
46	37.814	63.343	0	Drill hole	Zharkov and others (1982)
47	38.933	64.818	7	Drill hole	Zharkov and others (1982)
48	39.156	64.974	4	Drill hole	Zharkov and others (1982)
49	39.080	65.359	2	Drill hole	Zharkov and others (1982)
50	38.867	65.582	0	Drill hole	Zharkov and others (1982)

References Cited

Fedin, O.V., 1981, Otsenka perspektiv kaliyenosnosti verkhneyurskikh solyanykh otlozheniy yuga Sredney Azii [An evaluation of the prospects for potash-bearing capabilities in the Upper Jurassic salt deposits in southern Central Asia], *in* Yanshin, A.L., and Zharkov, M.A., eds., Stroyeniye i usloviya formirovaniya mestorozhdeniy kaliynykh soley [The structure and formation conditions of potash salt deposits]: Novosibirsk, USSR, Izd. Nauka, Sibirsk. Otdel., p. 171–176.

Khudaikuliev, K., 1986, Osnovniye chyerti stroyeniya vyerhnyeyoorskoy galogyennoy formatsii i yeye rol' v prognozirovanii po gryebyennih rifov v amudar'inskoy [Main structural features of the Upper Jurassic halogenous formation and its role in forecasting buried reefs in the Amu Darya syneclise], *in* Yanshin, A.L., and Merzlyakov, G.A., eds., Novye dannye po geologii solenosnykh basseinov Sovetskogo Soyuza [New data on the geology of saliferous basins of the Soviet Union]: Moscow, Nauka, p. 101–115.

Rayevskiy, V.I., and Fiveg, M.P., 1973, Mestorozhdeniya kaliynykh soley SSSR; metody ikh poiskov i razvedki [Deposits of potassium salts in the USSR; methods of exploration and surveying]: Leningrad, Izd. Nedra, Leningr. Otd., 344 p.

Sedletskiy, V.I., and Derevyagin, V.S., 1980, Stroyeniye i sostav kaliyenosnih otlozhyeniy Karlyukskogo myestorozhdyeniya [The structure and composition of the potassium-bearing Karlyukskogo deposits], *in* Zharkov, M.A., ed., Osobennosti stroeniia zalezhei bishofita i kaliinykh solei [Structural features of bischofite and potassium salt deposits]: Novosibirsk, Academiia Nauk SSSR, Institut geologgi i geofiziki, p. 70–90.

Sedletskiy, V.I., and Fedin, O.V., 1981, Lithofacies and potassium potential of Upper Jurassic halogen deposits in central Asia: Lithology and Mineral Resources, v. 16, no. 1, p. 83–92.

Vysotskiy, E.A., Garetskiy, R.G., and Kislik, V.Z., 1988, Kalienosnye basseiny mira [Potassium-bearing basins of the world]: Minsk, Izd. Nauka i Tekhnika, Byelorussian SSR, 387 p.

Zharkov, M.A., Blagovidov, V.V., Zharkova, T.M., and Merzlyakov, G.A., 1982a, Kvoprosu o stroyenii pozdnyeyoorskih solyenosnih otlozhyeniy Sryednyey Azii [The problem of the structure of Late Jurassic saliferrous sediments of Central Asia], *in* Yanshin, A.L., ed., Osobennosti stroenya osadocgnikh formatsiy [Structural characteristics of sedimentary formations]: Novosibirsk, Trudy Instituta Geologii i Geofiziki, p. 3–18.

Appendix F. Generalized SYSTAT Script for Estimation of Undiscovered Contained K_2O in Central Asia Salt Basin Tracts

By Greta J. Orris[1]

This appendix contains a list of variables (table F-1) and a generalized SYSTAT script for in-place ore and K_2O estimates for stratabound tracts in the Central Asia Salt Basin (table F-2). Initial estimates were made using average densities for sylvinite and carnallitite. The estimates were rerun in November, 2014, using a defined relationship between potash grade and density. The revised simulations use data from the Congo Basin (Rauche and others, 2013) that became available after the initial estimations were made; these new data allow a linear relationship between potash grade and density to be estimated using regressions for carnallitite and sylvinite (fig. F-1).

Potential users should note that literature for the area reported no data on the ratios of sylvite to carnallite in the Central Asia Salt Basin. Information was limited to reports of carnallitite as the dominant potash mineralization, with variably-sized local areas and horizons dominated by sylvite mineralization. Therefore, for the purposes of determining density, mineralization is assumed to be only carnallite when the grade is less than 16.9 percent K_2O and only sylvite when the grade is higher. This assumption leads to a discernable linear feature that corresponds to this grade break when plotting the K_2O grades versus in-place ore tonnages estimated by the SYSTAT script Monte Carlo simulation (fig. F-2).

Distributions

Normal distribution: ZRN (mean, standard deviation)

Triangular distribution: TRRN (minimum, maximum, mode)

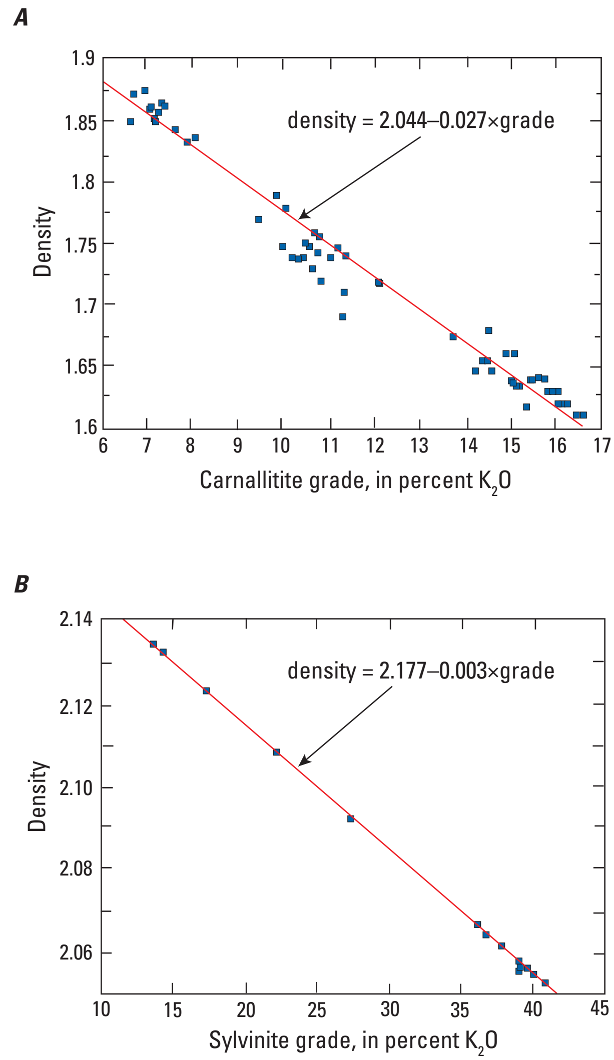

Figure F-1. Graphs showing relationship between grade (in percent K_2O [potassium oxide]) and density for carnallitite (*A*) and sylvinite (*B*). Resulting regression line and equation are also shown.

[1]U.S. Geological Survey, Tucson, Arizona, United States.

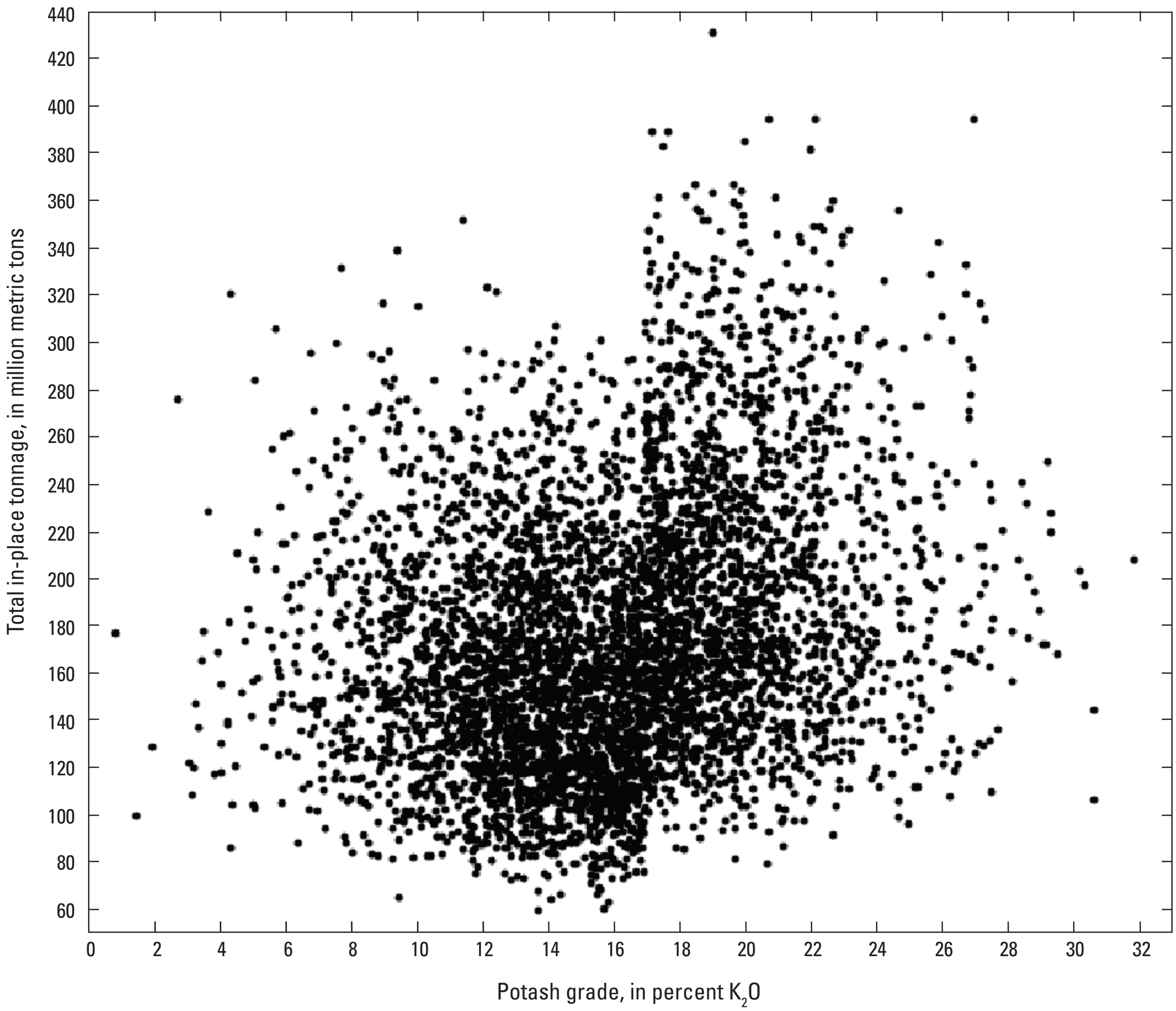

Figure F-2. Select plot showing potash grade and in-place tonnage estimations from the adaptive geometric estimation (AGE) method, SYSTAT Monte Carlo simulation. Grade break between carnallitite and sylvinite ore is discernable as a linear cluster of data points at about 17 percent K_2O (potassium oxide).

Variables

See table F-1.

Script

See table F-2.

References Cited

Rauche, Henry, van der Klauw, Sebastiaan, and Linsenbarth, Ralf, 2013, Update of the NI 43-101 Technical Report for MagMineral's Mengo Permit area, Kouilou region, Republic of Congo: Erfurt, Germany, ERCOSPLAN Ingenieurgesellschaft Geotechnik und Bergbau mbH.

Table F-1. Variables used in the SYSTAT script to estimate undiscovered K_2O.

Variable	Definition
CDENSITY	Calculate, carnallitite density
COT	Calculate, carnallitite, ore tonnage
COTADJ	Calculate, carnallitite ore tonnage, adjusted for anomalies and embayments
CTK2OADJ	Calculate, contained K_2O in adjusted carnallitite ore tonnage
EMB	Input, adjustment for edge embayment, as distribution (in percent)
HOLES	Input, adjustment for anomalies, as distribution (in percent)
KGRADE	Input, K_2O grade, as distribution, in percent
KGRADE2	Conversion, KGRADE from percent to decimal number
KVOL	Input, volume of potash area, as distribution or single number, in cubic kilometers (km^3)
SDENSITY	Calculate, sylvinite density
SOT	Calculate, sylvinite, ore tonnage
SOTADJ	Calculate, sylvinite ore tonnage, adjusted for anomalies and embayments
STK2OADJ	Calculate, contained K_2O in adjusted sylvinite ore tonnage
TOTADJ	Calculate, HOLES + EMB
TOTADJ2	Conversion, TOTADJ from percent to decimal number
TOTALK2O	Calculate, total tons contained K_2O in place, in billions of metric tons (Bt) with known K_2O subtracted
TOTALORE	Calculate, total tons of ore/mineralized rock in-place, in billions of metric tons (Bt) with known resources subtracted

Table F-2. Generalized SYSTAT script.

[black text is script; red text indicates values that need to be input for each tract; blue italicized text is an explanation of script step]

Script	Explanation
CLASSIC ON	
OUTPUT "location for output filename"/NOSCREEN	*Specify location and name for output file*
KGRADE=0	*Set initial value to zero*
TOTADJ=0	*Set initial value to zero*
TOTADJ2=0	*Set initial value to zero*
CDENSITY=0	*Set initial value to zero*
SDENSITY=0	*Set initial value to zero*
COT=0	*Set initial value to zero*
COTADJ=0	*Set initial value to zero*
CTK20ADJ=0	*Set initial value to zero*
SOT=0	*Set initial value to zero*
SOTADJ=0	*Set initial value to zero*
STK2OADJ=0	*Set initial value to zero*
FOR I =1 TO 5000	*5,000 iterations*
KVOL=TRRN(min,max,mode)	*Specify tract volume as distribution in km^3*
KGRADE=ZRN(mean,s.d.)	*Specify potash grade distribution in percent*
KGRADE2=CGRADE/100	*Convert grade from percent to decimal*
IF KGRADE2<0.04 THEN KGRADE2=0.04	*Set lower limit of 4 percent K_2O for KGRADE2 (K team specified for Central Asia)*
IF KGRADE2>0.22 THEN KGRADE2=0.22	*Set upper limit of 22 percent K_2O for KGRADE2 (K team specified for Central Asia)*
HOLES=TRRN(min,max,mode)	*Specify distribution of anomalies (K team specified for each tract)*
EMB=TRRN(min,max,mode)	*Specify distribution of embayments (K team specified for each tract)*
TOTADJ=(HOLES+EMB)	*Calculate total adjustments (in percent)*
TOTADJ2=TOTADJ/100	*Convert total adjustments from percent to decimal*
IF KGRADE2<0.169 THEN BEGINBLOCK	*If grade is less than 16.9% K_2O, assume mineralization is carnallite and calculate following values*
CDENSITY=2.044-(KGRADE*0.027)	*Calculate carnallitite density*
IF CDENSITY<1.602 THEN CDENSITY=1.602	*Set lower density limit at that of 100% carnallite*
SDENSITY=0	*Set sylvinite density to 0*
COT=KVOL*CDENSITY	*Calculate in-place ore tonnage for carnallitite*
COTADJ=COT-(COT*TOTADJ2)	*Adjust in-place ore tonnage for areas of no mineralization*
CTK2OADJ=COTADJ*KGRADE2	*Calculate contained K_2O from adjusted ore tonnage*
ENDBLOCK	*End calculation resulting from grade <0.169*
ELSE BEGINBLOCK	*If KGRADE2 is NOT <0.169, assume mineralization is sylvinite and calculate the following values*
CDENSITY=0	*Set carnallite density to 0*
SDENSITY=2.177-(KGRADE*0.003)	*Calculate sylvinite density*
SOT=KVOL*SDENSITY	*Calculate in-place ore tonnage for sylvinite*
SOTADJ=SOT-(SOT*TOTADJ2)	*Adjust in-place ore tonnage for areas of no mineralization*
STK2OADJ=SOTADJ*KGRADE2	*Calculate contained K_2O from adjusted ore tonnage*
ENDBLOCK	*End calculations resulting from KGRADE2 NOT <0.169*
ENDIF	*End conditional calculations*
TOTALORE=COTADJ+SOTADJ-[total ore, known resources]	*Calculate total ore tons (minus known resources), Bt*
TOTALK2O=CTK2OADJ+STK2OADJ-[total K2O, known resources]	*Calculate contained K_2O tons (minus known resources), Bt*
PRINT KVOL, KGRADE, HOLES, EMB, TOTADJ, CDENSITY, COT, COTADJ, CTK2OADJ, SDENSITY, SOT, SOTADJ, STK2OADJ , TOTALORE, TOTALK2O	*Print variables*
NEXT	*Go to next iteration*
OUTPUT *	
CLASSIC OFF	
END	

Appendix G. Glossary of Terms Used in Description of Evaporites

By Mark D. Cocker[1] and Greta J. Orris[1]

Allochthonous salt Sheetlike salt bodies emplaced at stratigraphic levels above the autochthonous source layer. Allochthonous salt lies on stratigraphically younger strata; theoretically, allochthonous salt could overlie older strata, but such examples have not yet been reported (Jackson and Talbot, 1991).

Autochthonous salt Salt body resting on the original strata or surface on which it accumulated by evaporation (Jackson and Talbot, 1991).

Bittern The bitter liquid remaining after seawater has been concentrated by evaporation until most of the sodium chloride has crystallized out (Neuendorf and others, 2005).

Bittern salts Any of the salts that may be extracted from the bittern of a saltworks or from a comparable natural solution; such as magnesium chloride, magnesium sulfate, bromides, iodides, and calcium chloride (Neuendorf and others, 2005).

Brachyanticline A short, broad anticline (Neuendorf and others, 2005). A short anticlinal fold of layers of rock having an oval cross section. The layers of rock that form the brachyanticline slope away from the central part of its crest on all sides. A brachyanticline is represented on a geological map in the form of concentric oval rings, with the older rocks in the center; the rocks become progressively younger toward the periphery (Prokhorov, 1970–1979).

Cap rock [tectonics] In a salt dome, an impervious body of anhydrite and gypsum, with minor calcite and sometimes with sulfur that overlies the salt body, or plug. It probably results from accumulation of the less soluble minerals of the salt body during leaching in the course of its ascent (Neuendorf and others, 2005).

Carnallite A primary potash ore mineral, $KMgCl_3 \cdot 6H_2O$, and that also is a source of magnesium in some deposits. Usually occurs as crystalline or granular masses. Mode of occurrence—occurs chiefly as a component of extensive thick sedimentary saline deposits, often associated with kieserite, halite, sylvite, and polyhalite (Roberts and others, 1974; Neuendorf and others, 2005).

Carnallitite A rock largely composed of a mixture of carnallite and halite (salt).

Cycle Many sedimentary sections exhibit rhythmicity in the form of regularly alternating beds traceable over long distance, or a repetition of larger units which are referred to as sedimentary sequences or cycles. Rhythmic and cyclic sequences occur worldwide on various scales in presumably every environmental and stratigraphic system (Einsele, 2000).

Dewatering The expulsion of water from sediments during diagenesis or metamorphism. The water may have been present in the form of interstitial pore waters or water bound to hydrous minerals, such as certain clays or gypsum (see page 11, Friedman and others, 1992; Neuendorf and others, 2005).

Diapir [structural geology] A dome or anticlinal fold in which the overlying rocks have been ruptured by the squeezing-out of plastic core material. Diapirs in sedimentary strata usually contain cores of salt or shale (Neuendorf and others, 2005).

Evaporite A sedimentary rock primarily composed of minerals produced from a saline solution as a result of extensive or total evaporation of the solvent. Examples include gypsum, anhydrite, other diverse sulfates, halite (rock salt), primary dolomite, and various nitrates and borates (Neuendorf and others, 2005).

[1]U.S. Geological Survey, Tucson, Arizona, United States.

Gypsum A widely distributed mineral consisting of hydrated calcium sulfate: $CaSO_4 \cdot 2H_2O$. Usually occurs as crystalline masses, fine to coarse granular; fibrous; pulverent; concretionary. Mode of occurrence—occurs abundantly and widespread chiefly in sedimentary deposits; in saline lakes and playas; as efflorescence on certain soils, in the oxidized parts of ore deposits; and in deposits associated with volcanic activity (Roberts and others, 1974). It is the most common sulfate mineral, and is frequently associated with halite and anhydrite in evaporites, forming thick, extensive beds interstratified with limestone, shale, and clay (especially in rocks of Permian and Triassic age) (Neuendorf and others, 2005). It may alter to anhydrite under burial metamorphic conditions and release its water of hydration (Adams, 1970).

Halite NaCl, an abundant evaporite mineral. Usually occurs as crystalline masses, granular and rarely columnar or stalactitic. Mode of occurrence—occurs widespread chiefly as extensive sedimentary deposits ranging from a few centimeters to more than several thousand meters in thickness; as efflorescence in playa deposits, and as a sublimation product in areas of volcanism (Roberts and others, 1974; Neuendorf and others, 2005).

Halokinesis (1) A class of salt tectonics in which salt flow is powered entirely by gravity in the absence of significant lateral tectonic forces Jackson and Talbot (1991). (2) The deformation of halite by flowage. Mechanisms cited for this process include gravity flow, tectonic thrusting, and diapirism (Kyle and Posey, 1991; Neuendorf and others, 2005).

Hartsalz Hard salt, typically a mixture of sylvinite and kieserite, with some anhydrite, found in the Stassfurt salt deposits (U.S. Bureau of Mines, 1996).

Horizon (1) In geology, any given definite position or interval in the stratigraphic column or the scheme of stratigraphic classification. (2) An identifiable rock stratum regionally known to contain or be associated with rock containing valuable minerals (U.S. Bureau of Mines, 1996).

Horse A mining term for a barren mass of country rock occurring within a vein (Neuendorf and others, 2005).

Intracratonic basin A basin formed within the interior region of a continent, away from plate boundaries. It develops where there is subsidence of a part of a craton, probably owing to thermal subsidence or an unsuccessful rift (Neuendorf and others, 2005).

Potash (1) A generic industry term for potassium-bearing salts that includes the commodities potassium chloride, potassium sulfate, potassium nitrate, and potassium oxide; (2) A generic geologic term that mainly includes the minerals sylvite, carnallite, kainite, and langbeinite; (3) A generic geologic term for a sedimentary rock containing significant amounts (commonly more than 20 percent by weight) of soluble, precipitated potassium- and magnesium-chloride and sulfate minerals intermixed or interlayered with halite and other bittern minerals. Variable amounts of insoluble minerals such as gypsum, anhydrite, clay, quartz, and hematite are generally present.

Rim syncline A fold having an arcuate or subcircular axial tract on the outer margin of a salt upwelling. Rim syncline is a nongenetic term, but in the context of salt tectonics a rim syncline typically results from salt withdrawal in the source layer. Peripheral sinks of sediments accumulate within rim synclines (Nettleton, 1934; Jackson and Talbot, 1991; Neuendorf and others, 2005).

Safety pillar A significant thickness, usually about 150 meters, of salt that is left in place below the brine saturated caprock and surrounding water-bearing strata to act as a seal in a diapiric salt structure (Heim and Potthoff, 1983). See "salt back."

Saline giant A term used to describe thick, basin-filling evaporite units; synonymous with mega-evaporites. Mineralogies are dominated by halite and (or) anhydrite, along with varying amounts of carbonates and potash salts (Warren, 2006, 2010).

Salt (1) A general term for naturally occurring sodium chloride, NaCl; (2) A geologic term for a sedimentary rock dominantly composed of halite formed by evaporation of saline water, usually seawater. Salt as a rock may contain lesser amounts of other evaporite-related minerals, including potassium- and magnesium-bearing minerals and variable amounts of insoluble minerals such as gypsum, anhydrite, clay, quartz, and hematite. Crystalline salt is found in playa lakes, bedded salt deposits, and salt structures (operational definition); (3) Usage as a commodity such as a food supplement, in industrial applications, or as a source of the chemicals sodium and chlorine.

Salts (1) A generic term for chemicals classified as chlorides, sulfates, bromides, and iodides; (2) A generic term for minerals classified as chlorides, sulfates, bromides, and iodides. This can include sylvite, carnallite, halite, and other minerals (operational definition; see appendix A for some of these minerals).

Salt anticline (1) A diapiric or piercement structure, like a salt dome except that the salt core is linear rather than equidimensional, such as the salt anticlines in the Paradox basin of the central Colorado Plateau (Neuendorf and others, 2005); (2) Elongated upwelling of salt having concordant overburden (DeGolyer, 1925; Harrison and Bally, 1988; Jackson and Talbot, 1991).

Salt back A significant thickness of salt above the mining horizon maintained to ensure a water seal between mine openings and overlying strata that contain groundwater. Salt back thickness depends on mining method and nature of water saturation and rock competency in overlying beds (Holter, 1969).

Salt diapir A mass of salt that has flowed ductilely and appears to have discordantly pierced or intruded the overburden. In its broadest sense, "diapir" includes (1) lateral or vertical intrusion of any shape, (2) upwelling of buoyant or non-buoyant rock or magma, or (3) emplacement by passive piercement or by faulting of prekinematic overburden (Mrazec, 1907; Jackson and Talbot, 1991).

Salt dome (1) A diapir or piercement structure with a central, nearly equidimensional salt plug, generally 1 to 2 kilometers (km) or more in diameter, which has risen through the enclosing sediments from a mother salt bed (source layer) 5 km to more than 10 km beneath the top of the plug. Many salt plugs have a cap rock of less soluble evaporite minerals, especially anhydrite. The enclosing sediments are commonly turned up and complexly faulted next to a salt plug, and the more permeable beds serve as reservoirs for oil and gas (U.S. Bureau of Mines, 1996); (2) An imprecise, general term for a domal upwelling comprising a salt core and its envelope of deformed overburden. The salt may or may not be discordant (Harris and Veatch, 1899; Jackson and Talbot, 1991).

Salt glacier Sheetlike extrusion of salt flowing from an exposed diapir and spreading subaqueously or subaerially (Jackson and Taylor, 1991).

Salt horse A dome-shaped barren zone generally consisting of halite that crosscuts potash-bearing salt beds. Bedding is continuous through the halite, but is thinner than the potash-bearing salt beds. Halite is believed to have replaced the potash-bearing salt beds in the salt horse through upward movement of saline brines (Linn and Adams, 1963).

Salt pillow A subcircular upwelling of salt having concordant overburden (Jackson and Talbot, 1991).

Salt plug The salt core of a salt dome. It is nearly equidimensional, about 1 or 2 km in diameter, and has risen through the enclosing sediments from a mother salt bed (source layer) 5 to 10 km below (Neuendorf and others, 2005).

Salt solutioning A partial to complete dissolution of salts, commonly resulting in collapse of overlying strata, attributed to ascending or descending less saline water or brine (Holter, 1969).

Salt stock (syn: salt plug; Trusheim, 1957; Jackson and Talbot, 1991; Neuendorf and others, 2005) A pluglike salt diapir having subcircular planform.

Salt structure A generic term used in petroleum, salt, and other geologic literature to refer to geologic structures formed partly or wholly from the movement and (or) deformation of salt (see halokinesis or salt tectonics); may include salt anticlines, salt diapirs, salt domes, salt pillows, salt stocks, salt plugs, salt walls, and other structures (operational definition).

Salt tectonics (syn: halotectonics): Any tectonic deformation involving salt, or other evaporites, as a substratum or source layer; it includes halokinesis (Trusheim, 1957;

Jackson and Talbot, 1986; Jackson and Talbot, 1991).

Salt wall An elongated upwelling of diapiric (discordant) salt, commonly forming sinuous, parallel rows (Trusheim, 1960; Jackson and Talbot, 1991).

Salt weld Surface or zone joining strata originally separated by autochthonous or allochthonous salt. The weld is a negative salt structure resulting from the complete or nearly complete removal of intervening salt. The weld can consist of brecciated, insoluble residue containing halite pseudomorphs or of salt too thin to be resolved in reflection-seismic data. The weld is usually but not always marked by a structural discordance. Another distinctive feature of welds is a structural inversion above them (Jackson and Talbot, 1991).

Salt withdrawal (syn: salt expulsion; Jackson and Talbot, 1991; Neuendorf and others, 2005) Mass transfer of salt over time without obvious change in salt area in cross section. Examples are the migration of salt from the flanks of a salt pillow into its core as it evolves into a diapir or the flow of salt along a salt wall into local culminations that evolve into salt stocks.

Source layer (syn: mother salt) Layer supplying salt for the growth of salt structures; the source layer is a particular type of substratum (Jackson and Talbot, 1991).

Stratabound Said of a mineral deposit confined to a single stratigraphic unit (Neuendorf and others, 2005).

Substratum An underlying layer; in salt tectonics, substratum refers to the ductile layer below a brittle overburden and above the subsalt strata or basement. “Substratum” is a term more general than source layer; the substratum mayor may not give rise to upwelling structures (Jackson and Taylor, 1991).

Subrosion (syn: postburial dissolution) Subrosion is the process by which soluble rocks in the underground are dissolved by groundwater or water penetrating from the surface. Subrosion takes place where soluble rocks are not protected by a layer of impermeable rocks (Rauche and van der Klauw, 2011).

Subsalt strata Sedimentary unit immediately underlying salt (Jackson and Talbot, 1991).

Sylvite The mineral sylvite, KCl, is the principal ore mineral of potassium. Usually in crystalline masses, compact to granular, as crusts, and columnar. Mode of occurrence: Occurs chiefly as extensive thick sedimentary deposits, typically associated with halite, gypsum, anhydrite, carnallite, polyhalite, kieserite, and kainite (Roberts and others, 1974; Neuendorf and others, 2005).

Sylvinite A mixture of halite and sylvite, mined as a potash ore; a rock that contains chiefly impure potassium chloride (Neuendorf and others, 2005).

Turtle-structure anticline (1) Mounded strata between salt diapirs having a flat base and rounded crest over a local primary increase in sedimentary thickness; the anticline may or may not be cored by a low salt pillow. The turtle structure forms between diapirs whose flanks subside because of regional extension or between salt structures evolving from pillows to diapirs (Trusheim, 1957; Neuendorf and others, 2005); (2) Strata mounded between salt diapirs and having a flat base and rounded crest over a sedimentary thick; the anticline mayor may not be cored by a low salt pillow. The turtle structure forms by structural inversion of a primary peripheral sink when salt is withdrawn from the margins of the peripheral sink by growing diapirs. The planform of turtle structures is typically highly irregular.

References Cited

Adams, S.S., 1970, Ore controls, Carlsbad Potash District, Southeast New Mexico, *in* Rau, J.L., and Dellwig, L.F., Third Symposium on salt, volume 1: Cleveland, Ohio, Northern Ohio Geological Society, p. 246–257.

DeGolyer, E.L., 1925, Discovery of potash salts and fossil algae in Texas salt dome: American Association of Petroleum Geologists Bulletin, v. 9, no. 2, p. 348–349.

Einsele, G., 2000, Sedimentary basins—evolution, facies, and sediment budget: New York, Springer, 792 p.

Friedman, G.M., Sanders, J.E., and Kopaska-merkee, D.C., 1992, Principles of sedimentary deposits—stratigraphy and sedimentology: New York, MacMillan Publishing Company, 43 p.

Harris, G.D., and Veatch, A.C., 1899, A preliminary report on the geology of Louisiana: Baton Rouge, Geological Survey of Louisiana Report, 324 p.

Harrison, J.C., and Bally, A.W., 1988, Cross sections of the Devonian to Mississippian fold belt on Melville Island, Canadian Arctic Islands: Canadian Society of Petroleum Geologists, v. 36, p. 311–332.

Heim, W.A., and Pothoff, A.H., 1983, Potash mining in steep deposits (salt domes), *in* McKercher, R., ed., Potash ’83: New York, Pergamon Press, p. 79–84.

Holter, M.E., 1969, The Middle Devonian Prairie Evaporite of Saskatchewan: Saskatchewan Department of Mineral Resources Report 123, 134 p.

Jackson, M.P.A., and Talbot, 1986, External shapes, strain rates, and dynamics of salt structures: Geological Society of America Bulletin, v. 97, p. 305–323.

Jackson, M.P.A., and Talbot, C.J., 1991, A glossary of salt tectonics: Texas Bureau of Economic Geology Geological Circular 91-4, 44 p.

Kyle, J.R., and Posey, H.H., 1991, Halokinesis, cap rock development, and salt dome mineral resources*, in* Melvin, J.L., ed., Evaporites, petroleum and mineral resources: New York, Elsevier, p. 413–474.

Linn, K.O., and Adams, S.S., 1963, Barren halite zones in potash deposits, Carlsbad, New Mexico, *in* Rau, J.L., ed., Second Symposium on Salt: Cleveland, OH, Northern Ohio Geological Society, p. 59–69.

Mrazec, L., 1907, Despre cute cu sîmbure de strapungere [On folds with piercing cores]: Romania, Buletinul Societatiide de ştiinţe, v. 16, p. 6–8.

Nettleton, L.L., 1934, Fluid Mechanics of Salt Domes: Bulletin of the American Association of Petroleum Geologists, v. 18, no. 9, p. 1175–1204.

Neuendorf, K.K.E., Mehl, Jr., J.P., and Jackson, J.A., 2005, Glossary of Geology (5th ed.): Alexandria, Virginia, American Geological Institute, 799 p.

Prokhorov, A.M., ed., 1970–1979, The Great Soviet Encyclopedia: New York, Macmillan Inc., 31 volumes and 3 volumes of indexes.

Rauche, H., and van der Klauw, S., 2011, Technical report and resource report for the Danakhil potash deposit, Afar State, State/Ethiopia: Erfurt, Germany, ERCOPSPLAN Ingenieurgesellschaft, 128 p. [plus appendixes.]

Roberts, W.L., Rapp, Jr., G.R., and Weber, Julie, 1974, Encyclopedia of minerals: New York, Van Nostran Reinhold Company, 693 p.

Trusheim, Ferdinand, 1957, Über halokinese und ihre bedeutung für die strukturelle entwicklung Norddeutschlands [On halokinesis and its significance for the structural development of North Germany]: Zeitschrift für Deutsche Geologische Gesellschaft, v. 109, p. 111–151.

Trusheim, Ferdinand, 1960, Mechanism of salt migration in northern Germany: Bulletin of the American Association of Petroleum Geologists, v. 44, no. 9, p. 1519–1540.

U.S. Bureau of Mines, 1996, Dictionary of mining, mineral, and related terms: U.S. Bureau of Mines Report SP-96-1, CD-ROM.

Warren, J.K., 2006, Evaporites—Sediments, resources and hydrocarbons: Berlin, Springer-Verlag, 1,035 p.

Warren, J.K., 2010, Evaporites through time—Tectonic, climatic, and eustatic controls in marine and nonmarine deposits: Earth-Science Reviews, v. 98, no. 3–4, p. 217–268.

Appendix H. The Assessment Team

Jeff Wynn, Ph.D., is a research geophysicist with the U.S. Geological Survey (USGS) at the Cascades Volcano Observatory in Vancouver, Washington. He has authored over 220 books, papers, and maps in geophysics, mineral resource assessments, astrophysics, and ocean engineering. He authored the first 3D geologic map, and the first age-correlated mineral resource assessment of southern Venezuela. He has served as a U.S. diplomat and USGS mission chief in Venezuela and Saudi Arabia. He served a 5-year assignment as chief scientist for volcano hazards of the U.S. Geological Survey, and holds three patents in mineral exploration technology and deep ocean geophysical mapping.

Greta J. Orris, Ph.D., is a research geologist with the USGS in Tucson, Arizona. She specializes in industrial minerals, tools and methodologies for quantitative assessment of these and other minerals, and is a senior USGS research scientist for mineral economics. She has served as a leader of mineral resource assessment teams evaluating a wide range of commodities in North and South America, Europe, Asia, and Africa.

Mark D. Cocker, Ph.D., PG, is an emeritus research geologist with the USGS. His background is in global potash assessment, lateritic, supergene rare earth elements, precious and base metals in the western US, industrial minerals in Georgia, and hydrocarbon exploration in Alaska. His work has involved field mapping, drilling, geochemical sampling, petrography, geophysical surveys, GIS mapping and analysis. He has authored over 170 papers, abstracts, maps, and digital publications. He has been a member of several mineral resource assessment teams.

Pamela Dunlap, M.S., is a geologist with the USGS in Tucson, Arizona. She worked as an exploration geologist for several mining companies in Nevada, Montana, Idaho, and Washington and also as a research geologist for various state geological surveys (Idaho, Montana, and Washington) prior to joining the USGS in 1992. She has done mineral-resource assessment work in Idaho (phosphate) and Montana (oil shale) under contract to the USGS. She has prepared many geologic map and mineral-resource assessment products in a geographic information system (GIS) while with the USGS.

James D. Bliss, M.S., is an industrial mineral and spatial modeling specialist with the USGS in Tucson, Arizona. He has developed grade and tonnage models suitable for use in quantitative assessment for a number of mineral-deposit types including low-sulfide gold quartz veins, and gold placers, among others. He has participated in a number of mineral resources assessment teams. He has developed models and grade and tonnage databases for numerous industrial minerals including graphite, diamonds, and pegmatites.

Bruce Lipin, Ph.D., is an emeritus geologist with the USGS in Reston, Virginia. He is a specialist in ultramafic rocks and their mineral resources, and mineral resource assessments.

Gregory T. Spanski, Ph.D., is an emeritus geologist with the USGS in Denver, Colorado. He is a mineral resource specialist for Africa, and a former university professor.

Chao Yang, Ph.D., is a senior oil and gas and evaporite geologist with Saskatchewan Energy and Resources, Regina, Saskatchewan, Canada.

Mirosław Słowakiewicz, Ph.D., is a sedimentary geologist with the Polish Geological Institute–National Research Institute, Warsaw, Poland.

Robert J. Ryan, Ph.D., is a geologist and section leader with the Nova Scotia Department of Natural Resources, Nova Scotia, Canada.

Menlo Park Publishing Service Center, California
Manuscript approved for publication, December 21, 2015
Edited by Sarah E. Nagorsen
Layout and design by Sharon L. Wahlstrom

USGS Wynn and others— **Geology and Undiscovered Resource Assessment of the Potash-Bearing Central Asia Salt Basin, Turkmenistan, Uzbekistan, Tajikistan, and Afghanistan**—Scientific Investigations Report 2010–5090–AA

ISSN 2328-0328 (online)
http://dx.doi.org/10.3133/sir20105090AA